

HEAT INTEGRATION AND CONTROLLABILITY ANALYSIS
OF HEAT EXCHANGER NETWORKS

by:

Ibrahim Tamer Masoud

A Thesis Presented to the Faculty of the
American University of Sharjah
College of Engineering
in Partial Fulfillment
of the Requirements
for the Degree of

Master of Science in
Chemical Engineering

Sharjah, United Arab Emirates

May 2014

© 2014 Ibrahim Tamer Masoud. All rights reserved.

Approval Signatures

We, the undersigned, approve the Master Thesis of Ibrahim M. Tamer Masoud Mohamed Ibrahim
Thesis Title: Heat Integration and Controllability Analysis of Heat Exchanger Networks

Signature

Date of Signature

Dr. Nabil Abdel Jabbar
Professor, Department of Chemical Engineering
Thesis Advisor

Dr. Rachid Chebbi
Professor, Department of Chemical Engineering
Thesis Co-Advisor

Dr. Zarook Shareefdeen
Associate Professor, Department of Chemical Engineering
Thesis Committee Member

Dr. Mohamed Gadalla
Professor, Department of Mechanical Engineering
Thesis Committee Member

Dr. Naif Darwish
Head, Department of Chemical Engineering

Dr. Hany El-Kadi
Associate Dean, College of Engineering

Dr. Leland Blank
Dean, College of Engineering

Dr. Khaled Assaleh
Director of Graduate Studies

Acknowledgments

All praises to Allah for giving me the strength and ability to finish this thesis.

I would like to sincerely thank my advisors, Dr. Nabil Abdel Jabbar and Dr. Rachid Chebbi for allowing me to pursue the research of my interest, for their continuous guidance and support, and for helping me pave the pathway in reaching the findings of this thesis.

I would like to express my appreciation to the thesis committee members: Dr. Zarook Shareefdeen and Dr. Mohamed Gadalla for their time and effort in reviewing this thesis.

I take this opportunity to express my utmost gratitude to my parents for their endless love, their continuous support in all aspects of life and for being my role models. I would like to genuinely thank my loving wife for her constant encouragement to peruse my dreams.

I also would like to thank Fahad Al-Sadoon, my true friend and colleague for making this journey unique and enjoyable.

Abstract

The objective of this research is to present a methodological framework for designing heat exchanger networks, which best addresses heat recovery, economics and controllability. The proposed framework formulates a systematic approach consisting of a series of simple design steps. The steps include heat integration techniques such that the design can achieve its energy recovery targets: a detailed cost analysis to minimize both capital and utility costs, and steady-state controllability measures to keep the design controllable. A heat exchanger network case study was used to test the proposed framework, and the results were compared with previous works in the literature. Pinch and Superstructure heat integration methods were applied to the case study; both designs achieved the system's required heat recovery, however, the Superstructure design showed lower costs than the Pinch design. Both heat integration methods were also compared in terms of their inner loop interactions by performing Relative Gain Array and Singular Value Decomposition analyses. The results showed that the Superstructure design had less inter-loop interactions than the Pinch design. Control of the heat exchanger networks was achieved by placing bypasses around some of the heat exchangers and manipulating the bypass fractions. All bypass fractions were set at 10%. It was found that bypass fractions marginally increase the capital cost of the HEN of about 2-4%. However, the increase in the bypass fractions did not affect the steady state controllability of the HEN system. The design with the proposed framework was further verified by a dynamic analysis and compared with a benchmark case from the literature. The closed-loop dynamic simulation was performed via ASPEN-HYSYS for different HEN the design that was obtained from the proposed framework in this study and the ones obtained in the literature. Dynamic simulation results revealed that our design exhibited better control characteristics in terms of disturbance rejection and set point tracking. Furthermore, it was found that the best control performance which was achieved in this study with the highest bypass fraction of 10%, had the highest capital cost for HEN design. This finding confirmed that there is a trade-off between the design and controllability of HENs.

Search Terms: Heat Integration, Heat Exchanger Networks, Heat Recovery, Economics, Minimum Costs, Framework, Bypass Placement, Bypass Fractions, Controllability

Table of Contents

Abstract	5
List of Figures	9
List of Tables.....	12
List of Abbreviations.....	14
Nomenclature	16
Chapter 1: Introduction	17
1.1 Problem Statement	17
1.2 Background and Literature Review.....	17
1.3 Research Objectives	22
1.4 Structure of the Report.....	23
Chapter 2: Research Methodology	24
2.1 Heat Integration Analysis.....	24
2.1.1 Pinch Design.....	24
2.1.2 Superstructure Design.....	26
2.1.3 Aspen HX-Net	26
2.2 Controllability Analysis	28
2.2.1 Relative Gain Array (RGA) Analysis.....	29
2.2.2 Singular Value Decomposition (SVD) Analysis	30
Chapter 3: Framework Development and Case Study Application.....	32
3.1 The Proposed Framework	32
3.2 The Case Study	39
3.3 Results and Discussion.....	40
3.3.1 Analyzing The Most Suitable Heat Integration Method, Pinch vs. Superstructure. 40	
3.3.1.1 Design A: Superstructure Design with 0.1 Bypass Fractions.....	42
3.3.1.2 Design B: Pinch Design with 0.1 bypass fractions.....	48
3.3.2 Bypass Placement Analysis	54
3.3.3 Bypass Fractions Analysis.....	56
3.3.3.1 HEN Cost Effect of Bypass Fractions Ranging from 0.01 to 0.1.....	56

3.3.3.2 HEN Controllability Effect of Bypass Fractions Ranging from 0.01 to 0.1	61
3.4 Steady State Comparison	64
Chapter 4: Dynamics, Control and Exergy Analyses.....	68
4.1 Steady State Simulation	68
4.2 Dynamic Simulation and Controller Design	69
4.3 Controller Performance Analysis	71
4.3.1 Step Change Disturbance in H1 Inlet Temperature.....	72
4.3.2 Step Change Disturbance in C1 Inlet Temperature.....	79
4.3.3 Step Change Disturbance in C2 Inlet Temperature.....	82
4.3.4 Step Change Disturbance in H2 Inlet Temperature.....	88
4.4 Exergy Analysis	92
Chapter 5: Conclusion and Recommendations.....	96
References	101
Appendix 1: Sample RGA and SVD Analysis MATLAB Files	104
Appendix 2: Sample Aspen HX-Net Simulation Report of the Proposed Framework Design	114
Appendix 3: Sample Aspen HYSY Simulation Report of the Proposed Framework Design	119
Vita	144

List of Figures

Figure 1.1: The overlap between heat recovery, economics and control for HEN.	22
Figure 2.1: Sample temperature interval diagram [3].....	24
Figure 2.2: Sample composite diagram [20].	25
Figure 2.3: Snapshot of Aspen HX-Net interface [21].....	27
Figure 3.1: General flow chart of the proposed framework	36
Figure 3.2: The proposed framework; choosing the best heat integration method flowchart .	37
Figure 3.3: The proposed framework; choosing the bypass placements flowchart.....	38
Figure 3.4: Grossman [24] et al.'s superstructure design of the HEN under study done by Konukman et al. [16].....	40
Figure 3.5: Linhoff et al.'s [1] pinch design of the HEN under study done by Konukman et al. [16].....	41
Figure 3.6 Snapshot of Aspen HX-Net simulation of Design A [21].....	43
Figure 3.7: Best control scheme for Design A.	48
Figure 3.8: Aspen HX-Net simulation of Design B	49
Figure 3.9: Best and chosen control scheme for Design B.....	53
Figure 3.10: Bypass placement comparison between the framework (green), Yan et al.'s [18] (blue) and Uzturk and Arkam's [23] design (red) approaches for the HEN under study.	64
Figure 4.1: Snapshot of Aspen HYSYS dynamic control simulation for the proposed framework design.....	70
Figure 4.2: Snapshot of Aspen HYSYS dynamic control simulation for Yan et al's [18] design.	71
Figure 4.3: H1 outlet temperature reaction to a +5 K step change in H1 inlet temperature of the framework's design.....	73
Figure 4.4: C1 outlet temperature reaction to a +5 K step change in H1 inlet temperature of the framework's design.....	73
Figure 4.5: C2 outlet temperature reaction to a +5 K step change in H1 inlet temperature of the framework's design.....	73
Figure 4.6: H1 outlet temperature reaction to a +5 K step change in H1 inlet temperature of Yan et al.'s [18] design.	74

Figure 4.7: C1 outlet temperature reaction to a +5 K step change in H1 inlet temperature of Yan et al.'s [18] design.....	74
Figure 4.8: C2 outlet temperature reaction to a +5 K step change in H1 inlet temperature of Yan et al.'s [18] design.....	75
Figure 4.9: H1 outlet temperature reaction to a +10 K step change in H1 inlet temperature of the framework's design.....	76
Figure 4.10: C1 outlet temperature reaction to a +10 K step change in H1 inlet temperature of the framework's design.....	77
Figure 4.11: C2 outlet temperature reaction to a +10 K step change in H1 inlet temperature of the framework's design.....	77
Figure 4.12: H1 outlet temperature reaction to a +10 K step change in H1 inlet temperature of Yan et al.'s [18] design.....	77
Figure 4.13: C1 outlet temperature reaction to a +10 K step change in H1 inlet temperature of Yan et al.'s [18] design.....	78
Figure 4.14: C2 outlet temperature reaction to a +10 K step change in H1 inlet temperature of Yan et al.'s [18] design.....	78
Figure 4.15: H1 outlet temperature reaction to a +5 K step change in C1 inlet temperature of the framework's design.....	79
Figure 4.16: C1 outlet temperature reaction to a +5 K step change in C1 inlet temperature of the framework's design.....	80
Figure 4.17: C2 outlet temperature reaction to a +5 K step change in C1 inlet temperature of the framework's design.....	80
Figure 4.18: H1 outlet temperature reaction to a +5 K step change in C1 inlet temperature of Yan et al.'s [18] design.....	81
Figure 4.19: C1 outlet temperature reaction to a +5 K step change in C1 inlet temperature of Yan et al.'s [18] design.....	81
Figure 4.20: C2 outlet temperature reaction to a +5 K step change in C1 inlet temperature of Yan et al.'s [18] design.....	81
Figure 4.21: H1 outlet temperature reaction to a +5 K step change in C2 inlet temperature of the framework's design.....	83
Figure 4.22: C1 outlet temperature reaction to a +5 K step change in C2 inlet temperature of the framework's design.....	83

Figure 4.23: C2 outlet temperature reaction to a +5 K step change in C2 inlet temperature of the framework's design.....	83
Figure 4.24: H1 outlet temperature reaction to a +5 K step change in C2 inlet temperature of Yan et al.'s [18] design.....	84
Figure 4.25: C1 outlet temperature reaction to a +5 K step change in C2 inlet temperature of Yan et al.'s [18] design.....	84
Figure 4.26: C2 outlet temperature reaction to a +5 K step change in C2 inlet temperature of Yan et al.'s [18] design.....	85
Figure 4.27: H1 outlet temperature reaction to a +1 K step change in C2 inlet temperature of the framework's design.....	86
Figure 4.28: C1 outlet temperature reaction to a +1 K step change in C2 inlet temperature of the framework's design.....	86
Figure 4.29: C2 outlet temperature reaction to a +1 K step change in C2 inlet temperature of the framework's design.....	87
Figure 4.30: H1 outlet temperature reaction to a +1 K step change in C2 inlet temperature of Yan et al.'s [18] design.....	87
Figure 4.31: C1 outlet temperature reaction to a +1 K step change in C2 inlet temperature of Yan et al.'s [18] design.....	87
Figure 4.32: C2 outlet temperature reaction to a +1 K step change in C2 inlet temperature of Yan et al.'s [18] design.....	88
Figure 4.33: H1 outlet temperature reaction to a +5 K step change in H2 inlet temperature of the framework's design.....	89
Figure 4.34: C1 outlet temperature reaction to a +5 K step change in H2 inlet temperature of the framework's design.....	89
Figure 4.35: C2 outlet temperature reaction to a +5 K step change in H2 inlet temperature of the framework's design.....	90
Figure 4.36: H1 outlet temperature reaction to a +5 K step change in H2 inlet temperature of the Yan et al.'s [18] design.....	90
Figure 4.37: C1 outlet temperature reaction to a +5 K step change in H2 inlet temperature of the Yan et al.'s [18] design.....	90
Figure 4.38: C2 outlet temperature reaction to a +5 K step change in H2 inlet temperature of the Yan et al.'s [18] design.....	91

List of Tables

Table 3.1: Heat exchanger network under study	39
Table 3.2: Heat exchanger areas and duties of design A.....	43
Table 3.3: Controlled variables of Design A.....	44
Table 3.4: Manipulated variables of Design A.....	44
Table 3.5: New values of CVs due to changes in MVs.....	45
Table 3.6: Controllability analysis results of Design A	47
Table 3.7: Summary of the best control scheme results for Design A	47
Table 3.8: Heat exchanger areas and duties of Design B.....	49
Table 3.9: Controlled variables of design B.....	49
Table 3.10: Manipulated variables of Design B.....	50
Table 3.11: New values of CVs due to the changes in MVs of Design B.....	50
Table 3.12: Controllability analysis results for Design B	52
Table 3.13: Summary of best control scheme results for Design B	52
Table 3.14: Summary of the best control schemes for each design	53
Table 3.15: HEN capital costs in USD with bypass fractions of $X_3=0.01$ and X_1 & X_2 ranging from 0.01 to 0.1.....	58
Table 3.16: HEN capital costs in USD with bypass fractions of $X_3=0.02$ and X_1 & X_2 ranging from 0.01 to 0.1.....	58
Table 3.17: HEN capital costs in USD with bypass fractions of $X_3=0.03$ and X_1 & X_2 ranging from 0.01 to 0.1.....	58
Table 3.18: HEN capital costs in USD with bypass fractions of $X_3=0.04$ and X_1 & X_2 ranging from 0.01 to 0.1.....	59
Table 3.19: HEN capital costs in USD with bypass fractions of $X_3=0.05$ and X_1 & X_2 ranging from 0.01 to 0.1.....	59
Table 3.20: HEN capital costs in USD with bypass fractions of $X_3=0.06$ and X_1 & X_2 ranging from 0.01 to 0.1.....	59
Table 3.21: HEN capital costs in USD with bypass fractions of $X_3=0.07$ and X_1 & X_2 ranging from 0.01 to 0.1.....	60
Table 3.22: HEN capital costs in USD with bypass fractions of $X_3=0.08$ and X_1 & X_2 ranging from 0.01 to 0.1.....	60

Table 3.23: HEN capital costs in USD with bypass fractions of $X_3=0.09$ and X_1 & X_2 ranging from 0.01 to 0.1.....	60
Table 3.24: HEN capital costs in USD with bypass fractions of $X_3=0.1$ and X_1 & X_2 ranging from 0.01 to 0.1.....	61
Table 3.25: RGA & SVD CNs of bypass fractions combinations with HEN costs close to 94,000 USD.....	62
Table 3.26: RGA & SVD CNs of bypass fractions combinations with HEN costs close to 94,500 USD.....	62
Table 3.27: RGA & SVD CNs of bypass fractions combinations with HEN costs close to 95,000 USD.....	63
Table 3.28: Comparison of steady state control parameters, heat exchanger areas and costs between the framework's proposed design, Yan et al.'s [18] and Uzturk and Arkam's [23] design approaches for the HEN under study	65
Table 4.1: HEN system parameters	69
Table 4.2: Effect of +5 (K) step change on H1 inlet temperature for the framework's and Yan et al.'s [18] control designs.....	76
Table 4.3: Effect of +10 (K) step change on H1 inlet temperature for framework's and Yan et al.'s [18] control designs.....	78
Table 4.4: Effect of +5 (K) step change in C1 inlet temperature on framework's and Yan et al.'s [18] control designs.....	82
Table 4.5: Effect of +5 (K) step change in C2 inlet temperature on framework's and Yan et al.'s [18] control designs.....	85
Table 4.6: Effect of +1 (K) step change in C2 inlet temperature on framework's and Yan et al.'s [18] control designs.....	88
Table 4.7: Effect of +5 (K) step change in H2 inlet temperature on framework's and Yan et al.'s [18] control designs.....	91
Table 4.8: Exergy analysis of the framework's design	94
Table 4.9: Exergy analysis of Yan el al.'s [18] design.....	95

List of Abbreviations

C	Cooler
C1	Cold Stream 1
C2	Cold Stream 2
CN	Condition Number
CV	Controlled Variables
DCN	Distillation Column Networks
DP	Disturbance Projection
HEN	Heat Exchanger Networks
H1	Hot Stream 1
H2	Hot Stream
HE1	Heat Exchanger 1
HE2	Heat Exchanger 2
HE3	Heat Exchanger 3
K	Steady State Gain Matrix
N_{byp}	Number of Bypasses
N_{hx}	Number of Heat Exchangers
MEN	Mass Exchanger Networks
MER	Maximum Energy Recovery
MV	Manipulated Variables
P	Eigenvalues of K Matrix
PL	Plan Life
RGA	Relative Gain Array
ROR	Rate of Return

S	Diagonal Array of Eigenvalues in Decreasing Order
SVD	Singular Value Decomposition
X1	Bypass Fraction 1
X2	Bypass Fraction 2
X3	Bypass Fraction 3
U	Orthogonal Array of Singular Left Vectors
V	Orthogonal Array of Singular Right Vectors

Nomenclature

e	Exergy Loss in kJ/kg
e_{HE}^i	Rate of Exergy Destruction in Heat Exchanger i in kW
\dot{E}	Rate of Exergy in kW
g	Gravitational Constant in m/s^2
h	Mass Enthalpy in kJ/kg
h_o	Mass Enthalpy at Ambient Conditions in kJ/kg
\dot{m}	Mass Flow Rate in kg/s
s	Specific Entropy in kJ/kg.K
s_o	Specific Entropy at Ambient Conditions in kJ/kg.K
T_o	Ambient Temperature in K
v	Velocity in m/s
z	Elevation in m
α	Eigenvalue
β	Diagonal Eigenvalue

Chapter 1: Introduction

1.1 Problem Statement

Heat exchanger networks are essential to any chemical process. The competitiveness of today's markets and the focus on energy efficiency requires improved heat-integrated heat exchanger networks. Heat integration methods aim to obtain the maximum heat recovery while minimizing capital and utility costs of a process unit but do not take into consideration the controllability aspects of the design. Heat integration of a process unit may increase the heat recovery and minimize the cost, but the process unit may become difficult to control. The aim of the present research is to incorporate the controllability aspects in the procedure of designing heat exchanger networks.

1.2 Background and Literature Review

Heat integration is a method where process design is optimized to minimize the energy consumption and maximize the heat recovery of a certain system. Heat integration synthesis of a heat exchanger network can be described as the design of heat exchangers and the matching of hot and cold streams in order to reach the streams' specified outlet temperatures using the minimum capital costs, and minimum utility costs by minimizing the utility consumption. There are two well-known techniques of heat integration: Pinch analysis and Superstructure analysis.

The Pinch analysis technique was first developed by Linhoff *et al.* [1, 2]. Pinch analysis is a methodology for minimizing energy consumption of chemical processes by calculating thermodynamically feasible energy targets and achieving them by optimizing heat recovery systems, energy supply methods and process operating conditions by following a series of heuristic steps of matching hot and cold streams together [3, 4, 5].

Contrary to the heuristic approach of the Pinch analysis, the Superstructure approach is a computer based analysis. All possible matching possibilities between the hot and the cold streams are analyzed through the design of a computer program based on linear and nonlinear equations. All matching possible scenarios are analyzed in terms of

heat recovery and economics. The most cost effective structure is chosen to be the optimum Superstructure design. The Superstructure approach is capable of designing large networks with complex constraints, but because the solution is very time consuming, computers are used to solve the linear and nonlinear equations and therefore computers choose the matches between the streams, eliminating the designer's input to the choice of the matches [4].

Heat integration of process streams can lead to process structures that are difficult to control, and in some cases this inhibits retrofit of existing processes. Supply stream temperatures and flow rates can act as disturbances to the system; therefore, a heat integrated system must cope with desired and undesired variations in operating conditions of the system.

Control and optimization always go hand in hand. Process control is the act of maintaining the operational requirements of a process through manipulation of one or more of the inputs to that process. Optimization is the choice of key set points such that the process operates at the best economic conditions. The control design objective is to maximize profits while satisfying product specifications, quality, safety, operational constraints and environmental regulations. A well-controlled process has less variability in the measured process variables, so the process can be operated close to the profitable constraint, i.e., at its steady state design.

Variables that affect, and are affected by the process, should be categorized as either controlled, manipulated or disturbances variables. Controlled variables are output variables which quantify the performance or quality of the final product. Manipulated variables are input variables that are adjusted dynamically to keep the controlled variables at their set points. Disturbance variables represent input variables that can cause the controlled variables to deviate from their respective set points. It is usually not possible to control all outputs. Thus, once the number of manipulated variables is defined, the controlled variables are chosen among the outputs according to the manipulated variables.

Design of a continuous chemical process is done at a steady state assuming that the process can be controlled and manipulated at the design conditions, no matter how complex the process is. The control system of a chemical process is often analyzed only

after the process design is defined, and it has traditionally been evaluated by designer expertise, heuristic rules and/or trial and error methods. Process synthesis and control system design are usually considered to be separate stages instead of an integrated procedure. Some unfavorable process dynamics may limit the effectiveness of the control system, and may lead to a process that is unable to meet the design specifications. Often design of chemical processes is based on economics and not on controllability. Thus, in the synthesis phase, an easily controllable process alternative can be rejected in favor of a more economical alternative that might be hard to control. Plants that are hard to control are normally not flexible, show no capacity to reject disturbances, and usually lead to additional operational costs to overcome the control difficulties. Controllability of a system, which is the ease with which a continuous plant can be held at a specified steady state of a system, does not depend on controller type; it is a function of the process and its interactions. Controllability can be altered by process modifications (type, size, etc.): location of sensors and actuators, addition of new equipment, new process lines (such as bypasses) and redefinition of control objectives (such as temperature targets).

Any chemical process is by default in a dynamic unsteady state or a transient system whose behavior changes with time. By definition, a dynamic system is a combination of components or subsystems working together towards a unified set of objectives. The variables affecting the interactions of each sub system can be categorized as either inlet or outlet variables. Inlet variables include a number of factors that act as disturbances driving the system from the designed steady state to the undesired unsteady state, such as variations in the inlet feed compositions, physical and chemical properties, cooling and heating medium properties and many more, thus affecting the outlet variables.

Control systems are therefore designed to control undesired changes, forcing the process to reach as much of the desired steady state as it could. Control design is done at a steady state, and although it can take into consideration a number of the expected dynamic interactions as a result of various subsystems working together, a dynamic simulation is always needed to validate the findings of the steady-state design.

Control measures such as controllability, switchability, and resiliency should be considered in the design phase of any chemical plant to achieve a process that is both

controllable and economical. Controllability is the ease with which a continuous plant can be held at a specified steady state. Switchability is the measure of ease with which a process can be moved from one desired stationary point to another. Resiliency is the measure of the degree to which a process can meet its design objectives despite external disturbances and uncertainties in the design conditions [4, 6, 7].

Once the design stage is finished, several methods are used to help the designer choose the best control scheme which produces the least interactions between the controllers and provides the best closed loop controller performances.

Interactions between process design and control for heat exchanger networks have been addressed by many researchers. Oliveira *et al.* [8] discussed the importance of taking into account preliminary control considerations in HEN synthesis, and analyzed in detail the interaction between process control and design of a particular HEN. They proposed a procedure to verify the controllability of a HEN using controllability measures based on steady-state information with minimal computational efforts. Relative Gain Array (RGA) analysis is a tool for decentralized multi-loop control; it provides a dimensionless measure of the interactions between control loops. RGA is also used to choose the most controllable control scheme between the proposed schemes. When RGA analysis produces similar results for more than one control scheme, Singular Value Decomposition (SVD) analysis is performed to choose the best control schemes from the ones proposed by RGA analysis [9, 10]. The procedure proposed by Oliveira *et al.* [8] must be employed at each step of the synthesis algorithm to identify unfeasible structures that must be eliminated to make the process both feasible and controllable. To make the process feasible and controllable Oliveira *et al.*'s [8] analysis suggests some process modifications which include the addition of bypasses and modification of the original heat transfer areas. These modifications present a trade-off between increasing the controllability and increasing the cost of the final HEN.

Westphalen *et al.* [11] state that the bulk of the literature discusses HEN control problems of existing networks that have already been designed and therefore cannot be used in the synthesis stage of design. They present a new controllability index for HEN to choose the best control scheme that does not depend on control strategy or manipulated

variables. Westphalen *et al.* [11] claim that this tool will enable process engineers to include process control issues at an early stage of the conceptual design.

Mathisen *et al.* [12, 13, 14, 15] studied different controllability measures, suggested several optimization problems and proposed to take controllability into account by adding control related constraints to the problem formulation. They concluded that all the critical targets of designs can be controlled by either the addition of utility streams, or by placing bypasses. They presented heuristics for bypass placement, selection of manipulated variables and pairing between controlled variables and manipulated variables.

Given a set of resiliency target constraints, Konukman *et al.* [16] proposed a new method for the retrofit design of a HEN at minimum cost satisfying those targets. They define a Design Resiliency Index (DRI) which indicates the maximum allowable deviation of magnitude in both directions that are caused by disturbances that causes the controllable variables to move away from their set points. The retrofit design they obtained was through the formulation of a single constrained nonlinear optimization problem that provides the individual heat exchanger areas and bypass fractions which minimize the annualized cost of a given HEN structure. The retrofit design resulting from this analysis is claimed to satisfy the target temperatures with a set of disturbances predefined in all possible directions.

Yang *et al.* [17] introduced a modeling approach to quantify disturbance projection in heat exchanger networks, mass exchanger networks, and distillation column networks at steady-state level based on first principles. The model can be used to estimate the maximum deviation of system outputs when it experiences the worst combination of various types of disturbances. The model is linear and applicable to networks of various complexities. But this model approach does not include terms representing feasibility and controllability. Yan *et al.* [18] further extended this model to include both disturbance propagation and control; the new model characterizes the system under control and economic constraints. The model is embedded into an iterative design procedure to produce optimal locations and nominal fractions of stream bypasses that have a minimized effect on the capital cost. The model also suggests the most controllable design scheme by the use of RGA analysis to non-squared systems.

Lersbamrungsuk *et al.* [19] proposed a systematic procedure to find a control scheme of heat exchanger networks that obey optimal operations ensuring all controlled temperatures are kept at their target values and utility cost is minimized. A degree of freedom analysis was used to identify whether the operation is structurally feasible and whether utility cost can be minimized. They formulated a linear programming problem that implies that optimal operations is an active constraint control problem, and was used to find the optimum control scheme.

1.3 Research Objectives

For each process there is a certain acceptable range of heat recovery, economics and controllability which the process has to operate within. The overlap between heat recovery, economics and controllability for heat exchanger networks is shown in Figure 1.1. Each circle represents the acceptable ranges of each objective; the green shaded area represents a design that satisfies all three objectives.

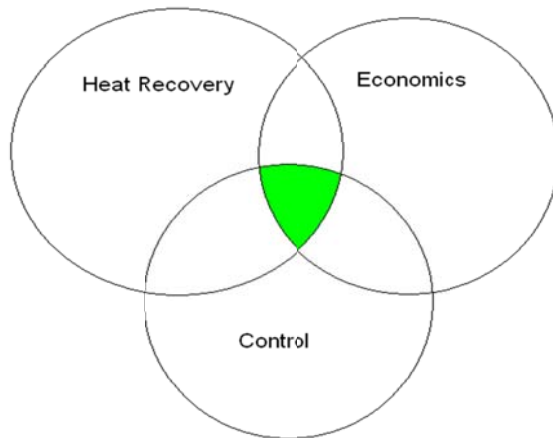


Figure 1.1: The overlap between heat recovery, economics and control for HEN.

The objective of this research is to develop a framework for designing heat exchanger networks, which address tradeoff between the three design objectives of heat recovery, economics and controllability. The framework will consist of a number of quick and easy-to-follow steps to design heat exchanger networks that satisfying the heat

recovery targets of the system, while optimizing its economics and fulfilling both the steady state and dynamic aspects of control. The results shall be proven, verified and judged against other well established methods of heat exchanger network design.

This research will allow process engineers working on the conceptual design phase of projects to design heat exchanger networks that are not only heat efficient and economical, but also controllable. It also aims to improve the existing heat integrated designs to make them more controllable without sacrificing the economics of the system.

1.4 Structure of the Report

This thesis is divided into five chapters. Chapter 1 introduces the research topic and includes the problem statement, the research objective and the literature review. The second chapter outlines the planned research methodology. Chapter 3 and 4 are considered as the heart of this research. In Chapter 3 the framework is formulated using analyses of heat integration, economics and steady state control; additionally the framework is applied to a case study and compared to the work of other researchers in the same field applied to the same case study. Chapter 4 studies the case study further in terms of dynamic control and exergy. The final chapter highlights the findings of the research by summarizing the framework, and sheds light on some recommendations for taking the research one step further.

Chapter 2: Research Methodology

During the course of this research, heat exchanger networks were studied using three types of analyses. First, the heat exchanger network is analyzed for the effectiveness of its heat recovery, then economically analyzed and lastly, analyzed for its extent of controllability.

2.1 Heat Integration Analysis

Heat integration methods are used to match hot and cold streams in heat exchanger networks to ensure the system achieves its maximum internal heat recovery while maintaining its economics at a minimum. There are two well-known methods of heat integration, Pinch Design and Superstructure Design.

2.1.1 Pinch Design

Pinch design is a heuristic approach based on calculating the maximum energy recovery targets of a heat exchanger network, and achieves the calculated targets by matching the hot and cold streams through a series of steps [1, 2].

The process data is represented as a set of energy streams, that are functions of mass flow rates, heat capacities, heat loads and inlet and outlet temperatures and are presented in what is called a temperature interval diagram, as shown in Figure 2.1.

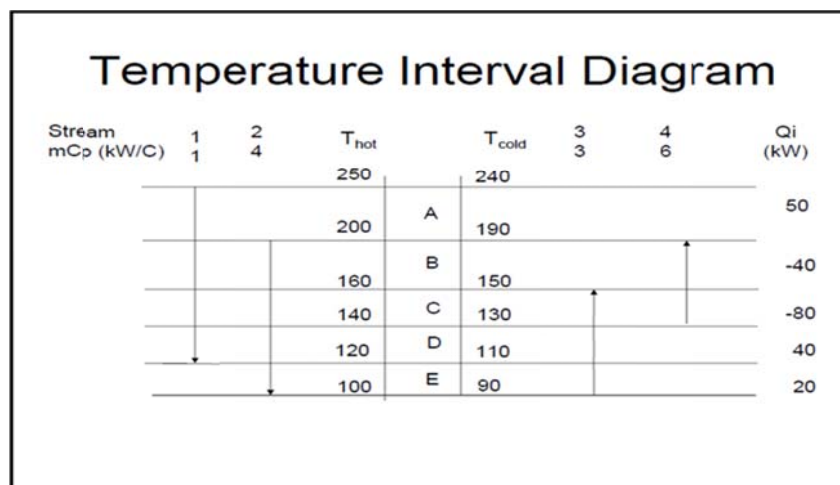


Figure 2.1: Sample temperature interval diagram [3].

These data are combined for all the streams in the plant to find the Maximum Energy Recovery, in other words, the minimum hot and cold utilities needed to satisfy all targets. Maximum Energy Recovery targets are found by using temperature interval diagrams and composite curves. A composite diagram is simply a temperature versus enthalpy diagram as shown in Figure 2.2.

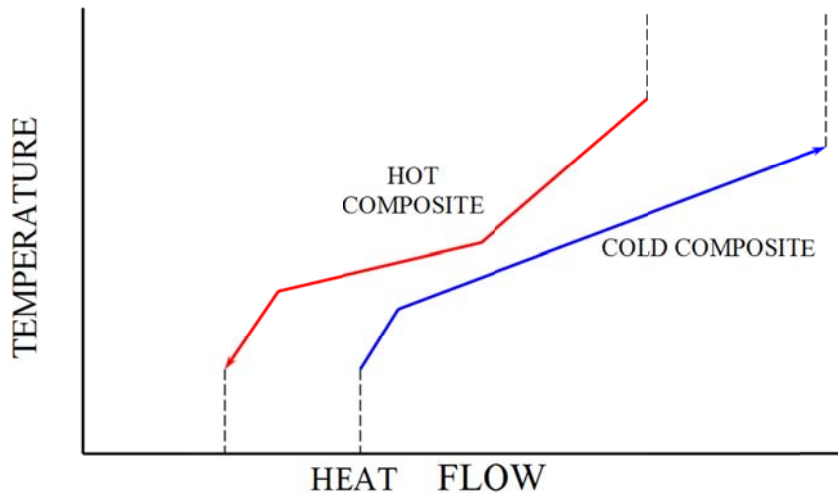


Figure 2.2: Sample composite diagram [20].

Composite curves are generated from the data for all the streams in the temperature interval diagram. Two separate curves are generated, one combining all hot streams (releasing heat) and the other combining all cold streams (requiring heat). The pinch point is the point of closest approach between the hot and cold composite curves. The pinch point has a hot stream pinch temperature and a cold stream pinch temperature; the difference between both pinch temperatures is the minimum approach temperature (ΔT_{\min}). The design is most constrained at the pinch point. Therefore, design, stream matching and heat exchanger placement, which are made to recover heat between hot and cold streams, starts at this point. Pinch Analysis proceeds in two separate designs, one design for all hot and cold streams above the pinch point and the other for those below the pinch point. Both designs are then integrated to come up with a final design for the network. Hot and cold utilities are placed when required by the design. Hot utilities are added to meet cold temperature targets and should not be used above the pinch. Cold utilities are added to meet hot temperature targets and should not be used below the

pinch. The total use of the utilities should not exceed what has been set by MER targets for the design to be efficient and feasible [3, 4, 5].

2.1.2 Superstructure Design

The Superstructure approach includes all heat exchanger network matching options between hot and cold streams; then through optimization, the unnecessary features of the design are removed [4]. By employing this method, the costs of each heat exchanger can be modeled by a linear equation that includes factors of area, duty, as well as inlet and outlet temperatures. The optimization is first simplified to a Mixed Integer Linear Programming (MILP) where the objective function is defined as the sum of all the linear equations of each heat exchanger. The network is then subjected to Mixed Integer Non-Linear Programming (MINLP) to allow for other features to be added, such as parallel or series configurations. The most economic structure will be chosen to serve as the optimum superstructure design [4].

2.1.3 Aspen HX-Net

The heat integration analysis tool used to analyze the efficiency aspects of the heat exchanger networks is Aspen HX-Net [21]. Aspen HX-Net is a conceptual design tool that provides an easy environment for performing optimal heat exchanger network design. It allows the user to calculate energy and capital investment targets of heat exchanger networks and enables the user to develop and/or to improve a heat integrated design in order to reduce operating costs, capital costs, to maximize the heat recovery of the design, and to minimize energy related emissions. Aspen HX-Net provides the tools for performing process optimization while allowing the user to connect to other process simulators such as Aspen HYSYS, and gives both graphical and algorithmic methods of calculation. The main advantage of Aspen HX-Net is that it allows the user to design the heat exchanger network according to the user's own analysis, experience or preference. It can also generate various design alternatives of the same heat exchanger network without the interference of the user. The designer can then choose amongst his/her design and the

Aspen HX-Net's design alternatives to formulate the most optimal design that maximizes the heat recovery of the system, uses the minimum amount of utilities and therefore minimizes costs. The interface of Aspen HX-Net is shown in Figure 2.3 [21].

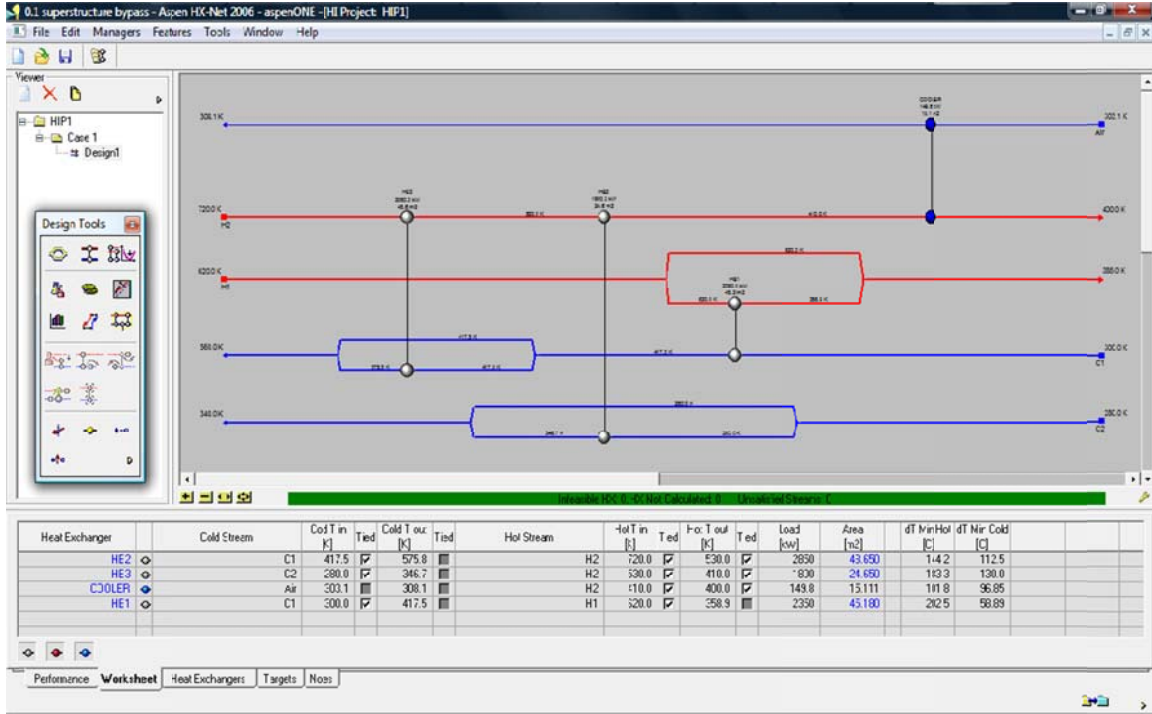


Figure 2.3: Snapshot of Aspen HX-Net interface [21].

Aspen HX-Net is able to calculate the capital cost, cost of utilities, operating costs and the total cost of the heat exchanger network. The capital cost is calculated using equation 2.1, which takes into consideration the areas and number of shells of the heat exchangers.

$$\text{Capital Cost Index (\$)} = a + \left[b \times \left(\left(\frac{\text{Heat Exchanger Area}}{\text{Number of Shells}} \right)^c \right) \times \text{Number of shells} \right] \quad (2.1)$$

where a, b and c are heat exchanger capital cost index parameters; Aspen HX-Net provides a default set of economic parameters for a typical heat exchanger. The parameters can be reset to values that the user specified according to their design expertise and best engineering practices. Aspen HX-Net has a database of utility data that enables it to calculate accurately the cost of utilities and the operating costs of any heat

exchanger network; it also enables the user to enter any additional utility that is not incorporated in the database. The total cost of the heat exchanger network takes into consideration an annualization factor which includes the Rate of Return (ROR) in percentage and the Plant Life (PL) in years of the network. The Annualization Factor is calculated using equation 2.2.

$$\text{Annualization Factor} = \frac{\left(\frac{1+\text{ROR}}{100}\right)^{\text{PL}}}{\text{PL}} \quad (2.2)$$

2.2 Controllability Analysis

Once the heat exchanger network is designed and optimized to attain the optimum heat recovery and cost, control design methods are applied to achieve all three objectives of the design: heat recovery, economics and control.

Heat exchanger networks use stream flow rates to control target temperatures. Two challenges arise while attempting to reach a well-controlled design. The first challenge is to allow the system to be controllable i.e. to ensure that the system has enough manipulated variables to control the controlled variables. The controlled variables of heat exchanger networks are the target temperatures while the manipulated variables are stream flow rates. Bypass streams and valves can be used to manipulate the stream flow rates. The challenge arises in the proper selection of the bypass streams and fractions to ensure that controllability is attained while not affecting the heat recovery or the economics of the process. This is achieved by various optimization methods, some using linear or nonlinear programming and others using different types of simulators.

The second challenge is pairing the controlled and manipulated variables together. This is done through steady state Relative Gain Array (RGA) and Singular Value Decomposition (SVD) analyses [9, 10, 21].

2.2.1 Relative Gain Array (RGA) Analysis

The RGA is a dimensionless measure of the interactions between control loops. The RGA is obtained from the Gain Array or the K matrix representing the steady state gain matrix of the system under study through equation 2.3 [22].

$$RGA_{i,j} = [K^{-1}]_{ij}^T \cdot K_{ij} \quad (2.3)$$

where K is the steady state gain matrix calculated as the ratio of difference in the controlled variable to the difference in manipulated variable.

The pairing of controlled variables and manipulated variables based on the RGA analysis is illustrated by the following example. K here represents the steady state gain matrix of a certain process:

$$K = \begin{bmatrix} 160 & -30 & -40 \\ 0 & 30 & -40 \\ 0 & 20 & 0 \end{bmatrix}$$

Substituting the K matrix into the equation 2.3 gives the RGA matrix as follows:

$$RGA = \left. \begin{array}{ccc} \text{Manipulated Variables} \\ y_1, & y_2, & y_3 \\ \left[\begin{array}{ccc} 1 & 0 & 0 \\ 0 & 0 & 1 \\ 0 & 1 & 0 \end{array} \right] & & \\ \left. \vphantom{\left[\begin{array}{ccc} 1 & 0 & 0 \\ 0 & 0 & 1 \\ 0 & 1 & 0 \end{array} \right]} \right\} \begin{array}{l} \text{Controlled Variables} \\ u_1, \\ u_2, \\ u_3 \end{array} \end{array} \right\}$$

The matching between the manipulated and the controlled variables is determined by choosing for each j^{th} column of controlled variable the i^{th} row of manipulated variables which has the element nearest to 1. Accordingly y_1 is matched with u_1 , y_2 is matched with u_3 and y_3 is matched with u_2 . The Condition Number (CN) of the RGA matrix is calculated as follows. [22]

$$CN = \frac{\sigma_1}{\sigma_2} \quad (2.4)$$

where

$$\sigma_1 = \sqrt{\alpha_1} \quad (2.5)$$

$$\sigma_2 = \sqrt{\alpha_2} \quad (2.6)$$

α_1 is the highest Eigenvalue of the $K \cdot K^T$ matrix

α_2 is the lowest Eigenvalue of the $K \cdot K^T$ matrix

The pairing with the lowest CN is the most robust and best conditioned pairing. If the RGA analysis is inconclusive, i.e. when more than one pairing has similar RGA CN, the SVD analysis is applied to choose among the best pairing indicated by RGA results.

2.2.2 Singular Value Decomposition (SVD) Analysis

The SVD analysis provides quantitative information about the controllability, sensor location and controller pairing. It indicates the controller pairings with the least open-loop interaction between controlled variables and manipulated variables. The SVD matrices are found according to equation 2.7. [22]

$$K_x = USV \quad (2.7)$$

where

K_x is the $n \times m$ square Gain Array matrix

U is an orthogonal array whose columns are singular left vectors

S is a diagonal array whose scalars are the Eigenvalues in decreasing order

V is an orthogonal array whose columns are singular right vectors

The U matrix is determined by solving equations 2.8 and 2.9 ... etc.

$$(K \cdot K^T - P_1) \cdot U_1 = 0 \quad (2.8)$$

$$(K \cdot K^T - P_2) \cdot U_2 = 0 \dots \dots \quad (2.9)$$

where

$P_1, P_2 \dots$ etc. are the Eigenvalues of the matrix $K \cdot K^T$

$U_1, U_2 \dots$ etc. are the columns of the U matrix

Similarly the V matrix is determined by solving equations 2.10 and 2.11 ... etc.

$$(K \cdot K^T - P_1) \cdot V_1 = 0 \quad (2.10)$$

$$(K \cdot K^T - P_2) \cdot V_2 = 0 \dots\dots\dots (2.11)$$

where

$V_1, V_2 \dots$ etc. are the columns of the V matrix

After determining the U and V matrices, the S matrix can be calculated through equation 2.7. The best pairing choice between controlled variables and manipulated variables that assures the least controller interactions is done by matching the largest magnitude element of the U1 vector (associated with the controlled variables) with the largest magnitude of the V1 vector (associated with the manipulated variable) without any regard to the signs of these values. Vectors U2, U3...etc. are matched with vectors V2, V3...etc. in the same way. This procedure continues until every controlled variable is paired with its corresponding manipulated variable. A condition number is also calculated for SVD matrices through equation 2.12; the pairing with the lowest CN is the most robust and best conditioned pairing. [22]

$$CN = \frac{\beta_1}{\beta_2} \quad (2.12)$$

where

β_1 is the highest diagonal Eigenvalue of the S matrix

β_2 is the lowest diagonal Eigenvalue of the S matrix

The first controllability analysis will be applied to a heat exchanger network that is designed by both pinch and superstructure approaches. The heat recovery, and economical and controllability results of each design will be considered together to draw a conclusion on the best design approach.

Chapter 3: Framework Development and Case Study Application

This chapter presents a number of analyses leading to the formulation of the methodological framework for design of HENs that achieve the objectives of optimized heat recovery, economics and controllability. First, a heat integration analysis is performed, comparing the two heat integration methods of Pinch and Superstructure in terms of heat recovery, economics and steady state control parameters. Second, a bypass placement analysis was performed to set the locations of the bypasses that will allow the control of the system, followed by a bypass fraction analysis. The application of this framework is shown via a case study.

3.1 The Proposed Framework

The proposed framework of designing heat exchanger networks consists of two simple steps. The first step is choosing the heat integration method to be used, which will take care of the heat recovery and economic targets. The second step is applying the steady state controllability parameters to ensure that design is controllable. Below is the outline of the proposed framework. In the next sections the framework is further discussed by applying it to a bench mark case study and is compared to the results of well-known researchers in the same field. The two steps are described in more detail as follows:

1. Analyze the most suitable heat integration method:

The first step to heat exchanger network design is to choose which heat integration method to apply. The choice lies between the heuristic approach of Pinch design or the computer based Superstructure design. The best way to choose is to run both designs and to select the design method that provides the best heat recovery results, the most minimized capital and utility costs and that holds the least inter-loop interactions.

2. Set the steady state control parameters

After the heat exchanger network is efficiently heat integrated, steady state control parameters are introduced to effectively control the network. Heat exchanger networks target temperatures are controlled by placing controllers on bypasses over the heat exchangers so as to be able to react to disturbances to the system by altering the flow rates of the streams through the bypasses. The steps below explain how the bypasses are placed, and what their bypass fractions will be.

The procedure below is a systematic method for providing the best bypass placements for HEN. It is based on the works of Mathisen *et al.* [14], Oliveira *et al.* [8] and Ogunnaike and Ray [22]

1. Calculate the possible number of bypass scenarios for the given HEN:

$$\text{Number of Bypass Scenarios} = 2^{N_{\text{byp}}} \left(\frac{N_{\text{hx}}!}{N_{\text{byp}}!(N_{\text{hx}} - N_{\text{byp}})!} \right) \quad (3.1)$$

where N_{hx} is the number of heat exchangers and N_{byp} is the number of bypasses to be placed. [14]

2. Identify and list all possible scenarios following step 1

The notation that will be followed is as follows e.g.: 1H2H3C. The HEN has 3 HEs, and bypasses are placed on

- The hot side of HE1
- The hot side of HE2
- The cold side of HE3

3. Draw a schematic diagram of each bypass scenario, if needed.

4. Identify the CVs and MVs for each scenario. [8, 21]

The above steps to list all the possible bypass scenarios. The following steps eliminate some of the scenarios to eventually come up with the preferred scenario.

5. Discard scenarios with both output temperatures of one heat exchanger set as controlled variables. [14]

Setting controllers on both outputs of the heat exchanger forces constant alterations of the MVs trying to satisfy both outputs, making the design very hard to stabilize and control.

6. Discard scenarios with bypasses on heat exchangers that have more than two paths to the output. [14]

Bypass placement scenarios that have two or more units between the CV and the MV tend to be ineffective, as the MV loses its magnitude through the paths, and because of no direct effect on the CV.

7. Prefer scenarios with bypasses that have a direct effect on the output, i.e. scenarios where the bypass is placed on the last HE, nearest to the output / target temperature. [14]

8. Prefer scenarios with bypasses that have a large effect on only one output. [14]

9. After eliminating a number of the bypass scenarios, decide on the most controllable scenario by doing the following [8, 21]:

- I. Simulate each scenario
- II. Perform RGA analysis on each scenario
- III. Perform SVD analysis on each scenario

The bypass placement analysis stated above drives the HEN under study to be the best controllable, economic and heat effective HEN.

After placing the bypass placements, the bypass fractions need to be set. According to Mathisen et al. [14], it is safe to assume that any bypass fraction ranging up to 0.1 of the streams is acceptable, as it does not affect much the controllability measures of HEN. In the following sections this claim is verified through extensive economic and controllability analyses. The claim is proven to be true and results of the analyses additionally show that the cost impacts for bypasses ranging up to 0.1 are considered minimal.

The designed HEN is analyzed dynamically to study how well the system rejects to disturbance that are introduced to the system which is explained in further detail in the next chapter. Figures 3.1 - 3.3, flowcharts for the proposed framework are illustrated through a number of easy to follow flow charts.

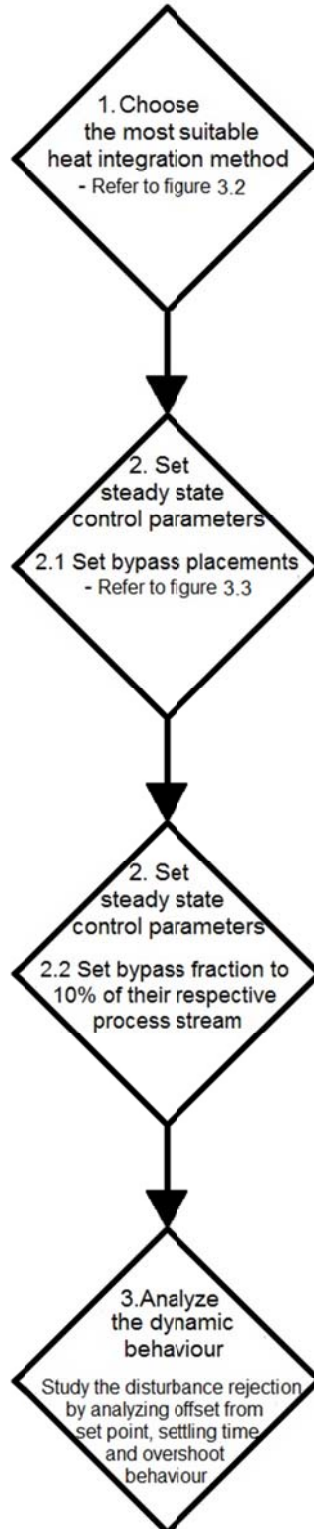
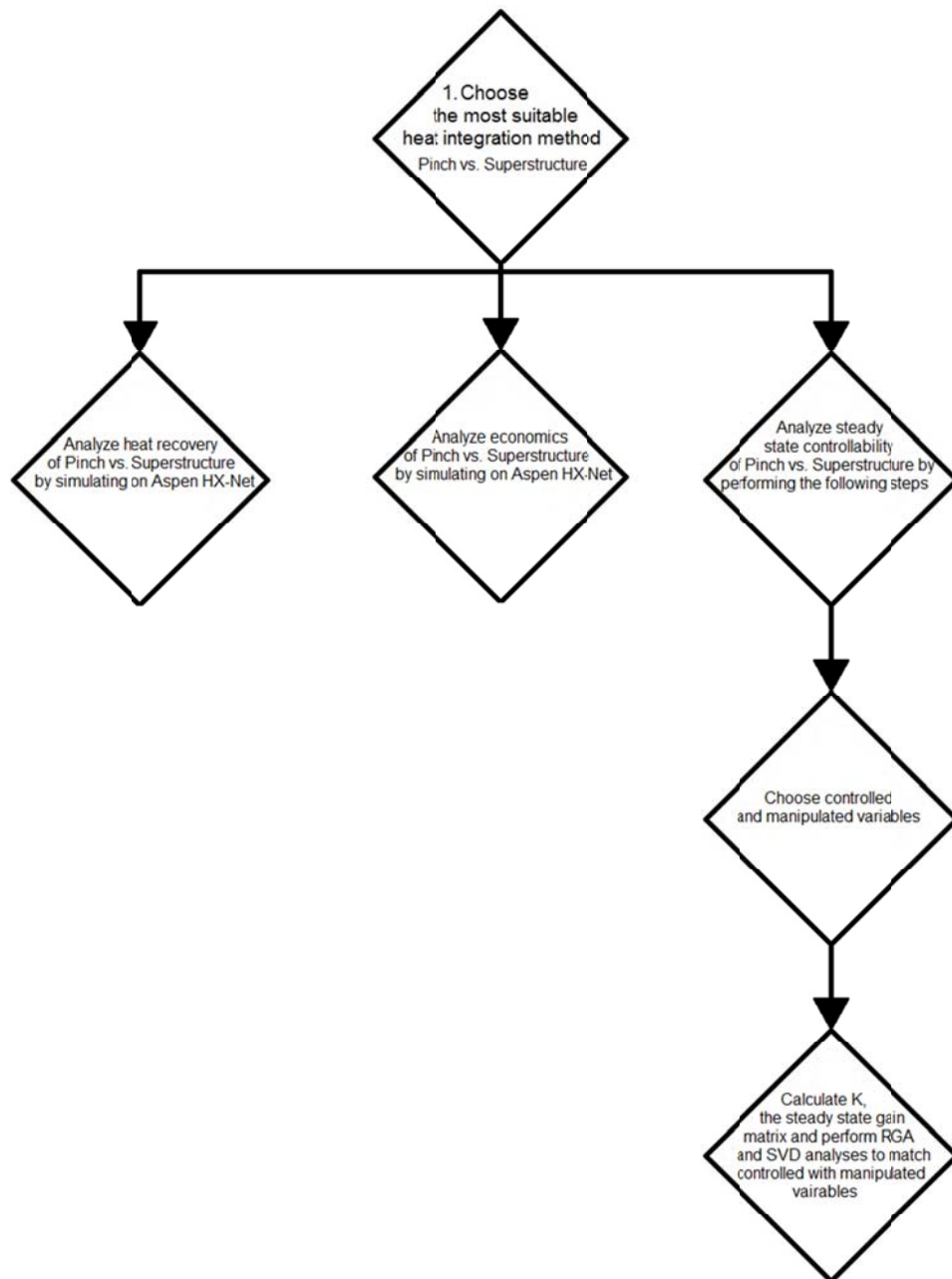


Figure 3.1: General flow chart of the proposed framework



Choose the heat integration method that gives better results of heat recovery, economics and steady state controllability parameters

Figure 3.2: The proposed framework; choosing the best heat integration method flowchart

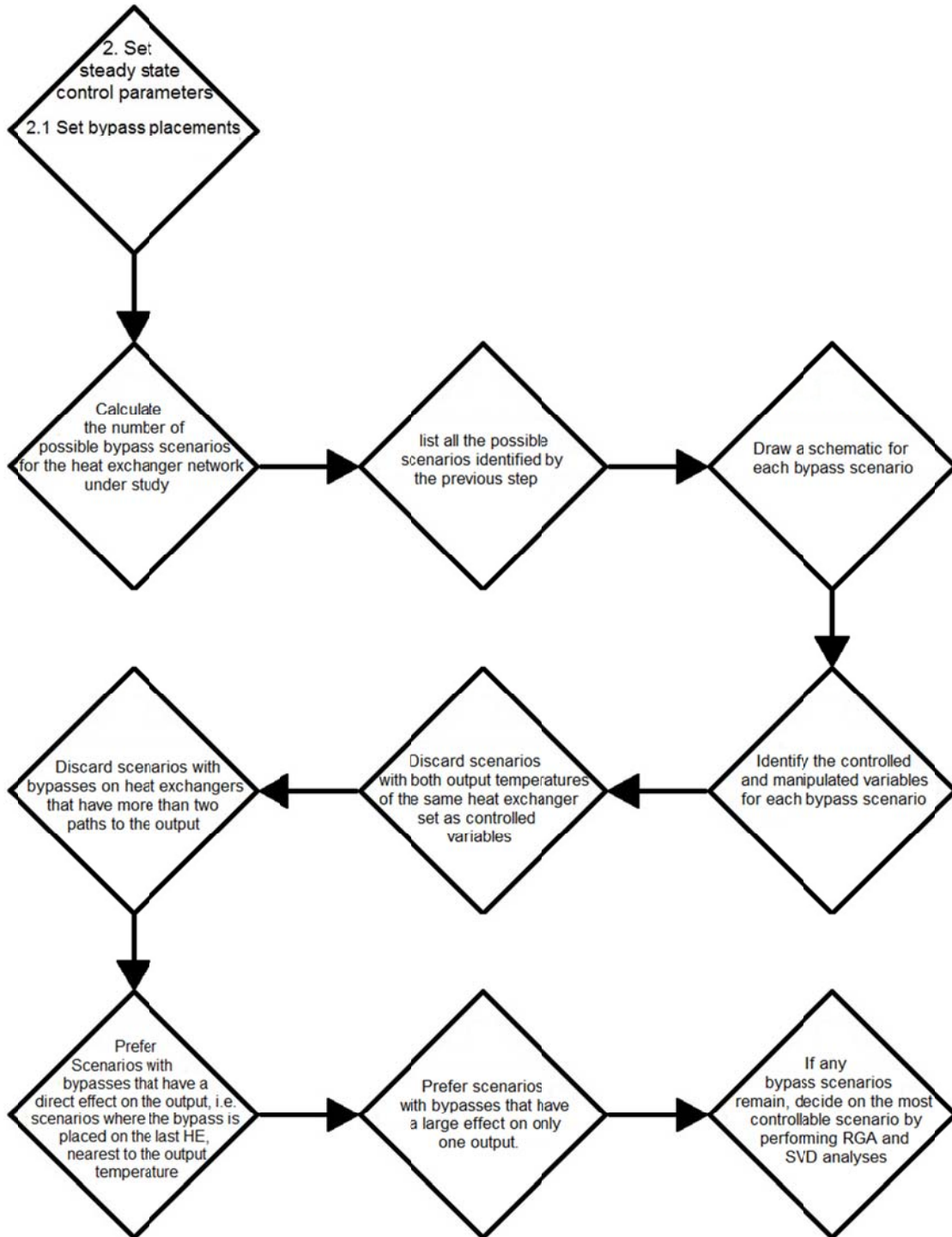


Figure 3.3: The proposed framework; choosing the bypass placements flowchart

3.2 The Case Study

Table 3.1 defines the heat exchanger network under study. The case study is simple, with limited constraints, and has been studied by various investigators to provide a basis for comparison and validation of results.

Table 3.1: Heat exchanger network under study

Stream	T _{in} (K)	T _{out} (K)	MCP (W/K)	Heat Transfer Coefficient (kW/m ² K)
H1	620	385	10000	1
H2	720	400	15000	1
C1	300	560	20000	1
C2	280	340	30000	1

Konukman *et al.* [16] used this case study to propose a new method of HEN design that satisfies a set of resiliency target constraints at minimum capital costs. Uzturk and Arkam [23] performed their own bypass design for the same HEN. Considering the same case study, Yang *et al.* [15] introduced a modeling approach to quantify disturbance projection in heat exchanger networks, mass exchanger networks and distillation column networks at steady state level. The model was used to estimate the maximum deviation of system outputs when it experiences the worst combination of various types of disturbances. This study was extended by Yan *et al.* [18] to include both disturbance propagation and control. The authors used the same HEN under study to develop an iterative design procedure to produce optimal locations and nominal fractions of stream bypasses that have a minimized effect on the capital cost. The model also suggests the most controllable design scheme is in line with the results of RGA analysis to non-squared systems. These studies performed on the same case study hold a paranormal importance for the purpose of comparison of results to the framework proposed in this research.

3.3 Results and Discussion

The proposed framework steps of section 3.1 and Figures 3.1 to 3.3 are applied to the bench mark case study of section 3.2 in this section.

3.3.1 Analyzing The Most Suitable Heat Integration Method, Pinch vs. Superstructure

Konukman *et al.* [16] studied the same HEN using two different synthesis algorithms to obtain two different heat integrated networks. The first solution shown in Figure 3.4 follows Yee and Grossman's [24] superstructure approach, based on Mixed Integer Linear and Non-Linear Programming (MILP and MINLP) to reach the minimum annualized cost.

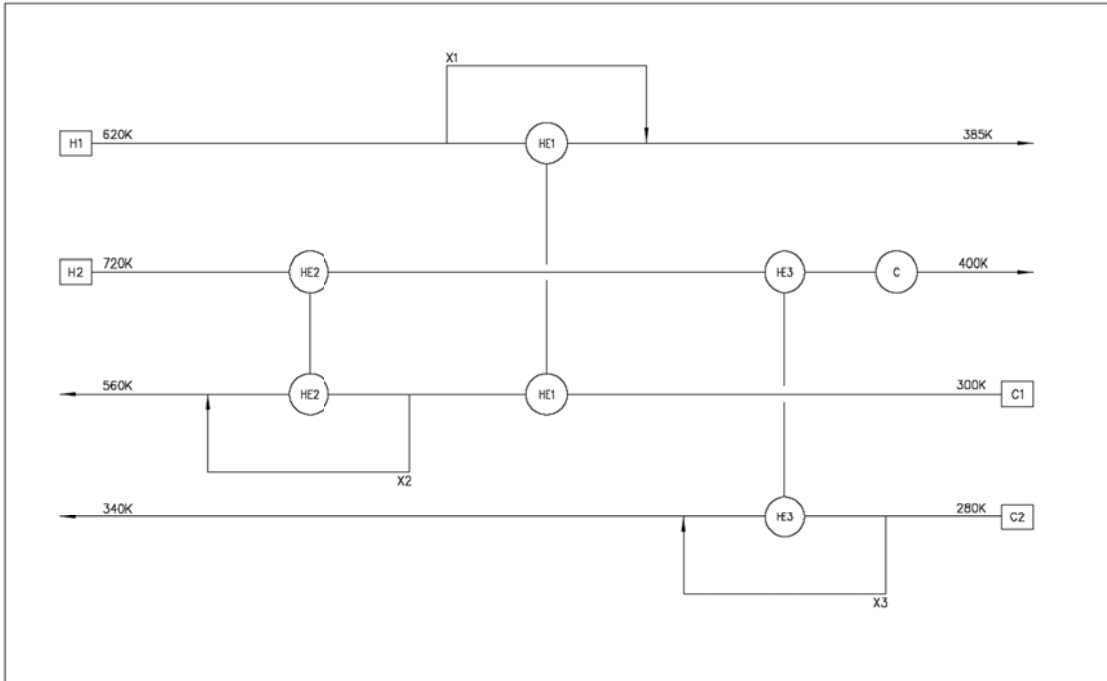


Figure 3.4: Grossman [24] *et al.*'s superstructure design of the HEN under study done by Konukman *et al.* [16].

Konukman *et al.* 's[16] second solution shown in Figure 3.5 follows Linhoff *et al.*'s [1] method of pinch design, based on optimization of the heat recovery system to attain the design with a minimum annualized cost through systematic design steps.

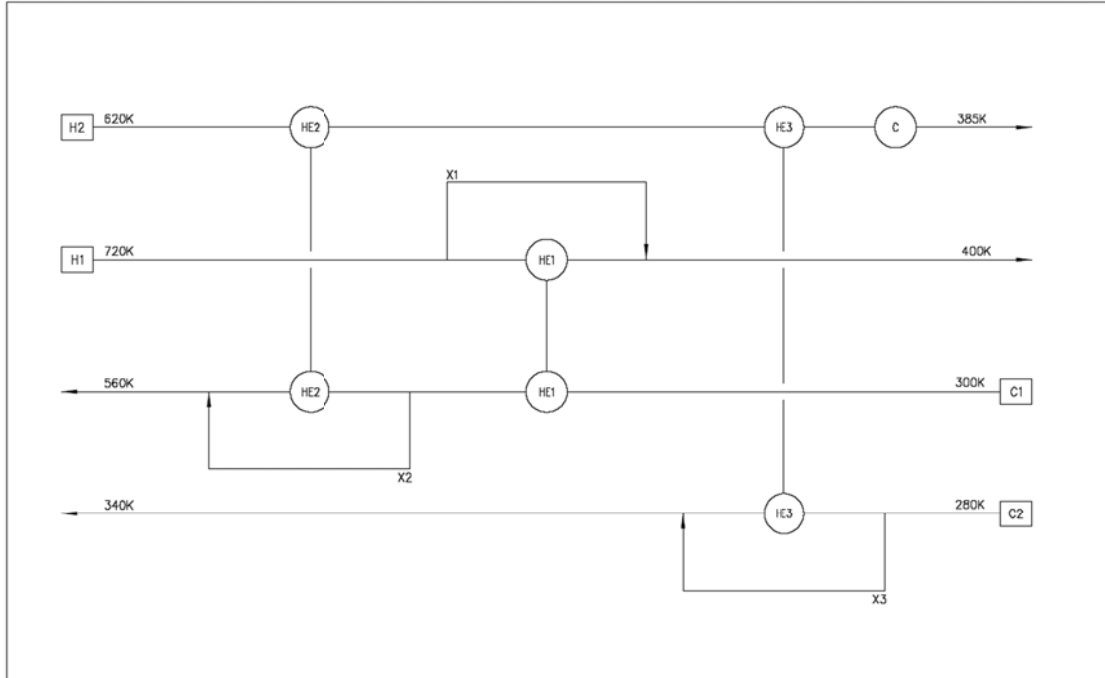


Figure 3.5: Linhoff *et al.*'s [1] pinch design of the HEN under study done by Konukman *et al.* [16].

Both heat exchanger networks which meet the maximum energy recovery targets, were designed with a minimum approach temperature of 10 K and contain three heat exchangers and one cooler. The duty of the cooler is the same in both designs; the difference between both designs lies in the matches of the hot and cold streams and the heat duties of the three heat exchangers.

Konukman *et al.* [16] obtained controllable designs of both heat exchanger network solutions by providing bypasses on the streams. This part of the research extends their research to define the heat integration method that best fits the HEN under study in terms of heat recovery, economics and controllability.

Konukman *et al.* [16] used bypass streams to control the system; however they did not specify the bypass fractions. For analysis purposes bypass fractions of 0.1 were assumed for all bypasses of the heat exchanger networks in each solution to proceed with the analysis. The chosen bypass fractions are justified in the bypass fractions analysis section. The system was analyzed using the following steps:

- Step 1: Simulating the Heat Exchanger Network
- Step 2: Choosing the Controlled and Manipulated Variables
- Step 3: Studying the Effect of each MV on the CVs.
- Step 4: Calculating the K matrix
- Step 5: Performing RGA and SVD Analyses

3.3.1.1 Design A: Superstructure Design with 0.1 Bypass Fractions

The first analysis is applied to Yee and Grossman's [24] solution shown in Figure 3.1 with a bypass fraction of 0.1 applied to all bypass streams. The heat exchanger network is analyzed through the following steps:

Step 1: Simulating the Heat Exchanger Network

The superstructure design is first simulated on Aspen HX-Net to obtain the energy targets, perform matching between the hot and cold streams and verify the areas, duties and capital cost of the system. The Aspen HX-Net simulation of the superstructure design is shown in Figure 3.6. The areas of the heat exchanger are kept constant in the simulation except for the area of the cooler which is left variable to change according to the inlet temperature (stream H2 entering the cooler) in order to reach the target temperature of the stream. The fixed heat exchanger areas simulation represents a real heat exchanger network where changes in the system can be monitored due to any change in the manipulated variables or any disturbances variables. The areas and duties of Design A are shown in Table 3.2. The superstructure design satisfies the heat recovery targets of the system; otherwise the simulation would not converge. Aspen HX-Net provides the heat recovery and cost results. The remaining steps will provide the controllability analysis of the system.

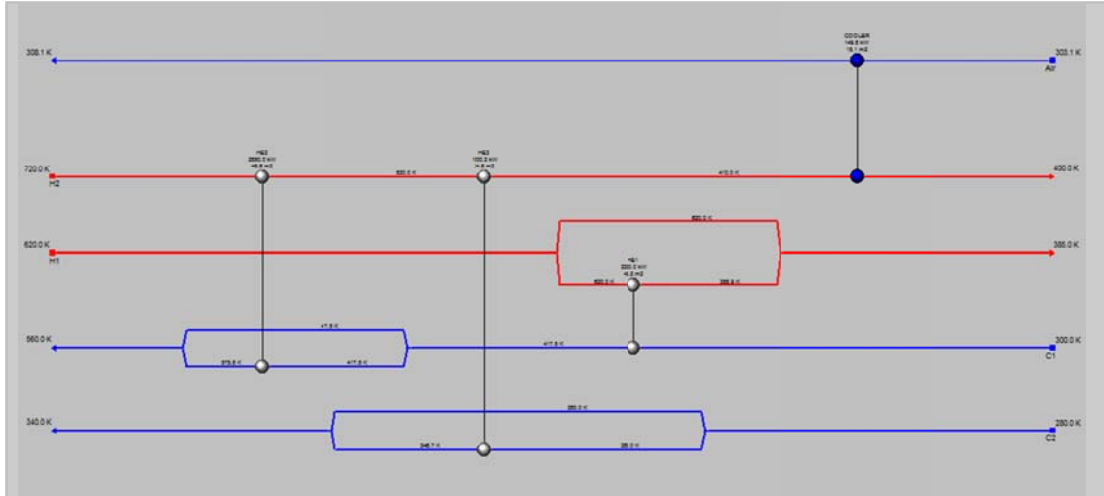


Figure 3.6 Snapshot of Aspen HX-Net simulation of Design A [21].

Table 3.2: Heat exchanger areas and duties of design A

	Area (m ²)	Duty (kW)
HE 1	45.2	2350
HE 2	48.7	2850
HE 3	24.7	1800
COOLER	15.1	150

Step 2: Choosing Controlled and Manipulated Variables

An important step of the controllability analysis is to define the controlled and manipulated variables of the design. The controlled and manipulated variables will then be paired together to form the control scheme of the system. The target temperatures of the hot and cold streams leaving the heat exchanger network are chosen to be the controlled variables, except for stream H2, where the target temperature is chosen to be the temperature after heat exchanger 3, just before the cooler. The cooler duty and area are not kept constant; they change according to the cooler inlet temperature of the cooler to achieve the target temperature of stream H2. The controlled variables are listed in Table 3.3. The manipulated variables are chosen to be the bypasses of the streams, and

are shown in Table 3.4. The bypass streams allow the heat exchanger network to be controllable and robust to disturbances from the system.

Table 3.3: Controlled variables of Design A

Stream	Description	Target Temperature (K)
T-H1	Outlet temperature of stream	385
T-H2	Outlet temperature from HE3 (before cooler)	410
T-C1	Outlet temperature of stream	560
T-C2	Outlet temperature of stream	340

Table 3.4: Manipulated variables of Design A

Manipulated Variable	Description
X1	Bypass fraction of stream H1 on HE1
X2	Bypass fraction of stream C1 on HE2
X3	Bypass fraction of stream C2 on HE3

Step 3: Studying the Effect of Each MV on the CVs

The objective of the controllability analysis is to provide matches between the controlled and the manipulated variables that result in the least interactions between the controllers, and therefore produces the best control scheme for the system. The interactions of the system are studied by changing the value of one manipulated variable at each instant while keeping the other two manipulated variables constant and monitoring the changes to the controlled variables. Each manipulated variable is increased by a value of 10%, therefore the bypass fraction of each stream will increase from a fraction of 0.1 to a fraction of 0.11 each time; i.e. first X1 will be set to 0.11 while X2 and X3 remain as 0.1, then X2 will be changed to 0.11 while setting X1 and X3 to 0.1 and finally X3 will be changed to 0.11 while X1 and X2 are set to 0.1. The new values of the controlled variables are given in Table 3.5.

Table 3.5: New values of CVs due to changes in MVs

	T-H1	T-H2	T-C1	T-C2
X1	386.6	409.7	559.6	339.9
X2	385	410.3	559.6	340.1
X3	385	410.2	560	339.9

Step 4: Calculating the K matrix

The results shown in Table 3.5 are used to calculate the Gain Array or the K matrix. Elements of the K matrix are calculated using equation 3.1 [22]

$$K_{ij} = \frac{\Delta CV_i}{\Delta MV_j} = \frac{CV_i - CV_{i,base}}{MV_j - MV_{j,base}} \quad (3.1)$$

where

CV_i is control variable i ,

$CV_{i,base}$ is control variable i in the base case,

MV_j is manipulated variable j ,

$MV_{j,base}$ is manipulated variable j in the base case,

The resulting Gain Array (K) is

$$K = \begin{pmatrix} 160 & -30 & -40 & -10 \\ 0 & 30 & -40 & 10 \\ 0 & 20 & 0 & -10 \end{pmatrix}$$

Step 5: Perform RGA and SVD Analyses

The K matrix is used to pair the controlled variables to the manipulated variables. This is done using the Relative Gain Array (RGA) analysis described earlier. Whenever the RGA analysis fails to indicate the best pairing, the Singular Value Decomposition (SVD) analysis is used. RGA can only be calculated for square K matrices. As the

controlled variables are more than the manipulated variables, the K matrix calculated in the previous step is not adequate since it is a non-square matrix. Therefore 3x3 square matrices will be defined from the K matrix to include all possible combination of CVs to MVs. Manipulated variables remain constant in all the K matrices, while changing the controlled variables in each matrix. Therefore, four different control structures are examined and synthesized. The first K matrix includes T-H1, T-H2 and T-C1 as controlled variables and the resulting K matrix is

$$K_1 = \begin{pmatrix} 160 & -30 & -40 \\ 0 & 30 & -40 \\ 0 & 20 & 0 \end{pmatrix}$$

The second K matrix includes T-H1, T-H2 and T-C1 as controlled variables; the resulting K matrix is

$$K_2 = \begin{pmatrix} 160 & -30 & -10 \\ 0 & 30 & 10 \\ 0 & 20 & -10 \end{pmatrix}$$

The third K matrix includes T-H1, T-C2 and T-C2 as controlled variables; the resulting K matrix is

$$K_3 = \begin{pmatrix} 160 & -40 & -10 \\ 0 & -40 & 10 \\ 0 & 0 & -10 \end{pmatrix}$$

The fourth and final K matrix includes T-H2, T-C2 and T-C2 as controlled variables; the resulting K matrix is

$$K_4 = \begin{pmatrix} -30 & -40 & -10 \\ 30 & -40 & 10 \\ 20 & 0 & -10 \end{pmatrix}$$

The RGA and SVD calculations are performed by MATLAB; sample MATLAB files are shown in Appendix I. The controllability analysis results of the superstructure design with bypass fractions of 0.1 (Design A) are shown in Table 3.6

Table 3.6: Controllability analysis results of Design A

Set of CVs & MVs	RGA Pairings	CN of RGA	SVD Pairings	CN of SVD
TH1, TH2, TC1 X1, X2, X3	TH1 – X1	1	TH1 – X1	11.3
	TH2 – X3		TH2 – X3	
	TC1 – X2		TC1 – X2	
TH1, TH2, TC2 X1, X2, X3	TH1 – X1	5	TH1 – X1	11.8
	TH2 – X2		TH2 – X2	
	TC2 – X3		TC2 – X3	
TH1, TC1, TC2 X1, X2, X3	TH1 – X1	1	TH1 – X1	17.2
	TC1 – X2		TC1 – X2	
	TC2 – X3		TC2 – X3	

The fourth set of CVs TH2, TC1 and TC2 produce inconclusive results of the pairings and therefore are discarded. According to RGA and SVD analyses TH1 – X1, TH2 – X3, TC1 – X2 pairings give a slightly better controllability than TH1 – X1, TC1 – X2, TC2 – X3 because of the lower SVD CN. However, we can consider the SVD CN difference as also inconclusive, as the difference has to be at least one order of magnitude so that it can be considered conclusive. Therefore we shall implement the third criterion which is the physical closeness of the controllers to the streams. In this case, TH1 – X1, TC1 – X2, TC2 – X3 is concluded to be the best chosen scenario. The cost of the heat exchanger network is based on a rate of return of 10% and a plant life of 5 years. Table 3.7 shows a summary of the best control scheme for Design A and Figure 3.7 shows the control scheme using the best pairing based on the results.

Table 3.7: Summary of the best control scheme results for Design A

Pairing	RGA CN	SVD CN	Capital Cost (\$)	Total Cost (\$/Year)	Total Area (m ²)
TH1 – X1 TC1 – X2 TC2 – X3	1	17.2	97,340	31,380	133.6

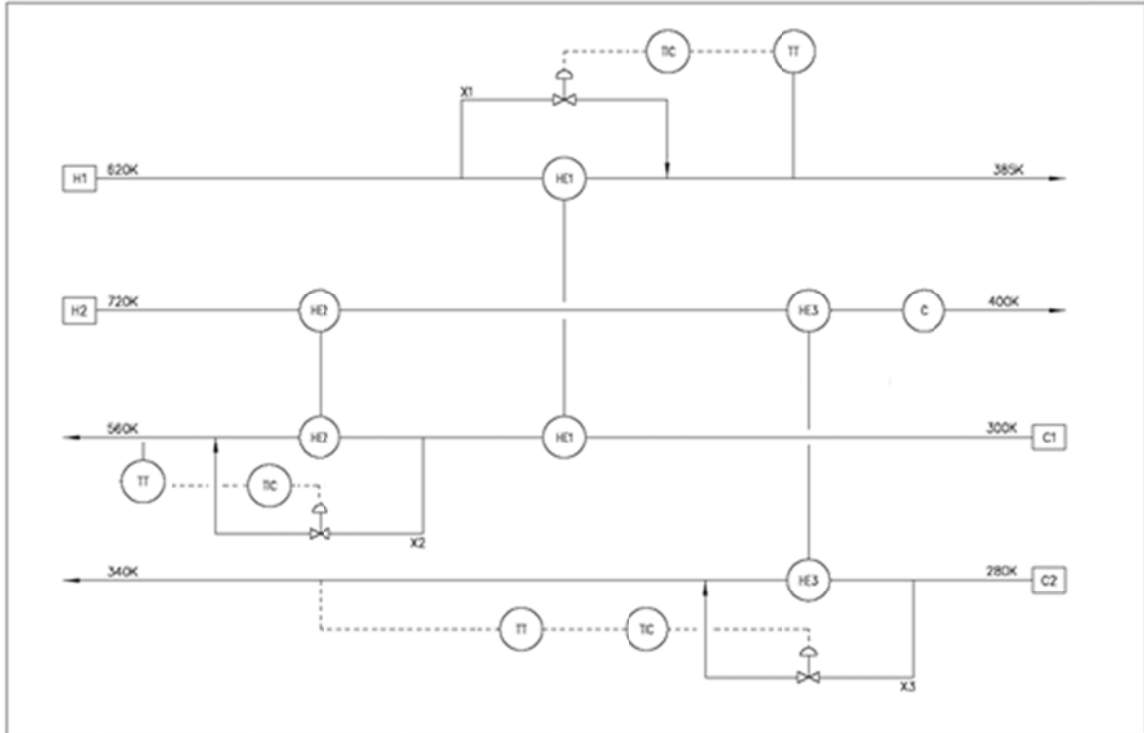


Figure 3.7: Best control scheme for Design A.

3.3.1.2 Design B: Pinch Design with 0.1 bypass fractions

The same design steps were applied to the pinch design with bypass fractions of 0.1 for the process stream H2, C1 and C2 (see Figure 3.5). The Pinch design satisfies the heat recovery targets of the system; otherwise the simulation would not converge. Aspen HX-Net provides the heat recovery and cost results; the remaining steps provide the controllability analysis of the system. The Aspen HX-Net simulation is shown in Figure 3.8 and the areas and duties of the heat exchangers are given Table 3.8.

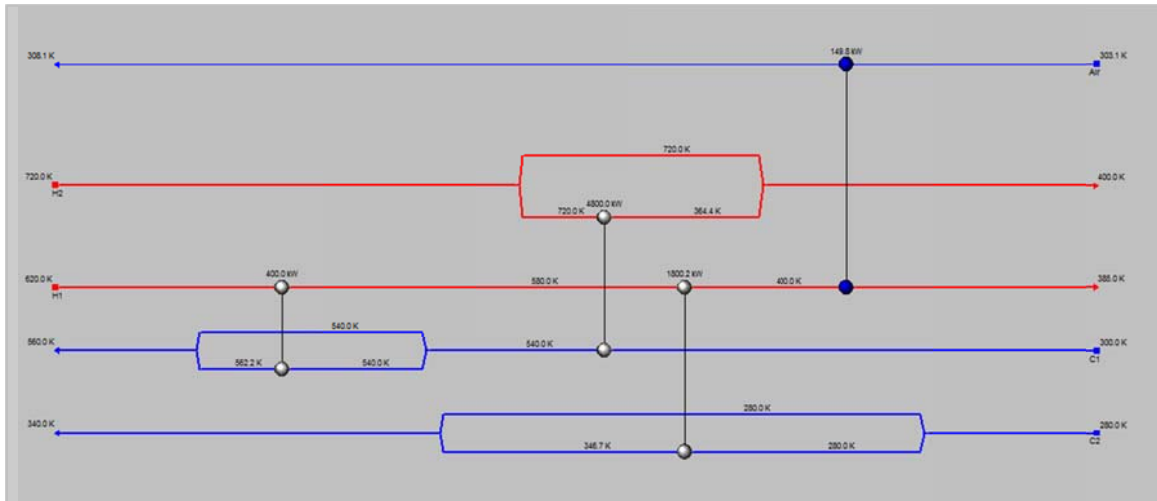


Figure 3.8: Aspen HX-Net simulation of Design B

Table 3.8: Heat exchanger areas and duties of Design B

	Area (m ²)	Duty (kW)
HE 1	99.4	4800
HE 2	17.8	400
HE 3	22.8	1800
COOLER	17.3	150

The controlled and manipulated variables are shown in Table 3.9 and Table 3.10, respectively.

Table 3.9: Controlled variables of design B

Stream	Description	Target Temperature (K)
T-H1	Temperature of outlet stream from HE3 (before cooler)	400
T-H2	Temperature of outlet stream	400
T-C1	Temperature of outlet stream	560
T-C2	Temperature of outlet stream	340

Table 3.10: Manipulated variables of Design B

Manipulated Variable	Description
X1	Bypass fraction of stream H2 entering HE1
X2	Bypass fraction of stream C1 entering HE2
X3	Bypass fraction of stream C2 entering HE3

The interactions of the system are studied by changing the value of one manipulated variable at each step while keeping the other two manipulated variables constant and monitoring the changes to the controlled variables. A 10% increase in each manipulated variable does not produce enough deviation in the controlled variables to be able to study the system interactions. Therefore each manipulated variable is increased by a value of 20% at a time. The new values of the controlled variables, due to the changes in the manipulated variables, are shown in Table 3.11.

Table 3.11: New values of CVs due to the changes in MVs of Design B

	T-H1	T-H2	T-C1	T-C2
X1	399.3	404.3	557.6	339.7
X2	400	400	559.9	340
X3	400.5	400	560	339.8

The resulting Gain Array or K matrix from the results shown in Table 3.11 is

$$K = \begin{pmatrix} -35 & 215 & -120 & -15 \\ 0 & 0 & -5 & 0 \\ 25 & 0 & 0 & -10 \end{pmatrix}$$

The K matrix is used to perform the RGA and SVD analyses, but since these analyses can only be applied to square matrices, 3x3 square matrices are extracted from the K matrix to include all possible combinations of CVs and MVs. As done before, manipulated variables remain the same as all are extracted from K matrices, while changing the controlled variables in each extracted matrix, which again results in four

control structures. The first extracted K_1 matrix includes T-H1, T-H2 and T-C1 as controlled variables.

$$K_1 = \begin{pmatrix} -35 & 215 & -120 \\ 0 & 0 & -5 \\ 25 & 0 & 0 \end{pmatrix}$$

The second extracted K_2 matrix includes T-H1, T-H2 and T-C1 as controlled variables.

$$K_2 = \begin{pmatrix} -35 & 215 & -15 \\ 0 & 0 & 0 \\ 25 & 0 & -10 \end{pmatrix}$$

The third extracted K_3 matrix includes T-H1, T-C2 and T-C2 as controlled variables.

$$K_3 = \begin{pmatrix} -35 & -120 & -15 \\ 0 & -5 & 0 \\ 25 & 0 & -10 \end{pmatrix}$$

The fourth and final K_4 matrix includes T-H2, T-C2 and T-C2 as controlled variables.

$$K_4 = \begin{pmatrix} 215 & -120 & -15 \\ 0 & -5 & 0 \\ 0 & 0 & -10 \end{pmatrix}$$

The RGA and SVD calculations are performed by MATLAB; sample MATLAB files are given in Appendix I. The controllability analysis results of the pinch design with bypass fractions of 0.1 (Design B) are shown in Table 3.12.

Table 3.12: Controllability analysis results for Design B

Set of CVs & MVs	RGA Pairings	CN of RGA	SVD Pairings	CN of SVD
TH1, TH2, TC1 X1, X2, X3	TH1 – X2 TH2 – X3 TC1 – X1	1	TH1 – X2 TH2 – X3 TC1 – X1	57.0
TH1, TC1, TC2 X1, X2, X3	TH1 – X3 TC1 – X2 TC2 – X1	29	TH1 – X2 TC1 – X3 TC2 – X1	115.4
TH2, TC1, TC2 X1, X2, X3	TH2 – X1 TC1 – X2 TC2 – X3	1	TH2 – X1 TC1 – X2 TC2 – X3	56.5

The second set of controlled variables TH1, TH2 and TC1 produces inconclusive results of the pairings and is therefore discarded. According to RGA and SVD analyses TH2 – X1, TC1 – X2, TC2 – X3 pairings structure gives better controllability than TH1 – X2, TH2 – X3, TC1 – X1 and meets the criterion of physical closeness of the controllers to the streams. Table 3.13 shows a summary of the best control scheme for Design B and Figure 3.9 shows the control scheme of the best pairing based on the results.

Table 3.13: Summary of best control scheme results for Design B

Pairing	RGA CN	SVD CN	Capital Cost (\$)	Total Cost (\$/Year)	Total Area (m ²)
TH2 – X1 TC1 – X2 TC2 – X3	1	56.5	105,100	33,870	157.3

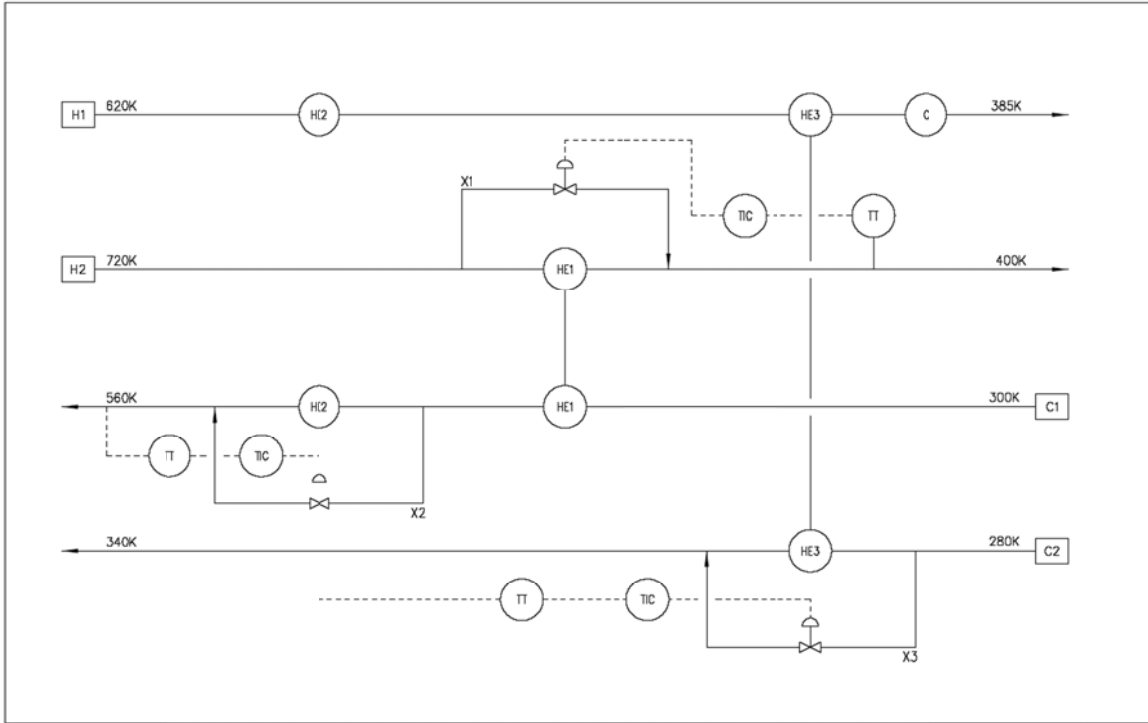


Figure 3.9: Best and chosen control scheme for Design B

A Comparison of the results of both designs is shown in Table 3.14.

Table 3.14: Summary of the best control schemes for each design

Design	Design Description	Pairing	RGA CN	SVD CN	Capital Cost (\$)	Total Area (m ²)
A	Superstructure bypass fraction=0.1	TH1 – X1 TC1 – X2 TC2 – X3	1	17.22	97,340	133.6
B	Pinch bypass fraction=0.1	TH2 – X1 TC1 – X2 TC2 – X3	1	56.51	105,100	157.3

Provided that both the superstructure and the pinch designs of the heat exchanger network achieve the maximum energy recovery targets, the results in Table 3.14 show that the superstructure design is more controllable and economical than the pinch design. The superstructure design is more economical with a capital cost of \$ 97,340 and more

controllable with an RGA CN of 1 and an SVD CN of 11.31. Since Superstructure design is better controlled than the Pinch design, it will be selected as the case study for the upcoming analyses.

3.3.2 Bypass Placement Analysis

The HEN under study is stripped of all its bypasses as per Konukman's [16] paper and is analyzed according to the steps mentioned in the prior section.

1. Indicate the possible number of bypass scenarios for the given HEN:

$$\text{Number of Bypass Scenarios} = 2^{N_{\text{byp}}} \left(\frac{N_{\text{hx}}!}{N_{\text{byp}}!(N_{\text{hx}} - N_{\text{byp}})!} \right) = 8 \quad (3.2)$$

where $N_{\text{hx}}=3$ and $N_{\text{byp}}=3$.

2. Identify and list all possible scenarios; the total number is obtained from step1:

- I. 1H2H3H
- II. 1H2H3C
- III. 1H2C3H
- IV. 1H2C3C
- V. 1C2H3H
- VI. 1C2H3C
- VII. 1C2C3H
- VIII. 1C2C3C

3. Draw a schematic diagram for each bypass scenario: not needed for this specific case

4. Identify CVs and MVs:

CVs: Target Temperatures of streams H1, C1 and C2

MVs: Bypass Streams

5. Discard scenarios with both output temperatures of one heat exchanger set as controlled variables:

Does not apply, as none of the listed scenarios have both of their outlets of a single heat exchanger set as controlled variables.

6. Discard scenarios with bypasses on heat exchangers that have two or more paths to the output:

All configurations with 2H can be discarded as there is a heat exchanger and a cooler between the bypass stream and the output temperature. The following scenarios are discarded:

- 1H2H3H
- 1H2H3C
- 1C2H3H
- 1C2H3C

Therefore we are left with the following eligible scenarios:

- 1H2C3H
- 1H2C3C
- 1C2C2H
- 1C2C3H

7. Prefer scenarios with bypasses that have a direct effect on the output:
out of the remaining eligible scenarios left only 1H2C3C has no paths between the bypass and the outlet.

Since the best scenario is identified in the 7th step, there is no need to go through the remaining steps. It is worth mentioning that this result is identical to Konukman *et al.*'s [16] bypass placements of the same HEN. The RGA, SVD and costing analysis of the 1H2C3C scheme has been analyzed as Design A of Table 3.14.

3.3.3 Bypass Fractions Analysis

Mathisen *et al.* [14] claimed the following: “*The different bypass alternatives (manipulated variables) are linearized with a nominal bypass fraction of 0.1% and scaled up to a constant bypass fraction of 10%. Note that most of the controllability measures are independent of the input scaling and thus not critically dependent on the exact values of the bypass fractions*”. They simply stated that bypass fractions in HENs ranging from 0.1% to 10% should not affect much the controllability measures of the HEN. Therefore it would be safe to assume a bypass fraction in the range 0.1% to 10% for analysis purposes, and this can be fine-tuned in a later stage when performing a rigorous optimization where disturbances and performance indicators of the controlled outputs are taken into consideration. Throughout the previous analyses, Mathisen *et al.*'s [14] above statement was considered as a heuristic, by setting all bypass fractions at 10%. Bypass fractions were set at the maximum of Mathisen *et al.*'s,[14] range to get the best controllability possible, as the system is better controlled with bigger bypass fractions, while not affecting much the cost of the system. In this section an analysis is performed considering the effects of both controllability and economics to changes in the bypass fractions to reconfirm Mathisen *et al.*'s [14] heuristic.

It is important to stress that the economical and the heat recovery targets of the HEN under study have already been satisfied in the heat integration analysis, and the controllability target has been already satisfied in the bypass placement analysis. The bypass fraction analysis is performed to only measure the effect of various bypass fractions on economics and controllability of the HEN. The purpose of the analysis is fine tuning the HEN, which is of less importance compared to the preceding analyses.

3.3.3.1 HEN Cost Effect of Bypass Fractions Ranging from 0.01 to 0.1

As mentioned in the previous section, the bypass placement option of 1H2C3C proved to be the best controllable combination. In this section, the HEN with 1H2C3C bypass placements undergoes an extensive study of a 1,000 scenarios of various bypass fractions combinations measuring the effect of the bypass fractions magnitude on the cost of the HEN. Using Aspen HX-Net the bypass fractions of the HEN under study (X1, X2

and X3) are all changed from 0.01 to 0.1 in intervals of 0.01 to make 1,000 different combinations, and Aspen HX-Net is used to calculate the corresponding capital cost of each. These costs are shown in USD (\$) in Tables 3.4.1 - 3.4.10.

The cost of the HEN increases proportionally with the increasing bypass fractions, as seen in Tables 3.15 - 3.24, where fixing any two bypass fractions and increasing the third increases the cost of the HEN. The heat exchanger network is originally designed to flow the majority of the flow rate through the heat exchangers while allowing a small portion of the flow rate to flow through the bypasses to allow for control against any disturbance rejections. The area of the heat exchangers is calculated based on the worst case scenario of the design. The worst case scenario is when the valve on the bypasses closes entirely, rerouting all the flow rate through the heat exchanger. In this case the heat exchanger has to cope with its originally designed flow rate in addition to the extra flow rate that is being re-routed from the bypass streams. Therefore the larger the bypass fractions are, the more flow rate the heat exchangers have to be designed for. In case of the worst case scenario, the larger the heat exchangers have to be and therefore the higher the costs.

As expected, the best economical bypass combination is the one with the smallest bypass fractions, where X_1, X_2 and $X_3 = 0.01$. The cost of this combination is 93,490 USD, and the cost for the chosen bypass fractions throughout this research is 97,349 USD. The difference in capital cost is not significant; it is less than 3,000 USD which is less than 4% of the total capital cost. Besides the fact that such small bypass fractions may not attain the controllability targets of the HEN, disturbances and performance indicators of the controlled outputs are not taken into consideration. This is purely an economical comparison that does not offer a substantial economical edge.

Table 3.15: HEN capital costs in USD with bypass fractions of X3=0.01 and X1 & X2 ranging from 0.01 to 0.1

X1\ X2	0.01	0.02	0.03	0.04	0.05	0.06	0.07	0.08	0.09	0.1
0.01	93,490	93,591	93,696	93,804	93,917	94,035	94,157	94,285	94,418	94,557
0.02	93,701	93,802	93,906	94,015	94,128	94,245	94,368	94,495	94,628	94,768
0.03	93,926	94,026	94,131	94,240	94,353	94,470	94,593	94,720	94,853	94,992
0.04	94,166	94,267	94,371	94,480	94,593	94,711	94,833	94,961	95,094	95,233
0.05	94,424	94,525	94,630	94,738	94,851	94,969	95,091	95,219	95,352	95,491
0.06	94,702	94,803	94,908	95,016	95,129	95,247	95,369	95,497	95,630	95,769
0.07	95,003	95,104	95,208	95,317	95,430	95,548	95,670	95,798	95,931	96,070
0.08	95,330	95,430	95,535	95,644	95,756	95,874	95,996	96,124	96,257	96,396
0.09	95,686	95,787	95,891	96,000	96,113	96,230	96,353	96,480	96,613	96,752
0.1	96,077	96,177	96,282	96,391	96,504	96,621	96,744	96,871	97,004	97,143

Table 3.16: HEN capital costs in USD with bypass fractions of X3=0.02 and X1 & X2 ranging from 0.01 to 0.1

X1\ X2	0.01	0.02	0.03	0.04	0.05	0.06	0.07	0.08	0.09	0.1
0.01	93,511	93,611	93,716	93,825	93,938	94,055	94,178	94,305	94,438	94,577
0.02	93,721	93,822	93,927	94,035	94,148	94,266	94,388	94,516	94,649	94,788
0.03	93,946	94,047	94,151	94,260	94,373	94,491	94,613	94,740	94,879	95,013
0.04	94,187	94,287	94,392	94,501	94,613	94,731	94,853	94,981	95,114	95,253
0.05	94,445	94,545	94,650	94,759	94,872	94,989	95,112	95,239	95,372	95,511
0.06	94,723	94,824	94,928	95,037	95,150	95,267	95,390	95,517	95,650	95,789
0.07	95,023	95,124	95,229	95,337	95,450	95,568	95,690	95,818	95,951	96,090
0.08	95,350	95,451	95,555	95,664	95,777	95,894	96,017	96,144	96,278	96,417
0.09	95,706	95,807	95,912	96,020	96,133	96,251	96,373	96,501	96,634	96,773
0.1	96,097	96,198	96,302	96,411	96,524	96,642	96,764	96,892	97,025	97,164

Table 3.17: HEN capital costs in USD with bypass fractions of X3=0.03 and X1 & X2 ranging from 0.01 to 0.1

X1\ X2	0.01	0.02	0.03	0.04	0.05	0.06	0.07	0.08	0.09	0.1
0.01	93,532	93,632	93,737	93,846	93,959	94,076	94,198	94,326	94,459	94,598
0.02	93,742	93,842	93,948	94,056	94,169	94,287	94,409	94,537	94,670	94,809
0.03	93,967	94,068	94,172	94,281	94,394	94,511	94,634	94,761	94,890	95,034
0.04	94,207	94,308	94,413	94,522	94,634	94,752	94,874	95,002	95,135	95,274
0.05	94,466	94,566	94,671	94,780	94,893	95,010	95,133	95,260	95,393	95,532
0.06	94,744	94,845	94,949	95,058	95,171	95,288	95,411	95,538	95,671	95,810
0.07	95,044	95,145	95,250	95,358	95,471	95,589	95,711	95,839	95,972	96,111
0.08	95,371	95,472	95,576	95,685	95,798	95,915	96,038	96,165	96,299	96,438
0.09	95,727	95,828	95,933	96,041	96,154	96,272	96,394	96,522	96,655	96,794
0.1	96,118	96,219	96,323	96,432	96,545	96,662	96,785	96,912	97,046	97,185

Table 3.18: HEN capital costs in USD with bypass fractions of X3=0.04 and X1 & X2 ranging from 0.01 to 0.1

X1\ X2	0.01	0.02	0.03	0.04	0.05	0.06	0.07	0.08	0.09	0.1
0.01	93,553	93,654	93,759	93,867	93,980	94,098	94,220	94,348	94,481	94,620
0.02	93,764	93,865	93,969	94,078	94,191	94,308	94,431	94,558	94,691	94,830
0.03	93,989	94,089	94,194	94,303	94,415	94,533	94,655	94,783	94,916	95,055
0.04	94,229	94,330	94,434	94,543	94,656	94,774	94,896	95,024	95,157	95,296
0.05	94,487	94,588	94,693	94,801	94,914	95,032	95,154	95,282	95,415	95,554
0.06	94,765	94,866	94,971	95,079	95,192	95,310	95,432	95,560	95,693	95,832
0.07	95,066	95,167	95,271	95,380	95,493	95,610	95,733	95,860	95,994	96,133
0.08	95,392	95,493	95,598	95,706	95,819	95,937	96,059	96,187	96,320	96,459
0.09	95,749	95,849	95,954	96,063	96,176	96,293	96,416	96,543	96,676	96,815
0.1	96,140	96,240	96,345	96,454	96,567	96,684	96,806	96,934	97,067	97,206

Table 3.19: HEN capital costs in USD with bypass fractions of X3=0.05 and X1 & X2 ranging from 0.01 to 0.1

X1\ X2	0.01	0.02	0.03	0.04	0.05	0.06	0.07	0.08	0.09	0.1
0.01	93,575	93,676	93,781	93,889	94,002	94,120	94,242	94,370	94,503	94,642
0.02	93,786	93,887	93,991	94,100	94,213	94,330	94,453	94,580	94,714	94,853
0.03	94,011	94,111	94,216	94,325	94,438	94,555	94,678	94,805	94,938	95,077
0.04	94,251	94,352	94,457	94,565	94,678	94,796	94,918	95,046	95,179	95,318
0.05	94,509	94,610	94,715	94,823	94,936	95,054	95,176	95,304	95,437	95,576
0.06	94,787	94,888	94,993	95,101	95,214	95,332	95,454	95,582	95,715	95,854
0.07	95,088	95,189	95,293	95,402	95,515	95,633	95,755	95,883	96,016	96,155
0.08	95,415	95,515	95,620	95,729	95,842	95,959	96,081	96,209	96,342	96,481
0.09	95,771	95,872	95,976	96,089	96,198	96,315	96,438	96,565	96,698	96,838
0.1	96,162	96,262	96,367	96,476	96,589	96,706	96,829	96,956	97,089	97,228

Table 3.20: HEN capital costs in USD with bypass fractions of X3=0.06 and X1 & X2 ranging from 0.01 to 0.1

X1\ X2	0.01	0.02	0.03	0.04	0.05	0.06	0.07	0.08	0.09	0.1
0.01	93,598	93,699	93,803	93,912	94,025	94,143	94,265	94,393	94,526	94,665
0.02	93,809	93,909	94,014	94,123	94,236	94,353	94,476	94,603	94,736	94,875
0.03	94,033	94,134	94,239	94,347	94,460	94,578	94,700	94,828	94,961	95,100
0.04	94,274	94,375	94,479	94,588	94,701	94,818	94,941	95,068	95,202	95,341
0.05	94,532	94,633	94,738	94,846	94,959	95,077	95,199	95,327	95,460	95,599
0.06	94,810	94,911	95,016	95,124	95,237	95,355	95,477	95,605	95,738	95,877
0.07	95,111	95,212	95,316	95,425	95,538	95,655	95,778	95,905	96,039	96,178
0.08	95,437	95,538	95,643	95,751	95,864	95,982	96,104	96,232	96,365	96,504
0.09	95,794	95,894	95,999	96,108	96,221	96,338	96,461	96,588	96,721	96,860
0.1	96,184	96,285	96,390	96,499	96,611	96,729	96,851	96,979	97,112	97,251

Table 3.21: HEN capital costs in USD with bypass fractions of X3=0.07 and X1 & X2 ranging from 0.01 to 0.1

X1\ X2	0.01	0.02	0.03	0.04	0.05	0.06	0.07	0.08	0.09	0.1
0.01	93,622	93,722	93,827	93,936	94,049	94,166	94,288	94,416	94,549	94,688
0.02	93,832	93,933	94,038	94,146	94,259	94,377	94,499	94,627	94,760	94,899
0.03	94,057	94,158	94,262	94,371	94,484	94,601	94,724	94,851	94,985	95,124
0.04	94,297	94,398	94,503	94,611	94,724	94,842	94,964	95,092	95,225	95,364
0.05	94,556	94,656	94,761	94,870	94,983	95,100	95,222	95,350	95,483	95,622
0.06	94,834	94,934	95,039	95,148	95,261	95,378	95,501	95,628	95,761	95,900
0.07	95,134	95,235	95,340	95,448	95,561	95,679	95,801	95,929	96,062	96,201
0.08	95,461	95,562	95,666	95,775	95,888	96,005	96,128	96,255	96,388	96,528
0.09	95,817	95,918	96,022	96,131	96,244	96,362	96,484	96,612	96,745	96,884
0.1	96,208	96,309	96,413	96,522	96,635	96,752	96,875	97,002	97,136	97,275

Table 3.22: HEN capital costs in USD with bypass fractions of X3=0.08 and X1 & X2 ranging from 0.01 to 0.1

X1\ X2	0.01	0.02	0.03	0.04	0.05	0.06	0.07	0.08	0.09	0.1
0.01	93,646	93,746	93,851	93,960	94,073	94,190	94,313	94,440	94,573	94,712
0.02	93,856	93,957	94,062	94,170	94,283	94,401	94,523	94,651	94,784	94,923
0.03	94,081	94,182	94,286	94,395	94,508	94,626	94,748	94,876	95,009	95,148
0.04	94,322	94,422	94,527	94,636	94,749	94,866	94,988	95,116	95,249	95,388
0.05	94,580	94,681	94,785	94,894	95,007	95,124	95,247	95,374	95,507	95,646
0.06	94,858	94,959	95,063	95,172	95,285	95,402	95,525	95,652	95,785	95,924
0.07	95,158	95,259	95,364	95,473	95,585	95,703	95,825	95,953	96,086	96,225
0.08	95,485	95,586	95,690	95,799	95,912	96,029	96,125	96,279	96,413	96,552
0.09	95,841	95,942	96,047	96,155	96,268	96,386	96,508	96,636	96,769	96,908
0.1	96,232	96,333	96,437	96,547	96,659	96,777	96,899	97,027	97,160	97,299

Table 3.23: HEN capital costs in USD with bypass fractions of X3=0.09 and X1 & X2 ranging from 0.01 to 0.1

X1\ X2	0.01	0.02	0.03	0.04	0.05	0.06	0.07	0.08	0.09	0.1
0.01	93,671	93,771	93,876	93,985	94,098	94,215	94,337	94,465	94,598	94,737
0.02	93,881	93,982	94,087	94,195	94,308	94,426	94,548	94,676	94,809	94,948
0.03	94,106	94,207	94,311	94,420	94,533	94,650	94,773	94,900	95,034	95,173
0.04	94,346	94,447	94,552	94,660	94,773	94,891	95,013	95,141	95,274	95,413
0.05	94,605	94,705	94,810	94,919	95,032	95,149	95,271	95,399	95,532	95,671
0.06	94,883	94,983	95,088	95,197	95,310	95,427	95,550	95,677	95,810	95,949
0.07	95,183	95,284	95,389	95,497	95,610	95,728	95,850	95,978	96,111	96,250
0.08	95,510	95,611	95,715	95,824	95,937	96,054	96,177	96,304	96,437	96,577
0.09	95,866	95,967	96,071	96,180	96,293	96,411	96,533	96,661	96,794	96,933
0.1	96,257	96,358	96,462	96,571	96,684	96,801	96,924	97,051	97,185	97,324

Table 3.24: HEN capital costs in USD with bypass fractions of X3=0.1 and X1 & X2 ranging from 0.01 to 0.1

X1\ X2	0.01	0.02	0.03	0.04	0.05	0.06	0.07	0.08	0.09	0.1
0.01	93,696	93,797	93,902	94,010	94,123	94,241	94,363	94,491	94,624	94,763
0.02	93,907	94,008	94,112	94,221	94,334	94,451	94,574	94,701	94,834	94,973
0.03	94,132	94,232	94,337	94,446	94,559	94,676	94,798	94,926	95,059	95,198
0.04	94,372	94,473	94,577	94,686	94,799	94,917	95,039	95,167	95,300	95,439
0.05	94,630	94,731	94,836	94,944	95,057	95,175	95,297	95,425	95,558	95,697
0.06	94,908	95,009	95,114	95,222	95,335	95,453	95,575	95,703	95,836	95,975
0.07	95,209	95,310	95,414	95,523	95,636	95,753	95,876	96,003	96,137	96,276
0.08	95,535	95,636	95,741	95,849	95,962	96,080	96,202	96,330	96,463	96,602
0.09	95,892	95,992	96,097	96,206	96,319	96,436	96,559	96,686	96,819	96,958
0.1	96,283	96,383	96,488	96,597	96,710	96,827	96,949	97,077	97,210	97,349

3.3.3.2 HEN Controllability Effect of Bypass Fractions Ranging from 0.01 to 0.1

Controllability was analyzed for the chosen bypass fractions scenarios (Tables 3.15 - 3.24). To make a fair controllability comparison of the different bypass fractions scenarios, the costs need to be fixed. The combination of bypass fractions providing the closest total costs to 94,000 USD, 94,500 USD and 95,000 USD were selected from each table, totaling 30 scenarios for the controllability analysis. Each bypass fraction combination was analyzed for its RGA CN and SVD CN (as explained in chapter 2) in order to conclude a controllability trend. The results of the controllability analysis are shown in Tables 3.25 - 3.27. Sample RGA and SVD analysis mfiles can be found in Appendix I.

Although the RGA and SVD analyses are performed to choose the best pairing combination, the bypass fractions combination also has an effect on the outcomes of this analysis. The extent of this effect on the RGA and SVD analyses results is unidentified, however since we are analyzing the HEN in the steady state sense, RGA and SVD analyses may help in deciding the best controllable combination of various bypass fractions of the same HEN.

Table 3.25: RGA & SVD CNs of bypass fractions combinations with HEN costs close to 94,000 USD

Bypass Fractions			Exact Cost (USD)	RGA CN	SVD CN
X1	X2	X3			
0.02	0.04	0.01	94,015	1	17.0986
0.02	0.04	0.02	94,035	1	16.112
0.01	0.05	0.03	93,959	1	15.4524
0.01	0.05	0.04	93,980	1	14.8893
0.01	0.05	0.05	94,002	1	14.5676
0.02	0.03	0.06	94,014	1	14.6794
0.02	0.03	0.07	94,038	1	14.3141
0.01	0.04	0.08	93,960	1	13.765
0.01	0.04	0.09	93,985	1	13.2723
0.02	0.02	0.1	94,008	1	13.3053

Table 3.26: RGA & SVD CNs of bypass fractions combinations with HEN costs close to 94,500 USD

Bypass Fractions			Exact Cost (USD)	RGA CN	SVD CN
X1	X2	X3			
0.04	0.04	0.01	94,480	1	18.1669
0.04	0.04	0.02	94,501	1	17.1109
0.03	0.06	0.03	94,511	1	16.2761
0.01	0.09	0.04	94,481	1	15.324
0.05	0.01	0.05	94,509	1	16.2945
0.04	0.03	0.06	94,479	1	15.5793
0.04	0.03	0.07	94,503	1	15.1976
0.03	0.05	0.08	94,508	1	14.2823
0.03	0.05	0.09	94,533	1	13.9599
0.01	0.08	0.1	94,491	1	13.0258

Table 3.27: RGA & SVD CNs of bypass fractions combinations with HEN costs close to 95,000 USD

Bypass Fractions			Exact Cost (USD)	RGA CN	SVD CN
X1	X2	X3			
0.07	0.01	0.01	95,003	1	19.8624
0.05	0.06	0.02	94,989	1	17.62
0.04	0.08	0.03	95,002	1	16.7669
0.04	0.08	0.04	95,024	1	16.5976
0.06	0.03	0.05	94,993	1	17.1664
0.06	0.03	0.06	95,016	1	16.5637
0.05	0.05	0.07	94,983	1	15.6405
0.05	0.05	0.08	95,007	1	15.3539
0.04	0.07	0.09	95,013	1	14.5552
0.06	0.02	0.1	95,009	1	14.8459

The results above show an RGA CN of 1 for all the scenarios under study. This is the lowest possible CN; therefore this reconfirms that the HEN pairing under study (1H2C3C) is the most robust with the best conditioned pairing. However since the RGA cannot identify the best controllable bypass fractions combination, the analysis is inconclusive, and the SVD analysis is applied to choose the best controllable bypass combination. In each table of the above results, the SVD CNs are considered to be too close to each other to have a decisive decision of the best controllable bypass fractions combination. For the SVD CN comparison to be decisive, the bypass fractions combinations should differ by at least one order of magnitude. Since all the SVD CNs are of the same order of magnitude, this analysis is also considered inconclusive.

After an extensive study of the effects of bypass fractions ranging from 0.1 to 10% of the HEN, it can be concluded that their effect on cost and controllability are minor. The study may be considered inconclusive as it doesn't lead to the most economical and controllable bypass fraction combination. This finding reconfirms Mathisen *et al.*'s [14] claim that bypass fractions in HENs ranging from 0.1% to 10% should not affect much the controllability measures of the HEN, and adds to it that the differences in costs associated from ranging the bypass fraction from 0.1% to 10% are marginal. Most importantly the above analysis is time consuming, and shall not be

included in the framework, as one of the important aspects of the framework is to have quick and easy steps to follow. Alternatively, the framework shall include Mathisen *et al.*'s [14] heuristic, with a recommendation of performing rigorous optimization where disturbances and performance indicators of the controlled outputs are taken into considerations to fine tune the HEN.

3.4 Steady State Comparison

The above three analyses are the basis of the framework formulation. In this section the framework findings of the case study are compared with Yan *et al.*'s [18] and Uzturk and Arkam's [23] investigations and results for the same case study. The comparison is done in terms of bypass placements and capital costs.

Figure 3.10 shows the results of the bypass placements for three different studies shown on the same heat exchanger network. The green bypasses represent the placements based on this thesis' findings via the proposed framework. The blue line represents Yan *et al.*'s [18] bypass placements based on their design, and the red lines represent bypass placements based of Uzturk and Arkam's [23] design.

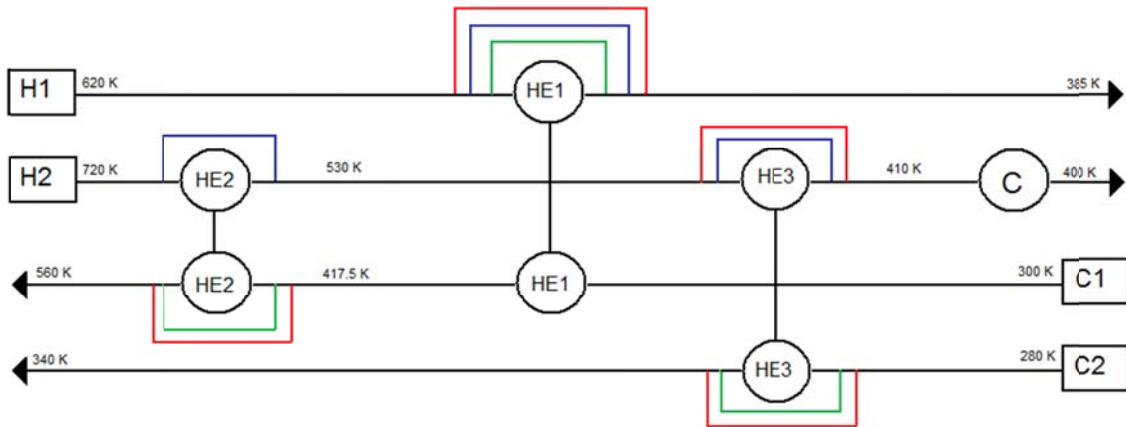


Figure 3.10: Bypass placement comparison between the framework (green), Yan *et al.*'s [18] (blue) and Uzturk and Arkam's [23] design (red) approaches for the HEN under study.

When comparing the framework's and Yan *et al.*'s [18] bypass placements, the following can be highlighted: the framework's design resulting in bypass placements 1H2C3C is based on a stepwise heuristic approach whereas Yan *et al.*'s [18] design 1H2H3H is based on a numerical model. The first bypass fraction 1H is shared by both designs, and the bypass placement on the hot side of HE1 directly controls the target temperature of stream H1. This can be considered as the logical dynamic choice, as this is the only HE for this stream.

Table 3.28 shows a brief comparison between the three designs. The calculations leading to the results shown in this table are given in Appendix 1. The comparison table shows that in terms of steady state controllability both the framework's and Yan *et al.*'s [18] designs share the same RGA CN of 1. However Yan *et al.*'s [18] design shows a lower SVD CN which means a better controllability in the steady state sense, but this does not prove a better controllability in the dynamic sense.

Table 3.28: Comparison of steady state control parameters, heat exchanger areas and costs between the framework's proposed design, Yan *et al.*'s [18] and Uzturk and Arkam's [23] design approaches for the HEN under study

Design	RGA CN	SVD CN	Total HE Areas (m²)	Capital Cost (\$)
Framework Proposed Design	1	17.34	133.7	97,380
Yan <i>et al.</i> [18]	1	6.73	126.4	94,820
Uzturk and Arkam [23]	31.39	1575.5	143.1	100,500

Although both the framework and Yan *et al.*'s [18] designs agree that the bypass of HE2 would control the target temperature of stream C1, they do not agree on the bypass placement side of the HE. In the framework 2C, the cold side of the HE, is selected, while Yan *et al.*'s [18] numerical model selected 2H, the hot side. The framework's placement, 2C, has a more direct influence on C1's target temperature than 2H because it is placed on the target stream itself, hence reducing the response time. The same applies to the placement of the last bypass placement, where both designs control stream C2's temperature. However the framework's placement of 3C affects the target

temperature of stream C2 in a faster and a more direct way than Yan *et al.*'s [18] 3H placement. The dynamic advantages that the framework bypass placements hold over Yan *et al.*'s [18] placements are verified in the dynamic analysis section.

Table 3.28 shows that Uzterk and Arkam's [23] design is not controllable in the steady state analysis as it has high RGA and SVD CNs. Uzterk and Arkam's [23] bypass placements were 1H2C3H3C; this is very close to the framework's placements except for the extra 3H bypass placements on HE3. The HEN has 3 heat exchangers and 4 bypasses, the author may have been trying to control the target temperatures of every stream. However the effect of placing two controllers on the same heat exchanger may have not been analyzed. Placing bypasses with controllers on both streams of the heat exchanger creates conflicting outputs, where each controller will try to stabilize its target temperature by changing its corresponding bypass fraction. However since both bypasses are placed on the same heat exchanger, they directly affect each other, causing unsteady stream temperatures that never reach the desired targets, and shattering of the control valves due to the constantly changing bypass fractions. Additionally, the cooler placed on H2 will be harmed as the inlet temperature will be constantly varying. A 3-heat exchanger system only needs 3 bypasses even if the system has 4 streams. Controlling 3 out of 4 target temperatures will result in controlling the fourth temperature by default.

To be able to fairly compare all three designs, the capital costs need to be calculated in the same manner. Therefore the capital costs of Yan *et al.*'s [18] and Uzterk and Arkam's [23] designs were recalculated using Aspen HX-Net, the same way the capital costs of the framework were calculated purely for comparison purposes. The capital costs are directly proportional to the sizes of the heat exchangers. The larger the areas of heat exchangers, the larger the capital costs required for the HEN. The sizes of the heat exchangers are also associated with the sizes of their corresponding bypass fractions; the larger the bypass fraction the larger the flow rate that the heat exchanger has to be designed for, in case of 0% bypass, and the larger the heat exchanger. Yan *et al.* [18] used numerical methods to minimize the bypass fractions and at the same time abided by the steady state controllability constraints, resulting in the lowest capital costs between the three compared designs. The framework's capital cost is next in line with bypass fractions all set at 10%, however the difference in capital cost is only around

\$2,500 which accounts for less than 2.7% increase over Yan *et al.*'s [18] design. Considering that this type of study is a preliminary one, without going into the details of heat exchanger design and flow lines design, analyzing in details the most economical utility alternatives; an increase in capital cost of 2.7% might be considered irrelevant, especially when leading to a less complex HEN and consuming less time on the analysis. Uzturk and Arkam's [23] design resulted in the largest heat exchangers and consequentially in the largest capital cost required for the HEN.

Chapter 4: Dynamics, Control and Exergy Analyses

This chapter investigates the dynamic controllability behavior of the designed system, and assures the reliability of the control system design in the dynamic phase. This chapter additionally gives an indication of how well the design consumes its useful energy through an exergy destruction analysis.

Steady-state simulations and steady-state based control analyses were used to formulate a framework to design a heat exchanger network that achieves efficient heat recovery, minimized capital costs and a controlled system. In this section dynamic simulations are used to assess and validate the framework's steady state design in terms of controllability and disturbance resiliency. The framework design is dynamically verified through first, performing the steady-state simulation, followed by adding control valves, turning the simulation to the dynamic mode, and finally introducing step changes. The system is then analyzed to see how well it reacts to the introduced changes. The same dynamic steps are applied to both the framework and Yan *et al.*'s [18] design to compare and determine which dynamic is favored.

4.1 Steady State Simulation

The steady-state system was simulated using Aspen HYSYS. To be able to perform the simulation, four basic pieces of information are needed for each stream; composition, temperature, pressure and flow rate. Inlet temperatures, outlet temperatures and specific heat capacities were the only pieces of information available; the other three needed to be assumed.

This framework is intended for industrial processes, more specifically hydrocarbon processes. In an attempt to make the system as less complicated as possible, all streams are considered to be 100% pure. Dodecane ($C_{12}H_{26}$) was the chosen alkane because it can attain the highest temperature while still in the liquid state. The pressure of each stream is chosen by a process of trial and error to make sure the streams remain in the liquid state for the entire range of inlet and outlet temperatures, while considering a safety margin of 5 bars. The heat capacity of each stream is evaluated at its median temperature, and the mass flow rates are calculated accordingly by dividing the known

specific heat capacities of each stream by their heat capacities at their respective median temperatures. After steady-state simulation, the flow rates are slightly adjusted in order to satisfy the target temperatures for each stream. Table 4.1 shows a summary of the system parameters. With the streams fully defined, the steady state simulation is completed by adding the heat exchangers and splitting the streams as per the bypass fractions specified above.

Table 4.1: HEN system parameters

Stream	T_{in} (K)	T_{out} (K)	MC_p (kJ/s·K)	Stream Median Temperature (K)	C_p at Median Temperature (kJ/kg·K)	Stream Pressure (bar)	Mass Flow Rate (kg/hr)
H1	620	385	10	502.5	2.916	17	11270
H2	720	400	15	560	3.158	51	18300
C1	300	560	20	430	2.616	9	29000
C2	280	340	30	310	2.1	6	48400

4.2 Dynamic Simulation and Controller Design

The most used feedback controller is the PID controller, which gives flexibility to tune all three parameters, K_c , the controller gain, τ_i , the integral constant, reducing the tracking error to zero and τ_d the derivative constant, reducing the noise and enhancing the predictive ability of the controller. However, for this simulation a PI controller is used instead of the PID controller for simplicity. Additionally, derivative actions may cause the controller to respond more nervously especially with the introduction of step changes, which is the core of the next section of the dynamic analysis. Moreover, whenever PI controllers are tuned properly and whenever the controller action is in the right direction and the PV range is defined wisely, the settings often give adequate performances [25].

After verifying that the steady state simulation correctly represents the system under study, the dynamic simulation process starts. Control valves are inserted into the system. Valves are left to be sized by HYSYS with a 50% opening for each, to allow flexibility in the system. A pressure drop of 0.5 bar is assumed through each valve on the basis of best engineering practice. Control valves are specified as PI controllers specifying the set points and the manipulated variables, as explained in the prior sections

and illustrated in Figure 3.10. The maximum and minimum operating parameters are set at 50K below and above the maximum and minimum stream temperatures, while satisfying the condition that the minimum temperature shall not go below 273 K. The controllers are set to Auto; the simulation is set to Auto tune to tune controller parameters accordingly. Finally, the system is turned on and left to stabilize, and is ready for further analysis. Snapshots of the Aspen HYSYS dynamic simulation s of both the proposed framework and Yan *et al.*'s [18] are shown in Figures 4.1 and 4.2.

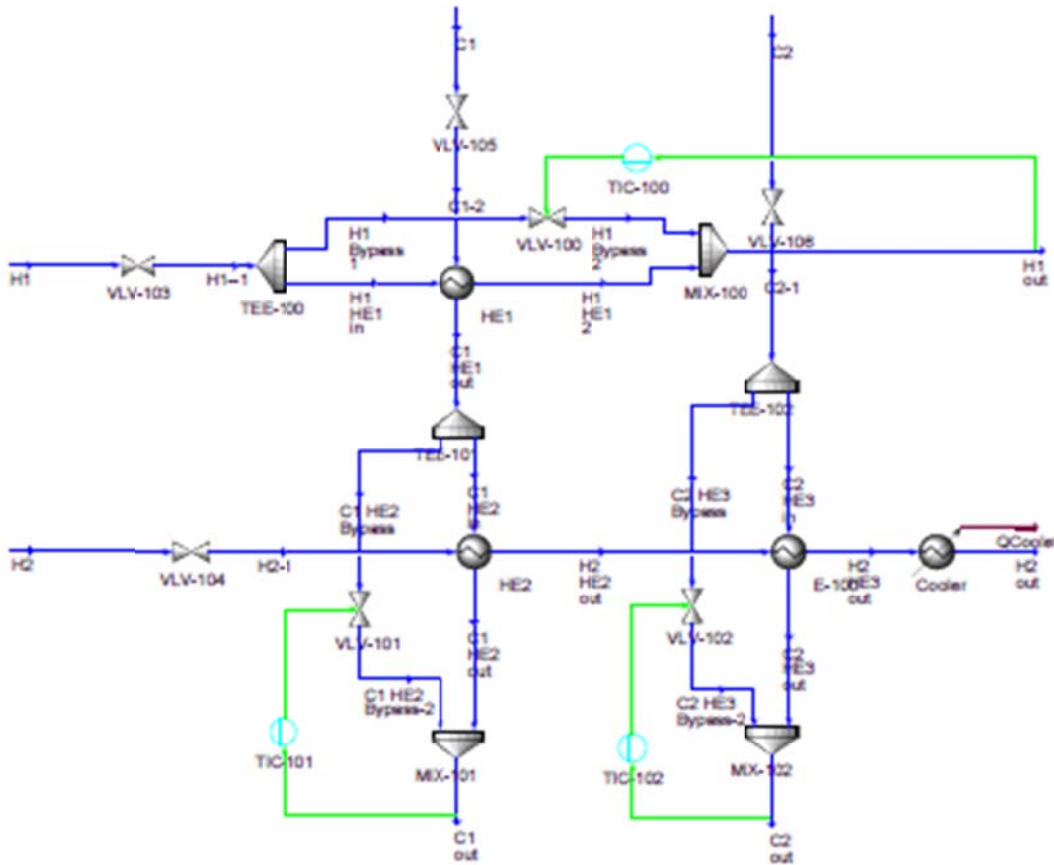


Figure 4.1: Snapshot of Aspen HYSYS dynamic control simulation for the proposed framework design.

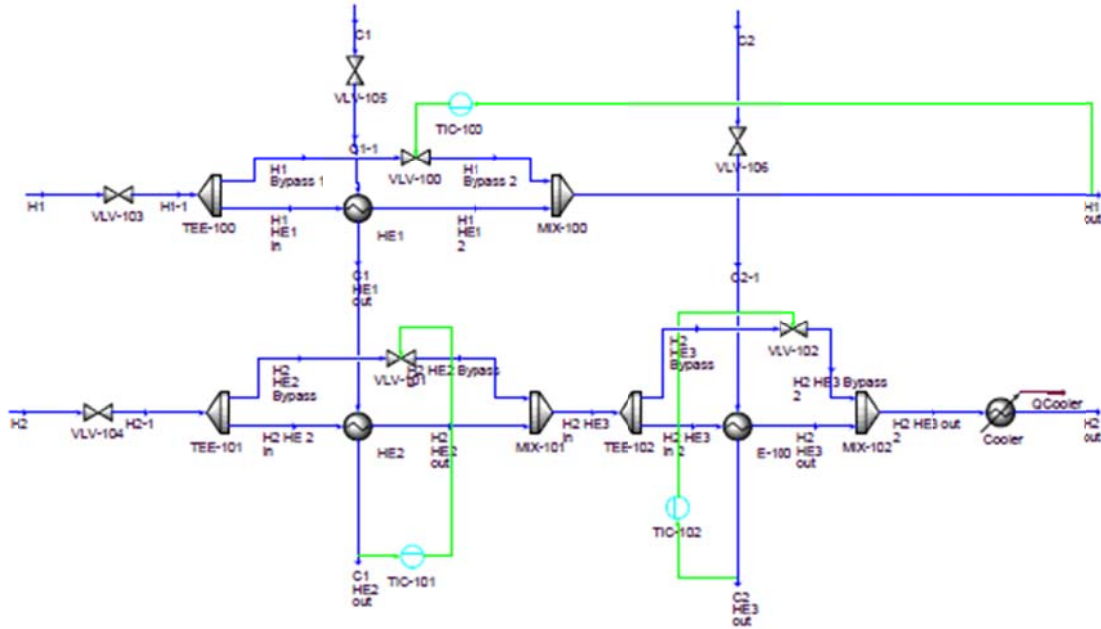


Figure 4.2: Snapshot of Aspen HYSYS dynamic control simulation for Yan *et al*'s [18] design.

4.3 Controller Performance Analysis

Verifying the controller performance of the system is done by introducing step change disturbances at the inlet temperatures of each stream one at a time, and observing and analyzing how the controllers react, as they try to alter the bypass fractions by changing the valve openings to push the system back to the original “set point” state. Each design has 3 controllers, TIC-100, TIC-101 and TIC-102 to control the outlet temperatures of streams H1, C1 and C2, respectively. The controller performance is assessed by control measures such as offset from the set point of each controlled outlet temperature, the overshoot behavior, and the settling time taken for the system to reach a steady-state. The settling time to reach steady state is usually defined as the time taken to reach $\pm 5\%$ of the set point [5], however since the effect of the step changes does not even exceed 1% of the set point as an overshoot, the settling time shall be considered to be the time taken for the temperature to reach an ultimate steady state behavior. In this analysis, the H2 outlet is uncontrolled, and is under the assumption that in a real situation, the utility system of the cooler would be designed to control the outlet temperature of H2.

The closed-loop dynamic behavior of the proposed framework design is compared to that of Yan *et al.* [18]. It is important to re-state the design parameters of each design as it does affect the dynamic behavior of each design. Both designs are heat integrated through the Superstructure approach. The bypass placements of each design are shown in Figure 3.10. The bypass fractions of the proposed framework are $X1=X2=X3=0.1$ and the bypass fractions of Yan *et al.* [18] are $X1=0.015$, $X2=0.053$ and $X3=0.082$. The effect of these parameter on the dynamic behavior of each design is explained in the following sections.

4.3.1 Step Change Disturbance in H1 Inlet Temperature

Two step changes of +5 K and +10 K were introduced into the inlet temperature of steam H1 in both the framework and Yan *et al.* [18] designs, and the systems were left to react to the changes. Overall, both designs managed to push the system back to its desired set points, however sometimes with some offsets.

As shown in Figure 3.10, both designs have the same bypass placement, where TIC-100 is placed over the bypass of the hot stream of HE1, to directly control the outlet temperature of stream H1, with the difference in bypass fractions. Figures 4.3 to 4.8 show the reaction of each controller to the step change of +5 K in stream H1's inlet temperature. Table 4.2 summarizes how effective each design is in terms of set point offset, time taken to stabilize the system and their respective overshoot.

As shown in Figures 4.3 - 4.5, the control scenario of the framework's design for the step change of +5 K in H1's inlet temperature is as follows: as the inlet temperature of H1 increased, it initially caused the outlet temperature of H1 to increase as well; however TIC-100 around HE1 reduced the valve opening to transmit the extra heat into C1 to push H1 outlet temperature to its set point. As a result C1 outlet temperature increased, and TIC-101 reacted by increasing the valve opening, reducing the flow rate of the heated stream and therefore pushing C1 back to its set point. Consequentially, the outlet temperature out of HE2 on stream H2 also increased, affecting the outlet temperatures of H2 and C2. For H2, the temperature out of HE3 increased; however it was compensated by the Cooler's duty to allow H2 to reach its set point temperature.

Stream C2's outlet temperature initially increased but TIC-102 reacted by increasing the valve opening, allowing C2's outlet temperature to go down to its set point.

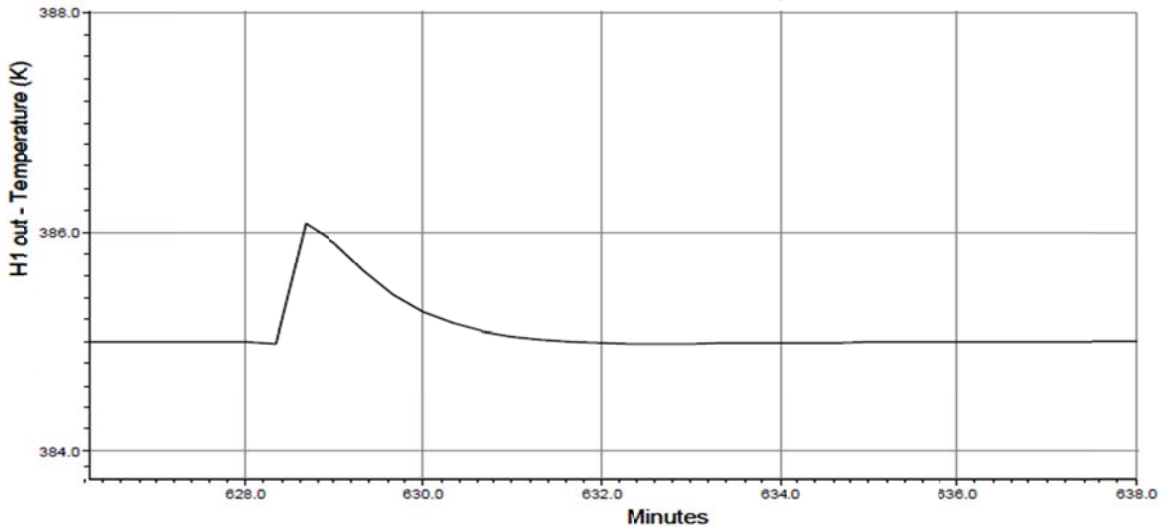


Figure 4.3: H1 outlet temperature reaction to a +5 K step change in H1 inlet temperature of the framework's design.

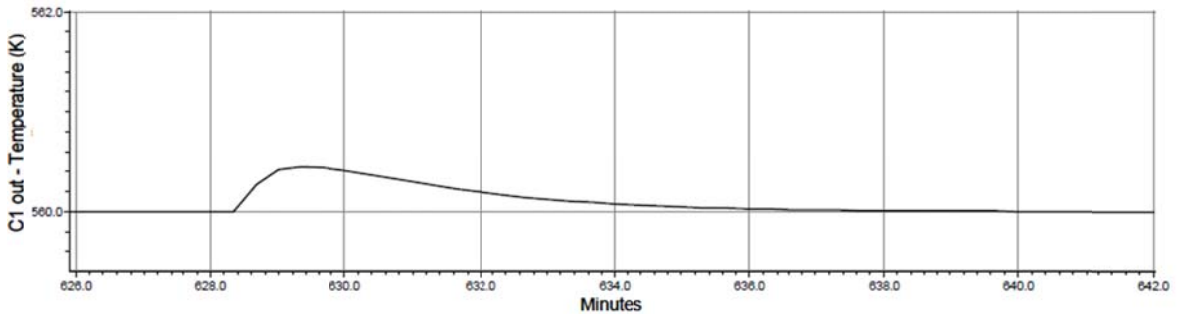


Figure 4.4: C1 outlet temperature reaction to a +5 K step change in H1 inlet temperature of the framework's design.

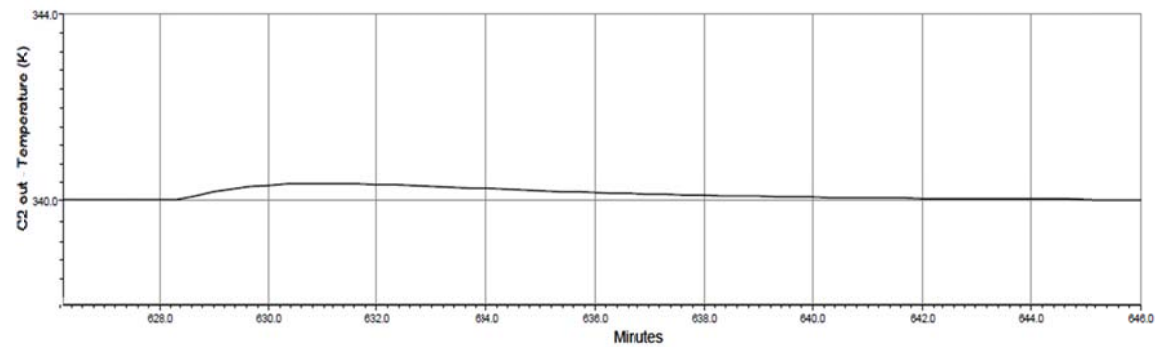


Figure 4.5: C2 outlet temperature reaction to a +5 K step change in H1 inlet temperature of the framework's design.

Yan *et al.*'s [18] design acted in a similar way to the step change of +5 K in H1's inlet temperature, however since the bypass placements are different it differed in the actions of its controllers. TIC-100 of Yan *et al.*'s [18] design acted in the same way as the framework's design did because the bypass placement is identical. TIC-101 increased the bypass opening over HE2 to allow C1 outlet temperature to drop, and TIC-102 also increased the valve opening to allow the outlet temperature of C2 to go back to its set point, leaving the cooler to stabilize H2 back to its set point. The above explanation is supported by Figures of 4.6 - 4.8 showing the reaction of each outlet temperature due to the step change.

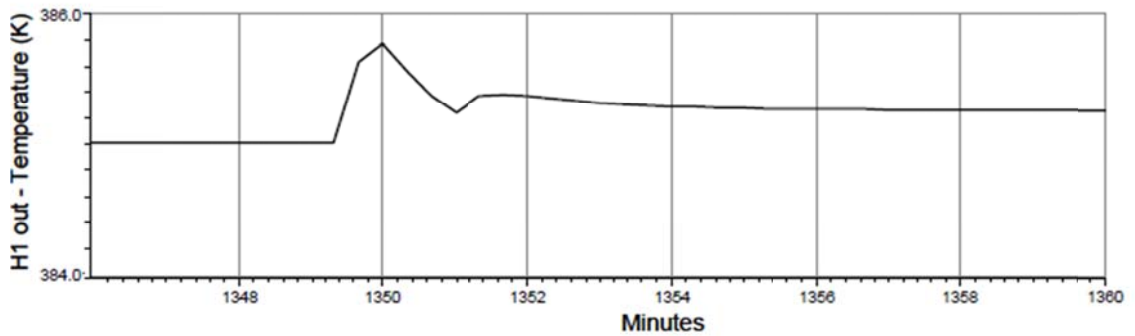


Figure 4.6: H1 outlet temperature reaction to a +5 K step change in H1 inlet temperature of Yan *et al.*'s [18] design.

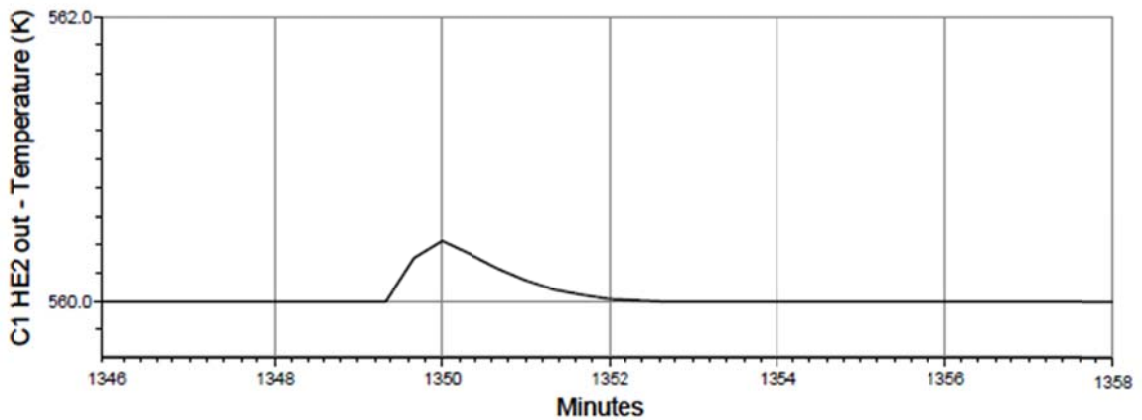


Figure 4.7: C1 outlet temperature reaction to a +5 K step change in H1 inlet temperature of Yan *et al.*'s [18] design.

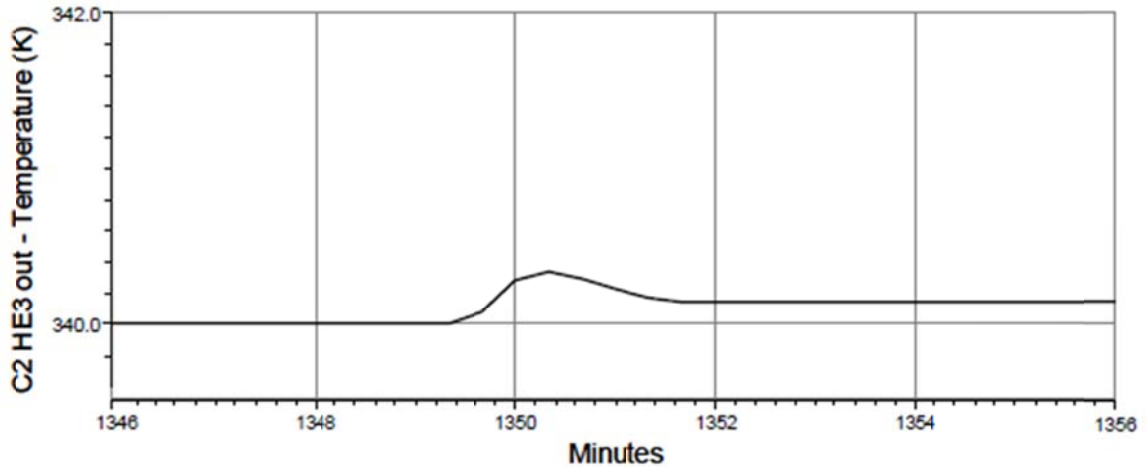


Figure 4.8: C2 outlet temperature reaction to a +5 K step change in H1 inlet temperature of Yan *et al.*'s [18] design.

As seen in Table 4.2, the framework's design shows zero offset for all the streams, while Yan *et al.*'s [18] design shows minor offsets in streams H1 and C2. This is mainly due to the difference in the bypass fractions between both designs. The proposed framework design holds higher bypass fractions around each heat exchanger than Yan *et al.*'s [18] design, which allows it to react more effectively to higher disturbances and obtains zero offsets from the set point target temperatures. On the other hand Yan *et al.*'s [18] design becomes saturated due to the limited bypass fractions and fails to obtain zero offset results from the set point target temperatures. In terms of the speed to return the system back to a steady-state like behavior, Yan *et al.*'s [18] design performed better, except for H1 where it was outperformed by the framework's design. The least offset was expected in the results of H1, since it is directly controlled by TIC-100, and with a disturbance occurring at the inlet for the same stream. The framework's design has controlled H1 stream better with zero offset and a shorter time of 7 minutes to reach a steady state behavior compared to Yan *et al.*'s [18] 0.3 K offset and stabilization time of 7.6 minutes. Yan *et al.*'s [18] design showed an overshoot from the set point that is slightly better than that of the framework's design, however the difference of overshoot is minor.

Table 4.2: Effect of +5 (K) step change on H1 inlet temperature for the framework's and Yan *et al.*'s [18] control designs

Step Change	Stream Name	H1			C1			C2		
	Measurement	Set Point Offset (K)	Settling Time (min)	Overshoot (K)	Set Point Offset (K)	Settling Time (min)	Overshoot (K)	Set Point Offset (K)	Settling Time (min)	Overshoot (K)
+5 (K) in H1 Inlet Temperature	Proposed Framework Design	0	7	1	0	8.9	0.2	0	16.6	0.3
	Yan <i>et al.</i> 's [18] Design	0.3	7.6	0.8	0	3.2	0.4	0.1	2.2	0.4

Introducing larger step changes into the system highlights more interesting observations. Figures 4.9 - 4.14 and Table 4.3 show the effect of +10 K step change in H1 in both designs. The design of Yan *et al.* [18] yields a significant drop, as it allows larger offsets and more time to stabilize the system compared to a lower step change. This is a result of the saturation of the controller actions due to the limited bypass fractions of Yan *et al.*'s [18] design. On the other hand the framework's design maintains zero offset in two out of the three set points as the bypass fraction around C2 is not big enough to react to this size of disturbance and therefore pushes the controller to saturation. The proposed framework design improves the time the system takes to reach a steady-state behavior at H1 and C2, as deduced from a comparison with the results in Table 4.2 for the +5K step change. Yan *et al.*'s [18] design remains to have a marginally better overshoot behavior than the framework's design only in C1 and C2, however the framework shows a better overshoot behavior in H1.

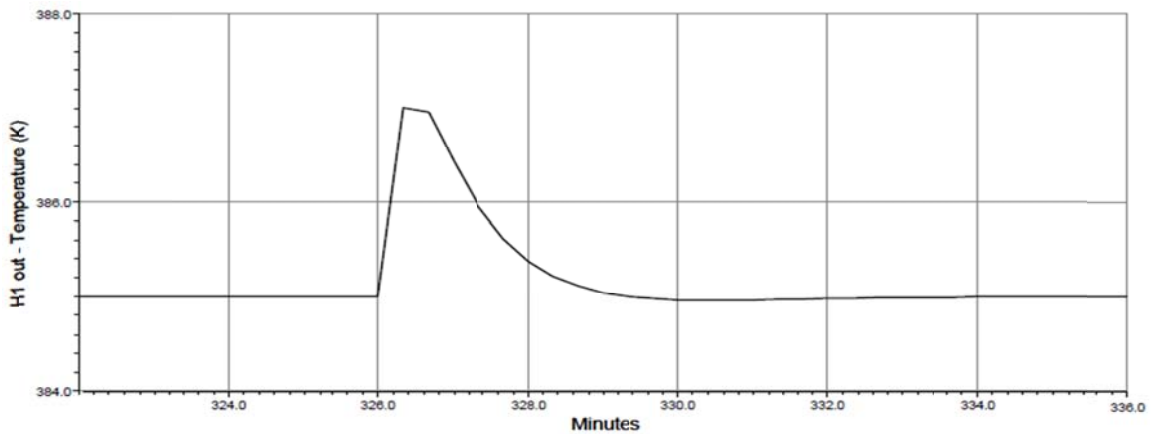


Figure 4.9: H1 outlet temperature reaction to a +10 K step change in H1 inlet temperature of the framework's design.

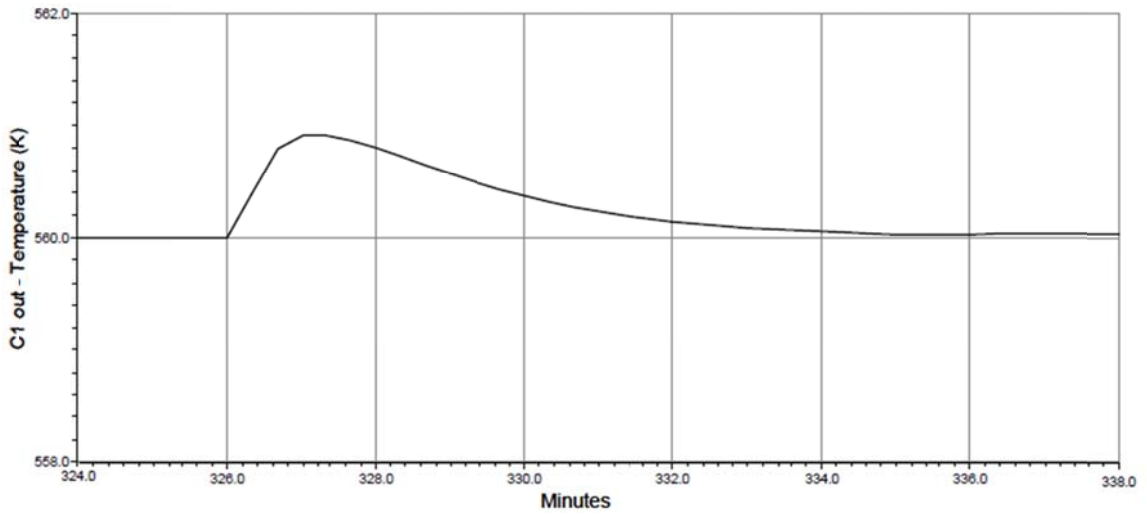


Figure 4.10: C1 outlet temperature reaction to a +10 K step change in H1 inlet temperature of the framework's design.

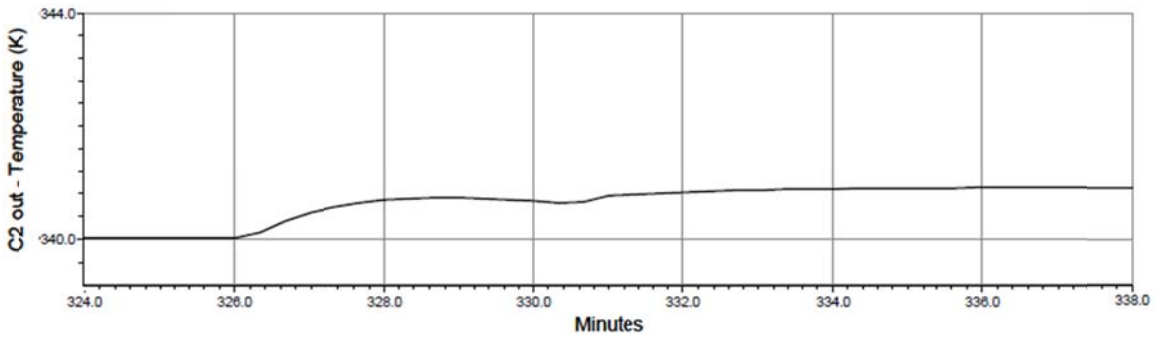


Figure 4.11: C2 outlet temperature reaction to a +10 K step change in H1 inlet temperature of the framework's design.

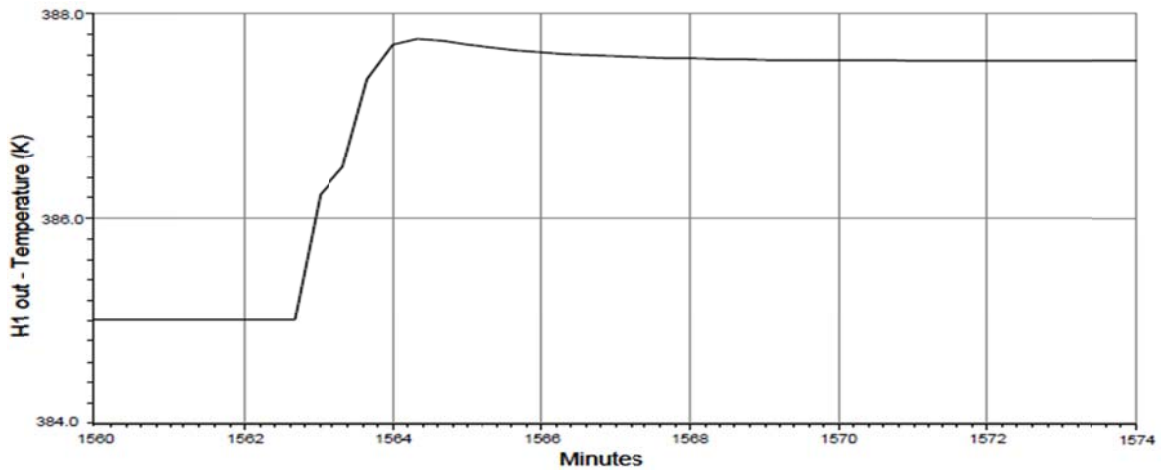


Figure 4.12: H1 outlet temperature reaction to a +10 K step change in H1 inlet temperature of Yan *et al.*'s [18] design.

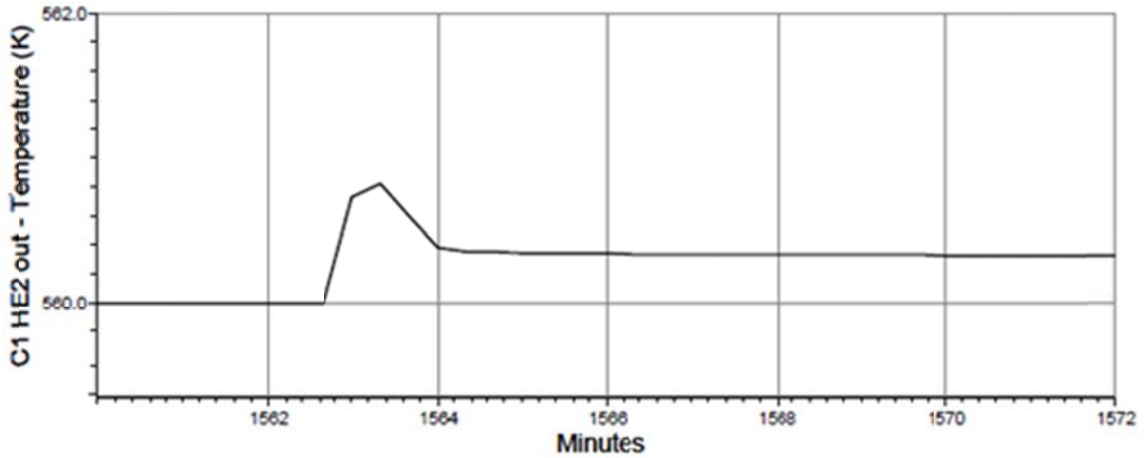


Figure 4.13: C1 outlet temperature reaction to a +10 K step change in H1 inlet temperature of Yan *et al.*'s [18] design.

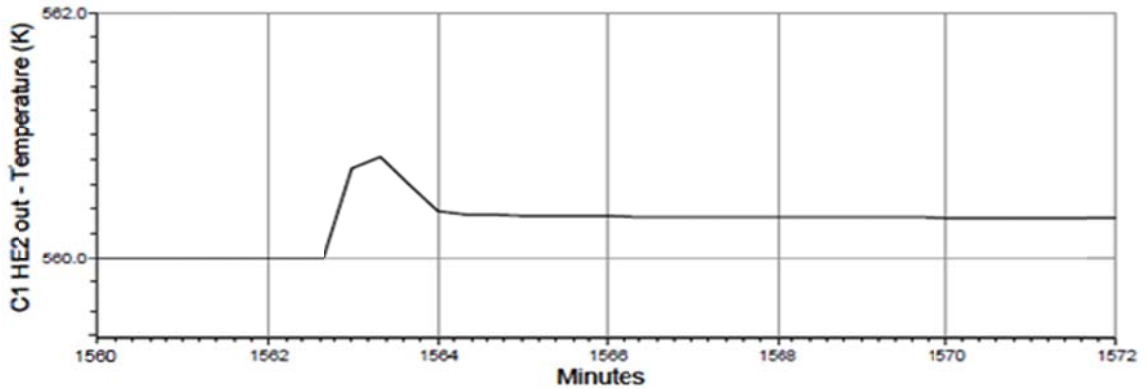


Figure 4.14: C2 outlet temperature reaction to a +10 K step change in H1 inlet temperature of Yan *et al.*'s [18] design.

Table 4.3: Effect of +10 (K) step change on H1 inlet temperature for framework's and Yan *et al.*'s [18] control designs

Step Change	StreamName	H1			C1			C2		
	Measurement	Set Point Offset (K)	Settling Time (min)	Overshoot (K)	Set Point Offset (K)	Settling Time (min)	Overshoot (K)	Set Point Offset (K)	Settling Time (min)	Overshoot (K)
+10 (K) in H1 Inlet Temperature	Proposed Framework Design	0	4	2	0	10.4	0.9	0.9	10	0.9
	Yan <i>et al.</i> 's [18] Design	2.5	8.2	2.6	0.3	7.2	0.8	0.7	3.7	0.7

4.3.2 Step Change Disturbance in C1 Inlet Temperature

Figures 4.15 - 4.17 help in visualizing the control reaction scenario of the framework to a +5 K step change in C1's inlet temperature in the following way. Initially the inlet temperature of stream H1 entering HE1 increased, yielding less heat transfer in HE1 between C1 and H1, causing H1 outlet temperature to increase. To fix that, TIC-100 reduced the valve opening of the bypass of HE1 on H1's side to allow for more heat exchange and ultimately regains H1's outlet set point temperature. Similarly a positive step change in C1's inlet temperature caused both the inlet and outlet temperatures of HE2 to increase. TIC-101 increased the valve opening, allowing more fluid to bypass HE2 to attain C1's outlet set point temperature. As a result the outlet temperature of HE2 increased as well; hence H2 entering and exiting HE3 increased accordingly. The cooler is assumed to take care of the outlet temperature of H2 by altering the rate of cooling medium that flows. An increased inlet temperature of H2 going through HE3 means more heat transfer to C2, therefore TIC-102 increased the valve opening, and hence the bypass to push the C2 outlet temperature back to its set point.

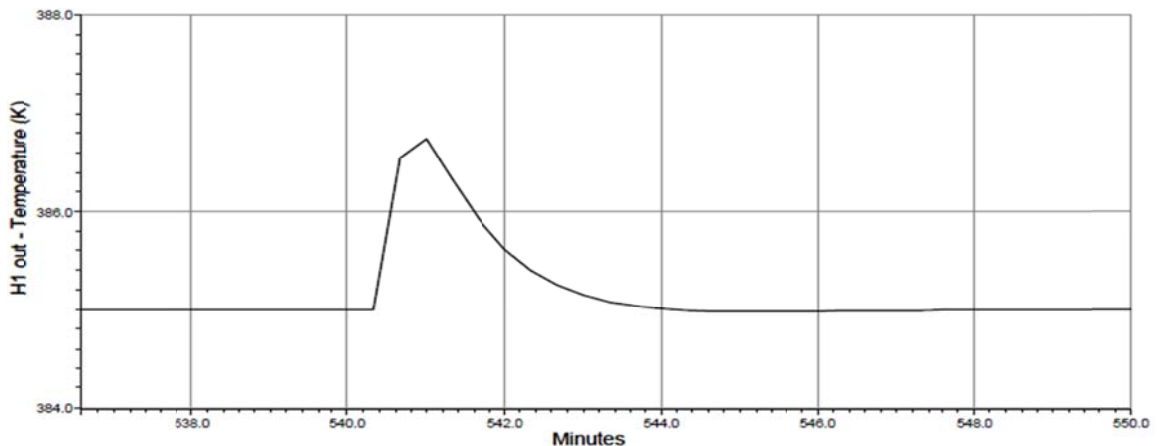


Figure 4.15: H1 outlet temperature reaction to a +5 K step change in C1 inlet temperature of the framework's design.

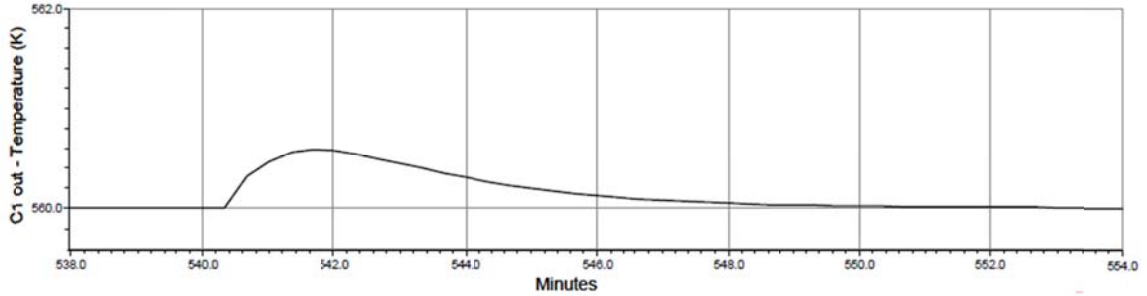


Figure 4.16: C1 outlet temperature reaction to a +5 K step change in C1 inlet temperature of the framework's design.

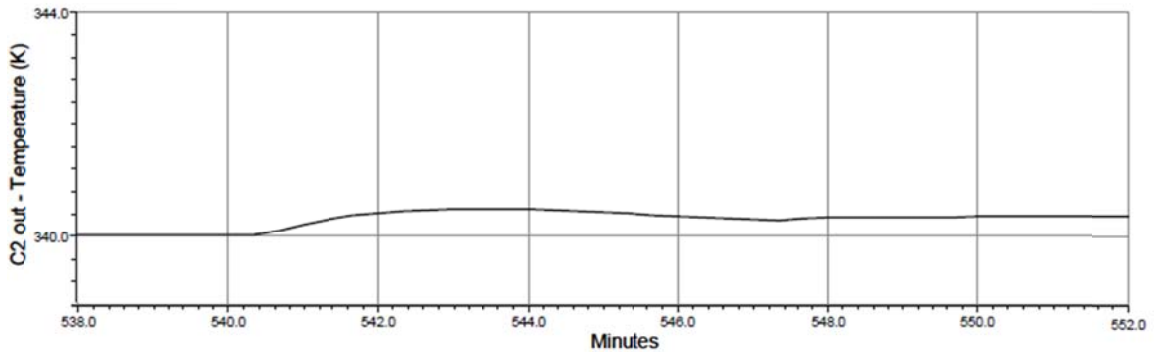


Figure 4.17: C2 outlet temperature reaction to a +5 K step change in C1 inlet temperature of the framework's design.

As for Yan *et al.*'s [18] design, the control scenario, due to a step change of +5 K in the inlet of C1, was as follows: TIC-100 would share the same type of response as the bypass placements are the same. The increase in temperature along C1 needed less heat to be exchanged through HE2 to push the C1 outlet temperature to its set point. Therefore TIC-101 in Yan *et al.*'s [18] design increased the valve opening allowing less fluid to flow through HE2, hence less was heat exchanged. The increased temperature of H2 as a whole affected C2; TIC-102 increased the valve opening allowing more flow through the bypass of HE3, less heat was exchanged and constraining C2 to reach its set point temperature. Finally as mentioned before, the cooler takes care of the set point of H2 through the utility system. Figures 4.18 - 4.20 show the reaction of the set points to the control scenario.

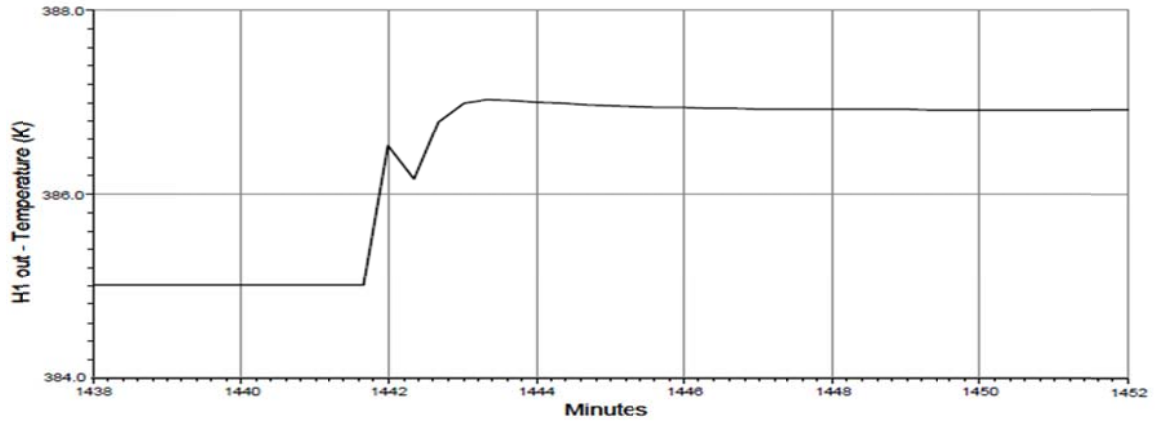


Figure 4.18: H1 outlet temperature reaction to a +5 K step change in C1 inlet temperature of Yan *et al.*'s [18] design.

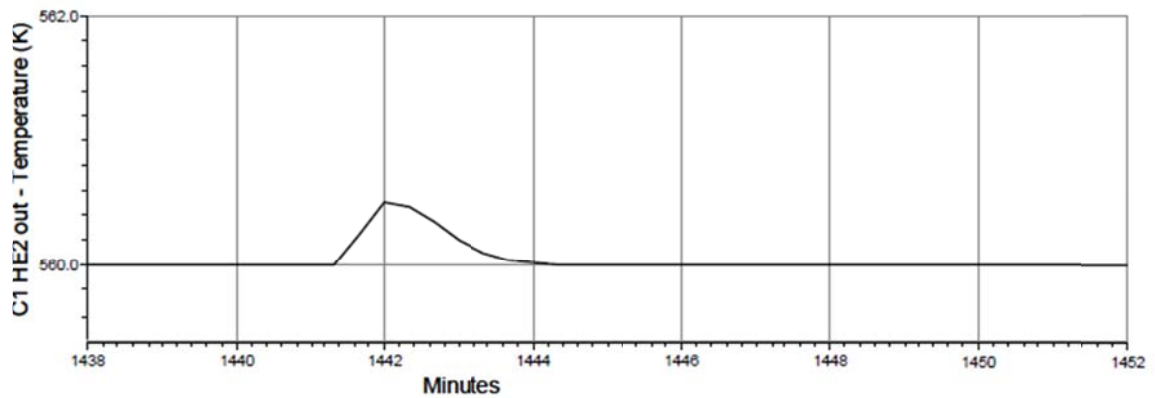


Figure 4.19: C1 outlet temperature reaction to a +5 K step change in C1 inlet temperature of Yan *et al.*'s [18] design.

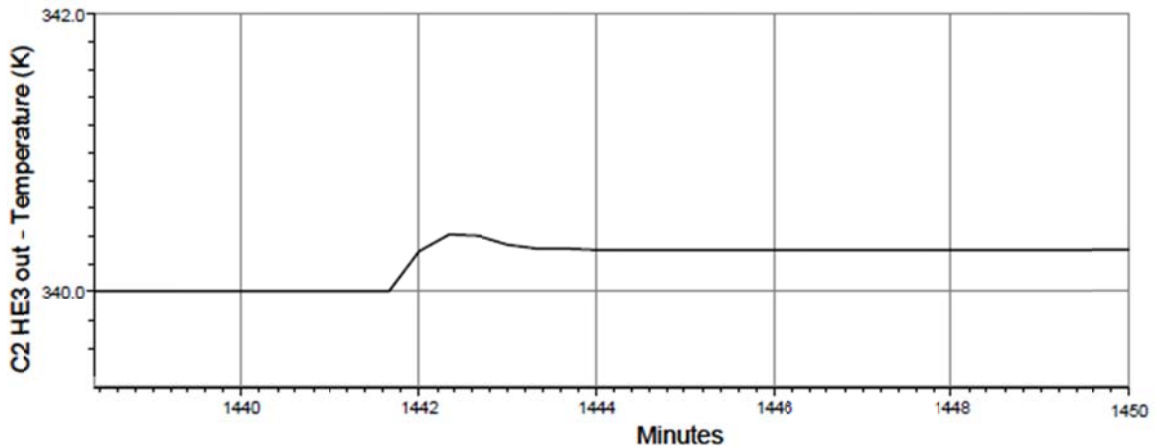


Figure 4.20: C2 outlet temperature reaction to a +5 K step change in C1 inlet temperature of Yan *et al.*'s [18] design.

Figures 4.15 - 4.20 show how effective each design was in controlling the system. The results summarized in Table 4.4 show that the framework attains better disturbance

rejection than Yan *et al.*'s [18] design as it is able to achieve zero set point offset for H1 and C1 and a 0.4 K offset for C2, while Yan *et al.*'s [18] design yields an offset of 1.9 K for H1, 0.3 K for C2, and zero offset C1. This is because of the bigger bypass fractions that allow for more effective control actions and reduces the saturations of the controllers. In terms of the speed at which the system reaches steady-state behavior again, both designs are the same for H1. However, the approach of Yan *et al.*'s [18] design to steady state is noticeably faster for C1 and C2. In terms of overshoot behavior, both designs had an identical behavior around C1, the framework's design showed a lower overshoot in H1 and Yan *et al.*'s [18] design showed a lower overshoot in C2, while all differences in overshoot remained marginal.

Table 4.4: Effect of +5 (K) step change in C1 inlet temperature on framework's and Yan *et al.*'s [18] control designs

Step Change	Stream Name	H1			C1			C2		
	Measurement	Set Point Offset (K)	Settling Time (min)	Overshoot (K)	Set Point Offset (K)	Settling Time (min)	Overshoot (K)	Set Point Offset (K)	Settling Time (min)	Overshoot (K)
+5 (K) in C1 Inlet Temperature	Proposed Framework Design	0	7.4	1.8	0	12.6	0.5	0.4	9.7	0.5
	Yan et al.'s [18] Design	1.9	7.4	2	0	2.9	0.5	0.3	2.2	0.4

4.3.3 Step Change Disturbance in C2 Inlet Temperature

An increase in the inlet temperature of C2 in the framework's design caused an increase of C2 outlet temperature. TIC-102 reacted by increasing the valve opening of the bypass over HE3, so less heat would be exchanged thus decreasing C2 outlet temperature to its set point. The reduced amount of heat exchanged affected the outlet temperature of H2, but a reduction in the cooler duty would be sufficient to drive it back to its set point. H1 was completely not affected by this change as it is not directly interconnected with C2, therefore TIC-100 made no changes to the bypass fraction. C1 is not directly connected with C2, however, it is interconnected through HE2 and HE3; HE2 connects C1 with H2 and HE3 connects H2 with C2. Due to this interconnection, TIC-101 reacted minimally to the temperature alterations H2 faces to fix C1 at its set point. In other words, due to the change in temperature of C2, H2 faced changes in temperatures that

were translated through HE2 and HE3 to drive the temperature of C1 to its set point. This can be shown in Figures 4.21 - 4.23.

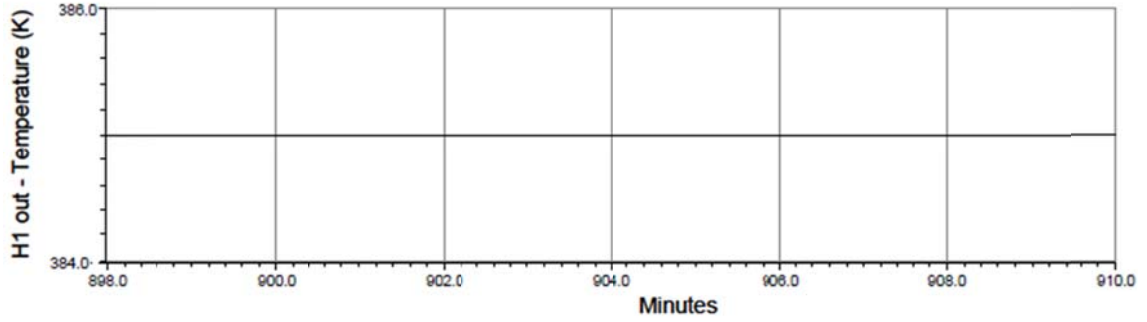


Figure 4.21: H1 outlet temperature reaction to a +5 K step change in C2 inlet temperature of the framework's design.

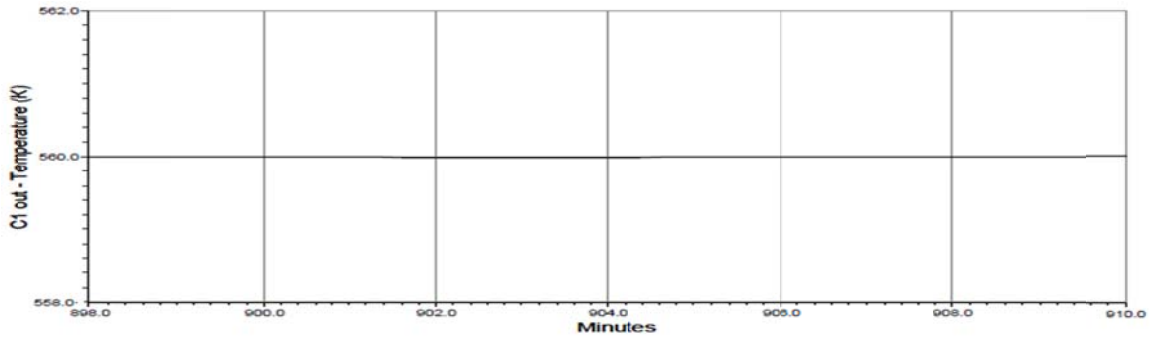


Figure 4.22: C1 outlet temperature reaction to a +5 K step change in C2 inlet temperature of the framework's design.

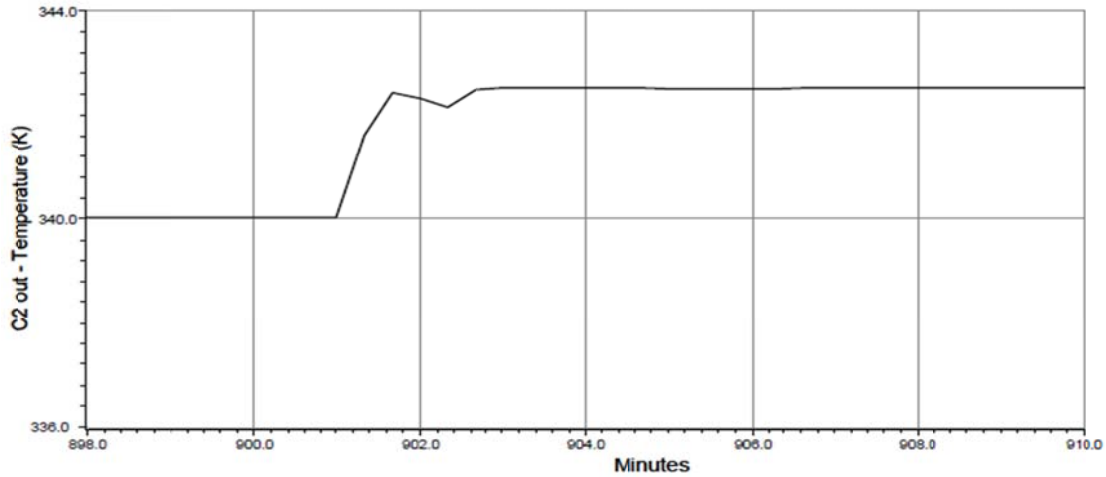


Figure 4.23: C2 outlet temperature reaction to a +5 K step change in C2 inlet temperature of the framework's design.

In Yan *et al.*'s [18] design case, Figures 4.24 - 4.26 shows that TIC-102 reacted to the increase in C2 inlet temperature by decreasing the valve opening on the bypass over HE3. As in the framework design, Yan *et al.*'s [18] design is also interconnected; changes in C2 cause temperature variations in H2 through HE3 and consequentially in C1 through HE2. This sudden change in temperature causes TIC-101 to alter the bypass fraction over HE3 in H2 as an attempt to regain the target temperatures; the bypass fraction initially increases, but then decreases again to its original bypass fraction and stabilizes quickly with no temperature changes for C1. Similar to the framework's design behavior, Yan *et al.*'s [18] design shows no changes in TIC-100's behavior, since H1 is not directly interconnected with C2, H1 was not affected by the change in inlet temperature of C2.

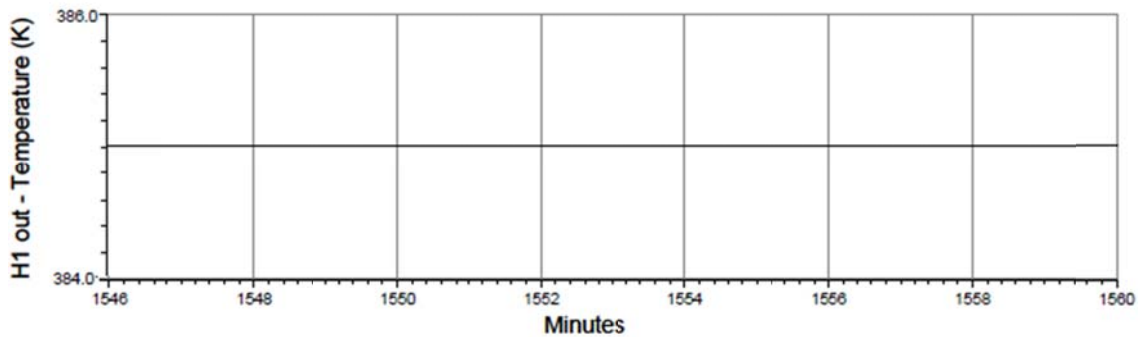


Figure 4.24: H1 outlet temperature reaction to a +5 K step change in C2 inlet temperature of Yan *et al.*'s [18] design.

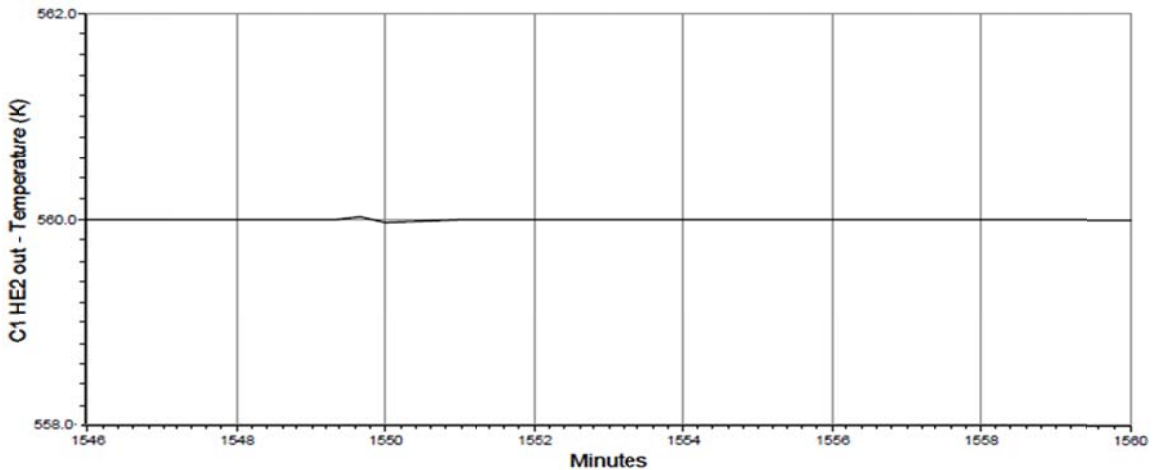


Figure 4.25: C1 outlet temperature reaction to a +5 K step change in C2 inlet temperature of Yan *et al.*'s [18] design.

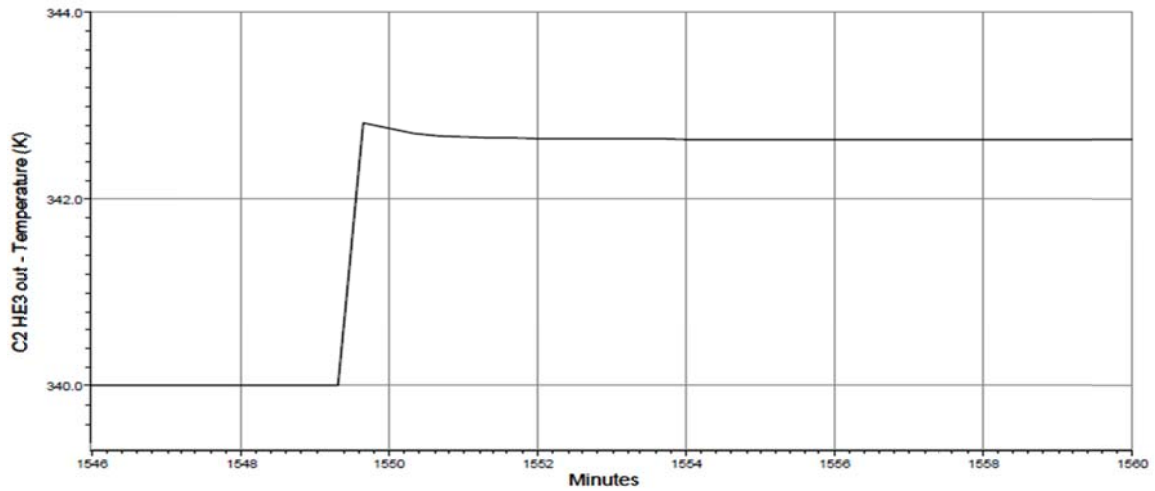


Figure 4.26: C2 outlet temperature reaction to a +5 K step change in C2 inlet temperature of Yan *et al.*'s [18] design.

Table 4.5 summarizes the effect of the +5 K step change on both designs. In both designs H1 shows zero set point offset and zero minutes to stabilize the system. This is due to the fact that H1 was unaffected by the changes in C2. Since minor interactions cause C1 to slightly react to the change in C2, its corresponding controllers react resulting in zero set point offset and 1.6 minutes to stabilize the system in Yan *et al.*'s [18] design, while in the framework design the system is stable with zero set point offset and zero minutes to stabilize. Changes in C2 cause both systems to have similar set point offsets of around 2.5 K; however, Yan *et al.*'s [18] design was quicker to stabilize the system. The framework's design showed a smaller overshoot in streams C1 and C2 compared to Yan *et al.*'s [18] design.

Table 4.5: Effect of +5 (K) step change in C2 inlet temperature on framework's and Yan *et al.*'s [18] control designs

Step Change	Stream Name	H1			C1			C2		
	Measurement	Set Point Offset (K)	Settling Time (min)	Overshoot (K)	Set Point Offset (K)	Settling Time (min)	Overshoot (K)	Set Point Offset (K)	Settling Time (min)	Overshoot (K)
+5 (K) in C2 Inlet Temperature	Proposed Framework Design	0	0	0	0	0	0	2.5	6.2	2.5
	Yan et al.'s [18] Design	0	0	0	0	1.6	0.04	2.6	4.3	2.8

In both systems, the controllers were not able to bring back C2's outlet temperature to its set point when a +5 K was introduced at its inlet due to the fact the a

+5 K step change might have been too big for the controllers and the bypass to react to. A smaller step change of +1 K was introduced. The results are shown in Figures 4.27 - 4.32 and summarized in Table 4.6, both systems showed improvements in disturbance rejection as all set point offsets were eliminated. In terms of speed to stabilize the system, the framework shows that it is able to bring back C1 to its target temperature faster than Yan *et al.*'s [18] design, while Yan *et al.*'s [18] design shows faster stabilization of C2's target temperature. In terms of overshoot, again the differences were negligible, were Yan *et al.*'s [18] design shows better results around C2 and the framework's design shows better results around C1.

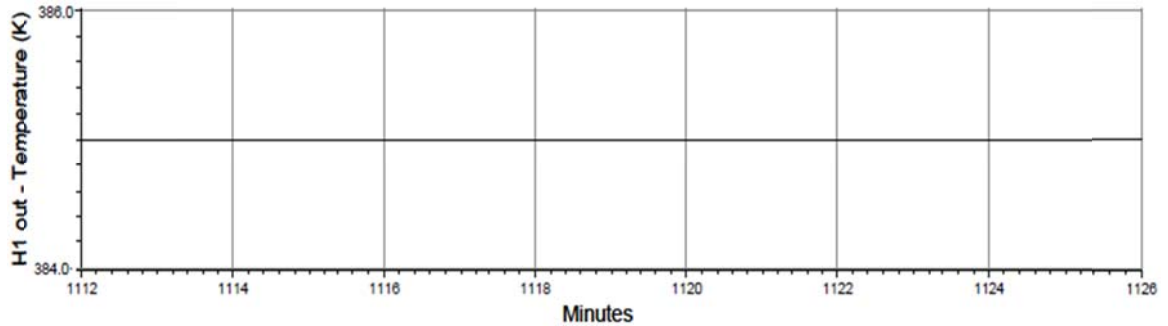


Figure 4.27: H1 outlet temperature reaction to a +1 K step change in C2 inlet temperature of the framework's design.

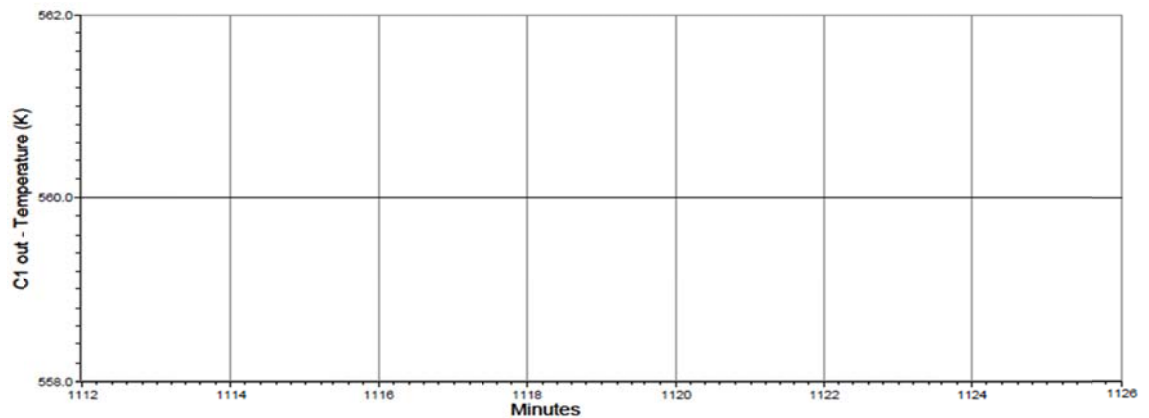


Figure 4.28: C1 outlet temperature reaction to a +1 K step change in C2 inlet temperature of the framework's design.

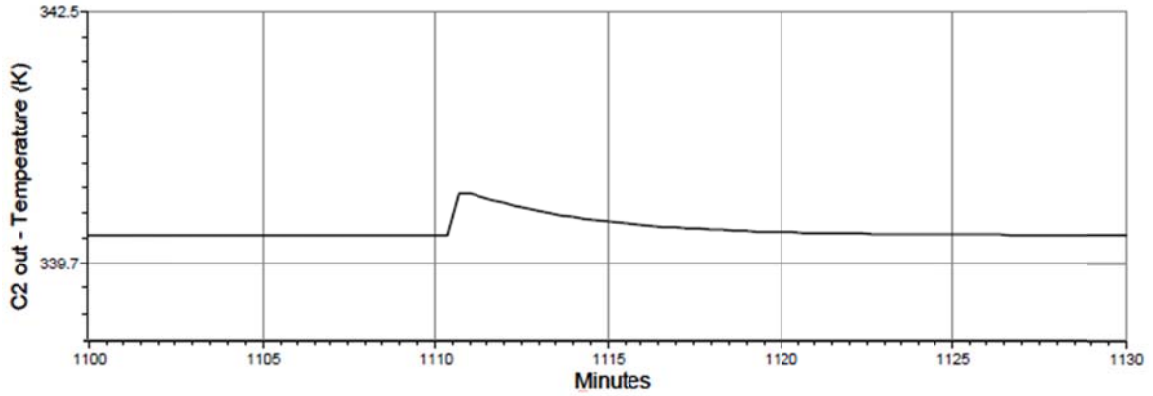


Figure 4.29: C2 outlet temperature reaction to a +1 K step change in C2 inlet temperature of the framework's design.

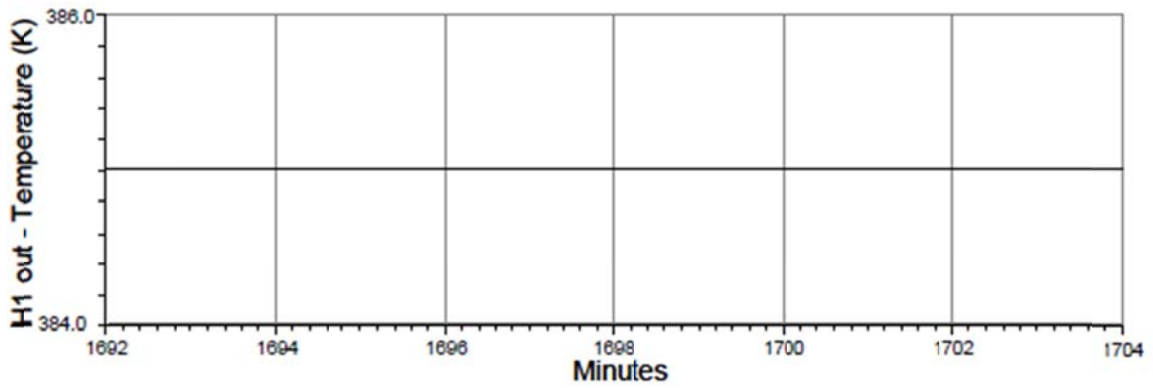


Figure 4.30: H1 outlet temperature reaction to a +1 K step change in C2 inlet temperature of Yan *et al.*'s [18] design.

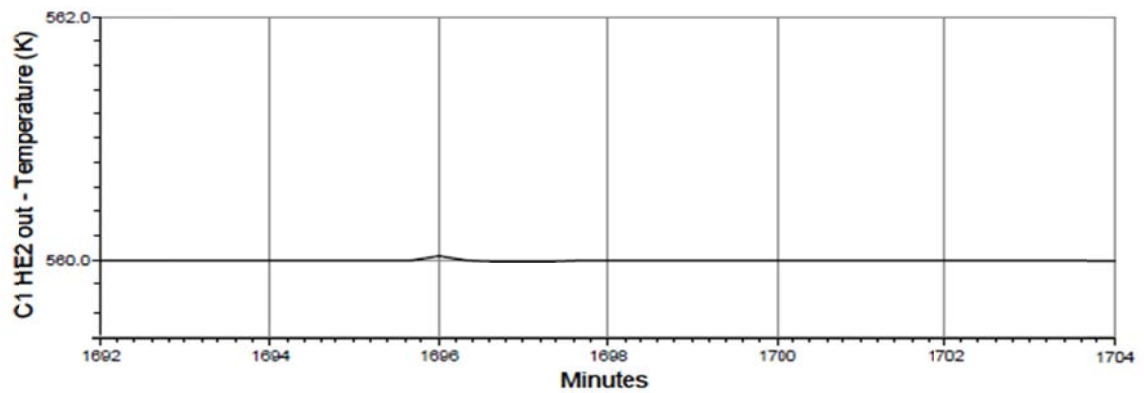


Figure 4.31: C1 outlet temperature reaction to a +1 K step change in C2 inlet temperature of Yan *et al.*'s [18] design.

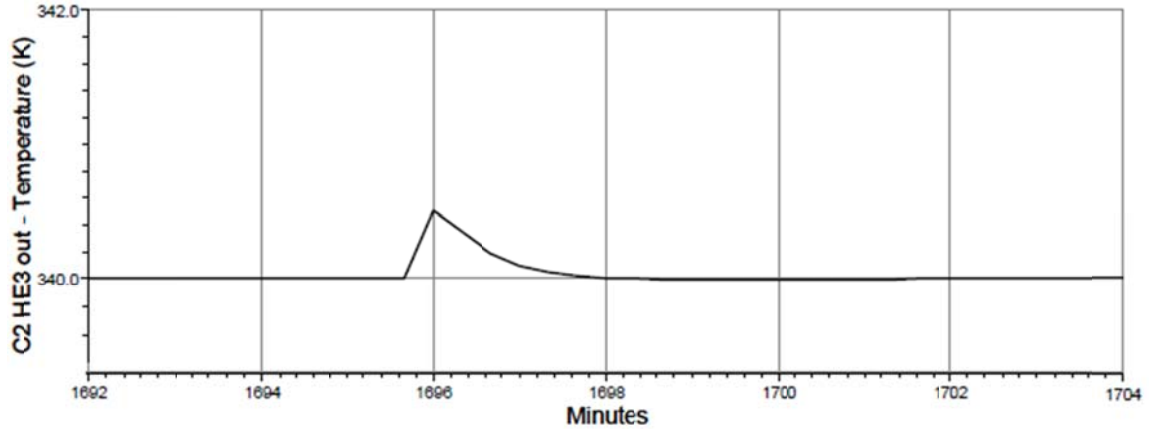


Figure 4.32: C2 outlet temperature reaction to a +1 K step change in C2 inlet temperature of Yan *et al.*'s [18] design.

Table 4.6: Effect of +1 (K) step change in C2 inlet temperature on framework's and Yan *et al.*'s [18] control designs

Step Change	Stream Name	H1			C1			C2		
	Measurement	Set Point Offset (K)	Settling Time (min)	Overshoot (K)	Set Point Offset (K)	Settling Time (min)	Overshoot (K)	Set Point Offset (K)	Settling Time (min)	Overshoot (K)
+1 (K) in C2 Inlet Temperature	Proposed Framework Design	0	0	0	0	0	0	0	16.1	0.55
	Yan <i>et al.</i> 's [18] Design	0	0	0	0	2	0.03	0	6	0.5

4.3.4 Step Change Disturbance in H2 Inlet Temperature

Introducing a positive step change of 5 K in the inlet temperature of H2 causes no change in H1's temperatures nor its controllers' actions in both designs, as H1 is not directly affected by H2. This is clearly shown in Figures 4.33 - 4.36 and summarized in Table 4.7, where both designs show zero set point offsets and do not need any time to stabilize as they have not been affected.

C1 experienced changes in temperatures in both designs due to the fact that the H2 step change directly affects it through HE2. In the framework's design, TIC-101 reacted to the step change by increasing the valve opening of the bypass over HE2 on C1. Yan *et al.*'s [18] design had a similar response of increasing valve opening of the bypass over HE2 on H2. Controller TIC-101 of both design has the same objective of maintaining the set point of C1. The reaction from each design is different because the bypass placements are different, the framework design has the bypass placed on the cold

side, C1 of HE2 and Yan *et al.*'s [18] has the bypass placed on the hot side of HE2, H2. Figures 4.34 and 4.37 show the above behavior. Table 4.7 summarized the findings and shows that the framework design has a better disturbance rejection due to its bigger bypass fractions that allow less saturation of the controllers that occur due to disturbances that are larger than the controller s could handle. The proposed framework design also has a smaller overshoot, however it takes a longer time to respond compared to Yan *et al.*'s [18] design.

Similarly C2 is directly affected by the changes in H2 through HE3. In both designs, TIC-102 aims to control the outlet temperature of C2, and in both designs the controller reacts to increase valve opening on the bypasses to bring C2 outlet temperature back to its set point. Figures 4.35 and 4.38 show the same trend. Table 4.7 summarizes the findings and shows that the framework design is better in term of set point tracking, again due to larger bypass fractions and shows a smaller overshoot. Yan *et al.*'s [18] design is better in terms of the speed needed to stabilize the system. H2's outlet temperature is controlled by the cooler as explained above.

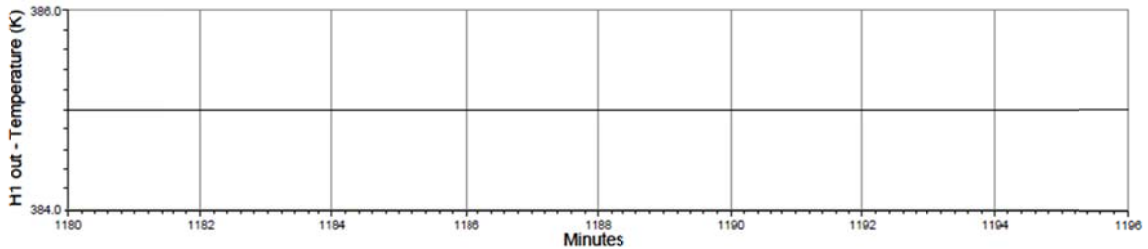


Figure 4.33: H1 outlet temperature reaction to a +5 K step change in H2 inlet temperature of the framework's design.

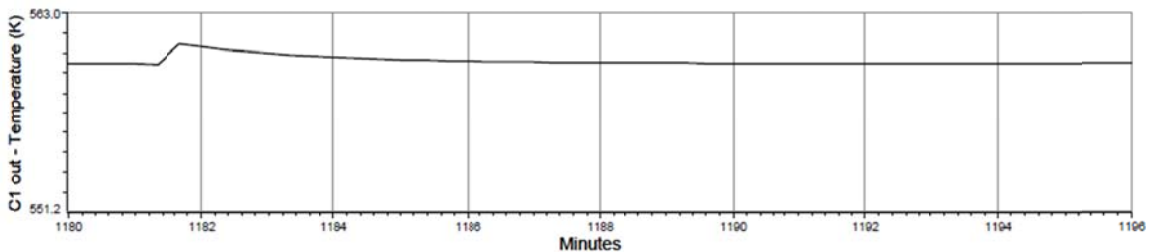


Figure 4.34: C1 outlet temperature reaction to a +5 K step change in H2 inlet temperature of the framework's design.

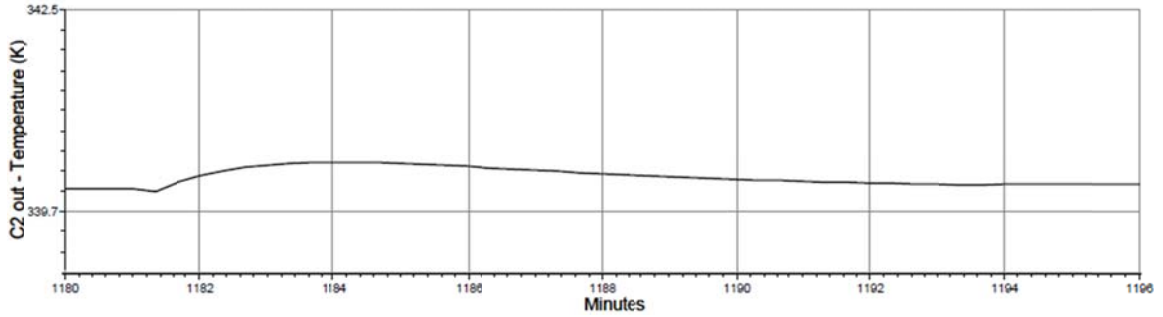


Figure 4.35: C2 outlet temperature reaction to a +5 K step change in H2 inlet temperature of the framework's design.

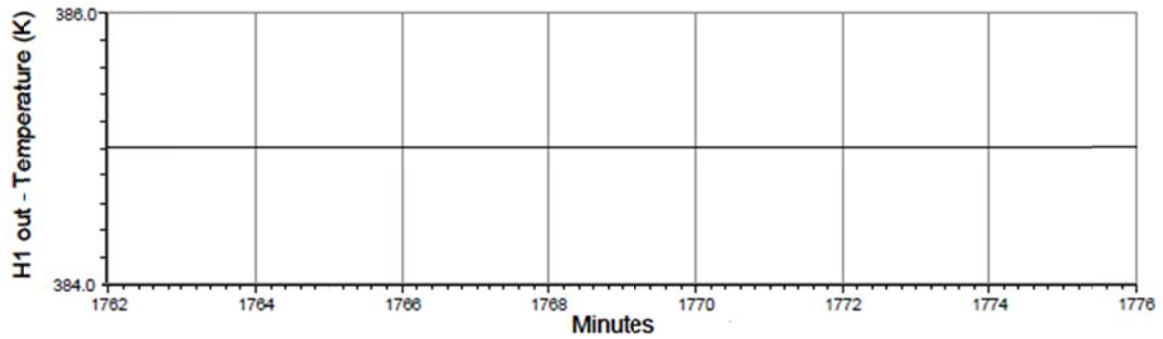


Figure 4.36: H1 outlet temperature reaction to a +5 K step change in H2 inlet temperature of the Yan *et al.*'s [18] design.

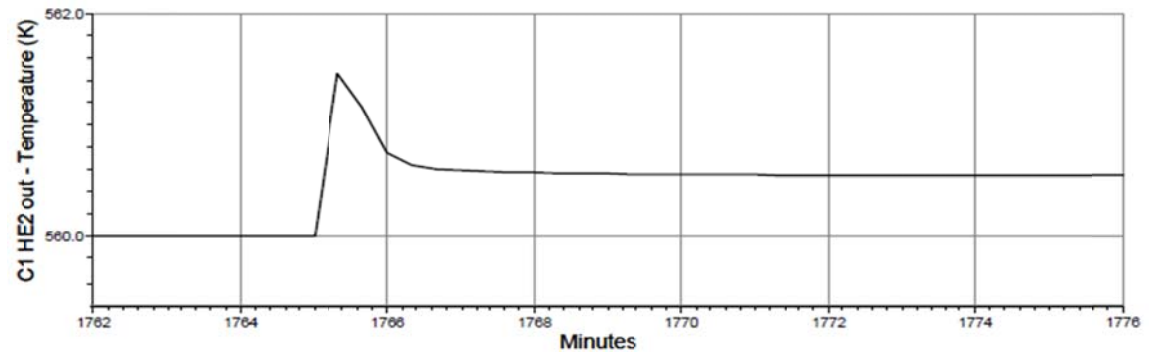


Figure 4.37: C1 outlet temperature reaction to a +5 K step change in H2 inlet temperature of the Yan *et al.*'s [18] design.

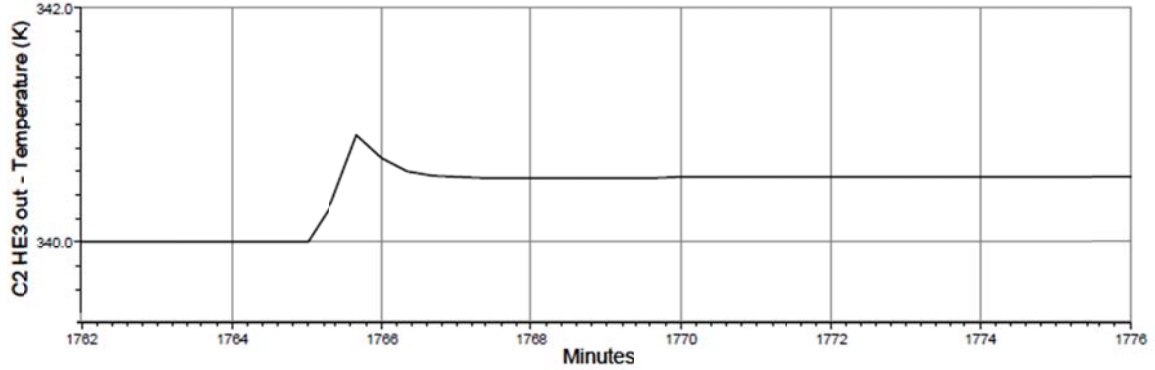


Figure 4.38: C2 outlet temperature reaction to a +5 K step change in H2 inlet temperature of the Yan *et al.*'s [18] design.

Table 4.7: Effect of +5 (K) step change in H2 inlet temperature on framework's and Yan *et al.*'s [18] control designs

Step Change	Stream Name	H1			C1			C2		
	Measurement	Set Point Offset (K)	Settling Time (min)	Overshoot (K)	Set Point Offset (K)	Settling Time (min)	Overshoot (K)	Set Point Offset (K)	Settling Time (min)	Overshoot (K)
+5 (K) in H2 Inlet Temperature	Proposed Framework Design	0	0	0	0	8.5	1	0.1	12.6	0.4
	Yan <i>et al.</i> 's [18] Design	0	0	0	0.5	6.2	1.4	0.6	4.8	1

In conclusion, both the framework and Yan *et al.*'s [18] control designs have performed well in the dynamic sense, in addition to their sound results in the steady-state analysis parameters. Both designs are dynamically successful in bringing their controlled variables back to their set points with a minor offset from the set points and bringing the system back to a steady state behavior in a reasonable amount of time. The general trend shows that the framework's design has a control scheme with a stronger disturbance rejection that has a lower set point offset compared to Yan *et al.*'s [18] design. On the other hand Yan *et al.*'s [18] design response is faster, and able to restore the system's steady state behavior in a shorter time compared to the framework's design. Both designs have very similar overshoot characteristics. Although both systems showed very promising steady state control results of RGA CN of 1 which meant that there are no interactions between the control loops that would affect the controllability of the system. Moreover, Yan *et al.*'s [18] design showed a lower SVD CN which gave an indication that it should be better controlled. This analysis shows that the system that produces the best steady state controllability results is not necessarily the best controlled in the dynamic manner. Due to the higher bypass fractions that the proposed framework design

holds over Yan *et al.*'s [18] design, it allowed the system to react to disturbances with zero offsets from the set point target temperatures. The bigger bypass fractions allowed the controllers to have higher saturation limits to the disturbances. Although the bigger bypasses increased the areas of the heat exchangers and therefore increased the cost of the heat exchanger network as a whole, it managed to control the system in a more efficient manner, allowing the system to operate at its pre-design optimum conditions, satisfying the designed product specifications and ultimately producing higher profits. The set point tracking has holds a higher weight of importance in a real industrial system than the time the system takes to stabilize, given the fact that the time taken to stabilize is still considered realistically acceptable, which is the case in this heat exchanger network. The dynamics of both designs can be improved if more extensive tuning methods are applied to the controllers.

4.4 Exergy Analysis

Exergy is a measure of the maximum available useful energy that can be achieved from a system going from a specified initial state to a final dead state, or an equilibrium state. The exergy at thermodynamic equilibrium is zero. Therefore a process will occur only in the direction of decreasing exergy, or increasing exergy destruction. The main purpose of exergy analyses is to identify the source and magnitude of the energy transfer throughout a process [26, 27].

The framework's design and Yan *et al.*'s [18] design of the HEN under study are investigated and compared in this section in terms of exergy to determine the system with the maximum available useful energy, and therefore the most efficient.

An exergy analysis around each heat exchanger in the heat exchanger network is performed. The exergy destruction rates around the heat exchangers are summed up, and the overall rates of exergy destruction are compared to conclude which design has the lowest loss of work, and therefore is the most efficient. An exergy balance performed on each heat exchanger expresses the exergy destroyed in the system as the difference in exergy of incoming and outgoing streams. The exergy balance for each heat exchanger is given by equation (4.1)

$$e_{HE}^i = \dot{E}_{in} - \dot{E}_{out} = \sum(\dot{m}e)_{in} - \sum(\dot{m}e)_{out} \quad (4.1)$$

where e_{HE}^i is the rate of exergy destruction in heat exchanger i in kW, \dot{E} is the rate of exergy in kW, \dot{m} is the mass flow rate in kg/s, e is the exergy loss in kJ/kg [27]; and “ e ” is the exergy destruction as shown in equation (4.2) as follows:

$$e = (h - h_o) - T_o(s - s_o) + \frac{v^2}{2} + gz \quad (4.2)$$

where h is the mass enthalpy in kJ/kg, h_o is the enthalpy at ambient conditions in kJ/kg, T_o is the ambient temperature in K, s is the specific entropy in kJ/kg.K, s_o is the specific entropy at ambient conditions in kJ/kg.K, v is the velocity in m/s, g is the gravitational constant in m/s², and z is the elevation in m.

Equation (4.3) represents the exergy balance after substituting equation (4.1) into equation (4.1). The terms $\frac{v^2}{2}$ cancel out because there is no change in the mass flow rate nor the pipes sizes either before or after any of the heat exchangers, and therefore the streams’ velocities remain constant. The gz terms cancel out because there is no elevation change within the system and finally h_o and s_o terms simply cancel out.

$$e_{HE}^i = \sum \dot{m}_H [(h_{in} - h_{out}) - T_o(s_{in} - s_{out})]_H + \sum \dot{m}_c [(h_{in} - h_{out}) - T_o(s_{in} - s_{out})]_c \quad (4.3)$$

The above balance was applied to each heat exchanger of the framework’s proposed design and Yan *et al.*’s [18] designs using input from the Aspen HYSYS steady-state simulations. Tables 4.8 and 4.9 show in detail all the values used in equation (4.3) to come up with a final value of the exergy destruction around each design. The cooling utility of the cooler of each design was not considered in the application of the balances, as the boundary of the exergy destruction analysis does not include the cooling utility system, however the hot stream entering and existing the cooler is included in the balance.

Table 4.8: Exergy analysis of the framework's design

	Heat Exchanger 1	Heat Exchanger 2	Heat Exchanger 3	Cooler	Total
Hot Streams					
m (Kg/s)	2.78	5.02	5.02	5.02	
T-in (K)	620	720	529.2	408.4	
T-out (K)	350.8	529.2	408.4	398.3	
h-in (kJ/kg)	-1152	-797.5	-1456	-1792	
h-out (kJ/kg)	-1934	-1456	-1792	-1817	
s-in (kJ/kg.K)	3.57	4.06	3.01	2.29	
s-out (kJ/kg.K)	1.93	3.01	2.29	2.23	
T ⁰ (K)	298	298	298	298	
Cold Streams					
m (Kg/s)	7.98	7.12	12.13		
T-in (K)	300	417.4	280		
T-out (K)	417.4	575.1	345.6		
h-in (kJ/kg)	-2054	-1773	-2086		
h-out (kJ/kg)	-1773	-1308	-1947		
s-in (kJ/kg.K)	1.59	2.35	1.45		
s-out (kJ/kg.K)	2.35	3.29	1.895		
T ⁰ (K)	298	298	298		
Exergy loss (kW)	380.25	418.57	530.62	31.25	1360.69

Table 4.9: Exergy analysis of Yan et al.'s [18] design

	Heat Exchanger 1	Heat Exchanger 2	Heat Exchanger 3	Cooler	Total
Hot Streams					
m (Kg/s)	3.09	4.71	4.46	5.08	
T-in (K)	620	720	533	414.2	
T-out (K)	381.4	516	395.6	404.3	
h-in (kJ/kg)	-1152	-797.5	-1445	-1777	
h-out (kJ/kg)	-1862	-1496	-1824	-1802	
s-in (kJ/kg.K)	3.55	4.06	3.03	2.33	
s-out (kJ/kg.K)	2.12	2.93	2.21	2.26	
T ⁰ (K)	298	298	298	298	
Cold Streams					
m (Kg/s)	7.99	7.99	13.38		
T-in (K)	300	418.4	280		
T-out (K)	418.4	560	340		
h-in (kJ/kg)	-2045	-1770	-2086		
h-out (kJ/kg)	-1770	-1359	-1960		
s-in (kJ/kg.K)	1.59	2.36	1.45		
s-out (kJ/kg.K)	2.36	3.2	1.86		
T ⁰ (K)	298	298	298		
Exergy loss (kW)	513.26	420.06	549.38	34.66	1517.36

Tables 4.8 and 4.9 show that the total exergy destruction from the heat exchanger network, integrated by the framework's design, is lower than that of Yan *et al.*'s [18] design, which implies that the framework's design produces a system that losses less energy and therefore is more efficient in this regard.

Chapter 5: Conclusion and Recommendations

Throughout this research, the framework was formulated to design a heat exchanger network that satisfies all three objectives of attaining best heat recovery, minimizing the capital and utility costs and sufficiently controlling the system, through a series of easy-to-follow steps.

The proposed framework steps start after choosing the heat exchanger network. The heat exchanger network can be chosen from an already designed chemical process where the purpose would be to improve the existing design through heat integration and control measures; or it could be a system that is still in the process of pre-design which comprises of hot and cold streams that need to be matched together.

The most well know methods of heat integration are Pinch and Superstructure methods. Both methods have been proven to meet the maximum energy recovery targets with the minimized costs, which satisfy two out of the three objectives of this research. Pinch design is an older method of heat integration which is based on the optimization of the heat recovery system to attain the design with the minimum annualized cost through defined design steps. The superstructure approach is considered as a more modern way of heat integration based on optimization through Mixed Integer Linear and Non-Linear Programming (MILP and MINLP) to reach the minimum annualized cost. Pinch design is more of a heuristic approach, while superstructure design is based on a programming tool to choose the best matching subject to the constraints set in the program. Pinch design allows the designer to have more control over the stream matching where engineering sense and best practices can be applied. Superstructure is capable of designing large networks with complex constraints; however it is limited to the settings of the solver, eliminating the designer's choice in matching the hot and cold streams. At the early stages of network design, the pinch approach is considered sufficient, whereas in the detailed engineering design stage the superstructure approach would be recommended. The best way to choose which approach to use is to run both of them and to select the system that provides the best heat recovery results along with the most minimized capital and utility costs. When comparing the Superstructure and the Pinch designs for the HEN case study, it was concluded that both designs were able to achieve the heat recovery

targets of the system, however the Superstructure design was able to achieve same heat recovery targets but with lower costs. In terms of steady state controllability, the RGA analysis showed that both designs were able to achieve an RGA CN of 1, however, the Superstructure method achieved a lower SVD CN, which meant that it experienced less inter-loop interactions. The above concludes that for the HEN understudy, the Superstructure heat integration technique managed to achieved a design that is more economical and better controlled in terms of the steady state control parameters.

After deciding on the heat integration model to adopt, that satisfies the heat recovery and the minimized costs objectives, the control parameters need to be set to attain the final objective of controllability. Heat exchanger networks target temperatures are controlled by placing bypasses over the heat exchangers, setting their bypass fractions and placing controllers to alter them accordingly when disturbances arise. Based on the works of Mathisen *et al.* [14], Oliveira *et al.* [8] and Ogunnaike and Ray [22], the proposed framework has set a systematic procedure made out of a series of nine steps to choose the best bypass placement locations. The procedure steps are split into two parts; the first part defines, lists and illustrates all the possible bypass placement scenarios of the HEN under study, while the second part eliminate scenarios based on control heuristics to eventually reach the most preferred controllable scenarios.

Once the most controllable bypass placement scenario is chosen, the bypass fractions are set to complete the design. Mathisen *et al.* [14] claimed that it is safe to assume that any bypass fraction ranging up to 10% of the streams is acceptable, as it does not affect much the controllability measures of HEN. This claim was challenged through rigorous cost and steady state controllability analyses. The controllability and cost analyses results confirmed Mathisen *et al.* 's [14] claim, that choosing any bypass fraction up to 10% does not affect the controllability of the system; and adds to it that the increase in costs incorporated with increasing the bypass fractions are considered to be marginal. Since the controllability is unaffected and the changes in costs are marginal, the chosen bypass fractions for the HEN understudy were chosen to be 10% of the process streams. The reason the bypass fractions were chosen to be on the upper limit is that in the dynamic phase a higher bypass fraction would allow more flexibility for the

controllers to react to any disturbances; this was further analyzed in detail in the dynamic analysis.

The above steps fully satisfy the three objectives of this research, maximum heat recovery, minimized capital and utility costs and a controllable system. The specified control parameters are considered effective in the steady state; however their dynamic effectiveness is not proven. Therefore, it is always recommended to dynamically simulate the controlled system and measure its disturbance rejection, set point tracking, speed to stabilize the system, over shoot behavior and its resiliency. To study the HEN case study dynamically the system was first simulated in the steady state phase. Next the simulation was turned into the dynamic phase by placing control valves, setting their design parameters and tuning them. The controller performances were evaluated by introducing step changes into the inlet temperatures of the system and measuring how the system would react in terms of set point tracking, speed to stabilize the system, over shoot behavior and resiliency. The results showed that although setting bypass fractions of 10% might have marginally increased the capital costs of the system compared to systems with lower bypass fractions, however, it allowed the system to react better to disturbances by achieving smaller offsets from the systems' set points; and therefore satisfying the product specifications of the design. Additionally the speed to stabilize the system and the overshoot behavior were satisfactory. Higher steps changes were introduced to test the control system's resiliency, and the system showed better results compared to a similar system of smaller bypass fractions.

The exergy analysis is not part of the proposed framework, however it is recommended as it would give an indication of the efficiency of the system by measuring the maximum available energy by performing a simple balance. This analysis is not time consuming as all the parameters needed in the balance are readily available from the previous framework steps.

Figures 3.1 to 3.3 illustrate the proposed framework in flowcharts made out of simple easy-to-follow steps. The above steps were formulated by extensively analyzing a case study for heat recovery, cost and control aspects, considering both being steady-state and dynamic analyses. The case study was compared with Yan *et al.*'s [18] and Uturk and Arkam's [23] work, in which the same case study was analyzed with the same

objectives. The framework proved to be an easy-to-follow scheme that attains very good results that matched and sometimes exceeded the results of Yan *et al.*'s [18] programming tool and Uzturk and Arkam's [23] design.

This research is aimed at process engineers who are involved in the conceptual design phase of chemical processes, and therefore the framework is designed to be as a series of easy-to-follow steps. If the framework is expanded to include the detailed engineering design phase of chemical processes it should be developed further with the same approach to include additional analyses.

This research is based on a heuristic approach in choosing the best heat integration method to adopt. In a detailed engineering phase the superstructure analysis should be further analyzed side by side with the best engineering practices. It would be a trial and improvement process to further explore the system for the best hot and cold stream matches where each design of possible matches that fits the system's constraints would be compared in terms of costs and feasibility, and not just the output of the heat integration method or the superstructure programming tool; there would be more designer inputs. This will be most effective in large-scale processes where tens or hundreds of streams are involved and where more constraints need to be added.

Bypass fractions would also become more sensitive in systems of a larger scale. Setting bypass fractions between 0.1 and 10% has been proven in this research for small scale subsystems to have a satisfactory control behavior while not affecting the capital and utility costs in a great manner; however this has not been tested for large scale systems. The analysis of the effect of controllability and cost due to changes in bypass fractions needs to be extended to cover such systems.

In this investigation, the performed dynamic analysis was intended to verify if the implemented steady state control parameters were sufficient enough to act in a dynamic manner. However, if a large scale industrial process was to be considered, the dynamic analysis would need to be extended to include the complex operational constraints. In this case study a number of factors have been assumed or left for HYSYS to calculate such as valve sizing, controller tunings and other factors. In a larger-scale system or project, a more detailed design at each phase of the simulation would be required. Valves would require a detailed analysis to size them before including them in the simulation. A design

of the utility system would be needed to control the coolers and heaters in the system, which would require a detailed control system design. The controllers were left for HYSYS simulator to tune. In a detailed engineering design phase of a project, the controllers would be sized after considering and analyzing different methods of tuning.

Overall a more detailed approach of design and analysis would be needed to extend the current framework if the intention is to use it in a detailed engineering phase of a project.

References

- [1] B. Linhoff, D. W. Townsend, D. Boland, G.F. Hewitt, B.E.A Thomas, A.R. Guy, R.H. Marsland. "A User Guide on Process Integration for the Efficient Use of Energy". *Permagon Press*, 1982
- [2] B. Linhoff, M. Morari, "Design of Resilient Processing Plants I. Process Design under Consideration of Dynamic Aspects" *Ind. Eng. Chem. Res.*, 1982
- [3] R. Turton, R. C. Bailie, W. B. Whiting, J. A. Shaeiwitz. *Analysis, Synthesis, and Design of Chemical Processes 2nd ed.* New Jersey: B.M. Goodwin, 2003, ch. 13, sec. 3, pp. 459-518.
- [4] R. Smith., *Chemical Process Design and Integration*, New Jersey: Wiley, 2005
- [5] W. D. Seider, J. D. Seader, D. R. Lewin and S. Widagdo, *Product and Process Design Principles*, New Jersey, Wiley, 2004.
- [6] P. Alberto, P. and A. Sala. *Multi Variable Control Systems*, London, UK: Springer, 2004
- [7] D. Seborg, T. F. Edgar, D. A. Mellichamp. *Process Dynamics and Control*, 2nd ed. New Jersey: Wiley, 2004
- [8] S.G. Oliviera, F. S. Liporace, O. Q. F. Araujo, E. M. Queiroz. "The Importance of Control Considerations for Heat Exchanger Network Synthesis: A Case Study" *Brazilian Journal of Chemical Engineering*, 2001
- [9] T. McAvoy, "Interaction Analysis", ISA, 1983
- [10] E. H. Bristol, E.H, "On a new measure of interactions for multivariable process control", *IEEE Trans. on Autom. Control*, AC-11, 133–13, 1966.
- [11] D.L. Westphalen, B. R. Young, W. Y. Svrcek, "Strategies for the Operation and Control of Heat Exchanger Networks" *Accepted for presentation at the Foundations of Computer-Aided Process Operations*, 2003

- [12] K. W. Mathisen, S. Skogestad, E. Wolff. “Controllability of Heat Exchanger Network”, *paper 152n presented in at AIChE Annual Meeting*, 1991
- [13] K. W. Mathisen, S. Skogestad, T. Gundersen “Optimal Bypass Placement in Heat Exchanger Networks” *paper 67e presented in at AIChE Annual Meeting*, 1992a
- [14] K. W. Mathisen, S. Skogestad, E. Wolff. “A Bypass Selection for Control of Heat Exchanger Networks” *Presented at the First European Symposium on Computer Aided Process Engineering – ESCAPE 1, Elsinore, Denmark, May 24-28*, 1992b
- [15] K. W. Mathisen, “Integrated Design and Control of Heat Exchanger Networks” Ph.D Thesis, University of Trondheim, 1994
- [16] Alp Er S. Konukman, Ugur Akman, and Mehmet C. Camurdan “Optimal Design of Controllable Heat Exchanger Networks Under Multi-Directional Resiliency Target Constraints” *Computers Chem. Eng. Vol 19 Pergamon*, 1995
- [17] Y. H. Yang, J. P. Gong; and Y. L. Huang. “ A Simplified System Model for Rapid Evaluation of Distribution Propagation through a Heat Exchanger Network” *Ind. Eng. Chem. Res.*, 1996
- [18] Q.Z. Yan, Y. H. Yang and Huang “Cost Effective Bypass Design of Highly Controllable Heat Exchanger Networks” *AIChE Journal*, 2001
- [19] V. Lersbamrungsuk, S. Skogestad and T. Srinophakun “A Simple Strategy for Operation of Heat Exchanger Networks” *International Conference on Modeling in Chemical and Biological Engineering Sciences*, 2006.
- [20] H. Cripps (2014). *Elements of Pinch Analysis*. HRC Consultants Ltd [online]. Available: http://www.hrcconsultants.co.uk/methodology/pinch_analysis.html
- [21] Aspen Energy Analyzer Tutorial Guide, Aspen Tech, 2009.
- [22] B. A. Ogunnaike and W. H. Ray, *Process Dynamics, Modeling and Control* Oxford University Press, New York, 1994

- [23] D. Uzturk and U. Akman, "Centralized and Decentralized Control of Retrofit Heat-Exchanger Networks," *Comput. Chem. Eng.*, 21S373, 1997
- [24] T. F. Yee and I.E Grossman. "Simultaneous Optimization Models for Heat Integration – II. Heat Exchanger Network Synthesis" *Comp. Chem. Eng.*, 1990
- [25] W. D. Seider, J. D. Seader, S. R. Lewin, *Process Design Principles, Simulation of Process Flowsheets: Synthesis, Analysis and Evaluation*, New Jersey: Wiley, 2004
- [26] Y. Cengel, M. R. Boles, *Thermodynamics, An Engineering Approach*, New York, McGraw-Hill, 2011
- [27] A. Ataei and C. Yoo, "Combined pinch and exergy analysis for energy efficiency optimization in a steam power plant" *International Journal of the Physical Sciences Vol. 5(7)*, 2010
- [28] D. L. Westphalen, B. R. Young, and W. Y. Svrcek "A Controllability Index for Heat Exchanger Networks" *Ind. Eng. Chem. Res.*, 2003
- [29] J. Douglas. *Conceptual Design of Chemical Processes*, New York: McGraw-Hill, 1998
- [30] B. R. Young, D. L. Westphalen, and W. Y. Svrcek, "Heat Exchanger Network Dynamic Analysis". *Dev. Chem. Eng. Mineral Process.*, 2006.

Appendix 1: Sample RGA and SVD Analysis MATLAB Files


```
'RGA of 1st K Matrix of Superstrucre-0.1 bypass design'  
K=[160 -30 -40;0 30 -40;0 20 0]  
Ki=inv(K);  
RGA=Ki'.*K  
LtL=RGA'*RGA;  
RGACN=sqrt(max(eig(LtL),[],1))/sqrt(min(eig(LtL),[],1))  
'SVD Anaylisis of 1st K Matrix of Superstrucre-0.1 bypass design'  
[U,S,V]=svd(K)
```

ans =

RGA of 1st K Matrix of Superstrucure-0.1 bypass design

K =

τ_{11}	160	-30	-40
τ_{12}	0	30	-40
τ_{21}	0	20	0

RGA =

	x_1	x_2	x_3
τ_{11}	1	0	0
τ_{12}	0	0	1
τ_{21}	0	1	0

RGACN =

1

ans =

SVD Anaylysis of 1st K Matrix of Superstrucure-0.1 bypass design

U =

τ_{11}	0.9994	-0.0203	-0.0273
	0.0268	0.9646	0.2622
	-0.0210	0.2628	-0.9646

S =

167.7242	0	0
0	51.4656	0
0	0	14.8285

V =

x_1	0.9534	-0.0632	-0.2950
x_2	-0.1765	0.6763	-0.7152
x_3	-0.2447	-0.7339	-0.6336

>> SVDCN=167.7242/14.8285

SVDCN =

11.3109

>>

```
'RGA of 2nd K Matrix of Superstrucure-0.1 bypass design'  
K=[160 -30 -10;0 30 10;0 20 -10]  
Ki=inv(K);  
RGA=Ki'.*K  
LtL=RGA'*RGA;  
RGACN=sqrt(max(eig(LtL),[],1))/sqrt(min(eig(LtL),[],1))  
'SVD Anaylysis of 2nd K Matrix of Superstrucure-0.1 bypass design'  
[U,S,V]=svd(K)
```

ans =

RGA of 2nd K Matrix of Superstrucure-0.1 bypass design

K =

160	-30	-10
0	30	10
0	20	-10

RGA =

	X_1	X_2	X_3
T_{H1}	1.0000	0	0
T_{H2}	0	0.6000	0.4000
T_{C2}	0	0.4000	0.6000

RGACN =

5.0000

ans =

SVD Analysis of 2nd K Matrix of Superstrucure-0.1 bypass design

U =

T_{H1}	0.9990	-0.0439	-0.0040
T_{H2}	-0.0393	-0.8477	-0.5291
T_{C2}	-0.0199	-0.5287	0.8486

S =

163.2462	0	0
0	35.4979	0
0	0	13.8052

V =

X_1	0.9792	-0.1978	-0.0460
X_2	-0.1933	-0.9772	0.0882
X_3	-0.0624	-0.0775	-0.9950

>> SVDCN=163.2462/13.8052

SVDCN =

11.8250

>>

```
'RGA of 3rd K Matrix of Superstrucure-0.1 bypass design'  
K=[160 -40 -10;0 -40 10;0 0 -10]  
Ki=inv(K);  
RGA=Ki'.*K  
LtL=RGA'*RGA;  
RGACN=sqrt(max(eig(LtL), [], 1))/sqrt(min(eig(LtL), [], 1))  
'SVD Anaylysis of 3rd K Matrix of Superstrucure-0.1 bypass design'  
[U,S,V]=svd(K)
```

ans =

RGA of 3rd K Matrix of Superstrucure-0.1 bypass design

K =

160	-40	-10
0	-40	10
0	0	-10

RGA =

	X1	X2	X3
T ₁₁	(1)	0	0
T _{C1}	0	(1)	0
T _{C2}	0	0	(1)

RGACN =

1

ans =

SVD Analysis of 3rd K Matrix of Superstrucure-0.1 bypass design

U =

T ₁₁	(0.9983)	0.0579	-0.0075
T _{C1}	0.0583	(0.9959)	0.0690
T _{C2}	0.0034	0.0693	(0.9976)

S =

165.4929	0	0
0	40.2462	0
0	0	9.6090

V =

X ₁	(0.9652)	0.2302	-0.1244
X ₂	-0.2554	(0.9323)	-0.2562
X ₃	-0.0570	-0.2791	(-0.9586)

>> SVDCN=165.4929/9.6090

SVDCN =

17.2227

>>

```
'RGA of 4th K Matrix of Superstrucre-0.1 bypass design'  
K=[-30 -40 -10;30 -40 10;20 0 -10]  
Ki=inv(K);  
RGA=Ki' .*K  
LtL=RGA'*RGA  
eigLtL=eig(LtL)  
RGACN=sqrt(max(eig(LtL), [], 1))/sqrt(min(eig(LtL), [], 1))  
'SVD Anaylysis of 4th K Matrix of Superstrucre-0.1 bypass design'  
[U,S,V]=svd(K)
```

ans =

RGA of 4th K Matrix of Superstrucure-0.1 bypass design

K =

```
-30  -40  -10
  30  -40   10
  20   0  -10
```

RGA =

	X1	X2	X3
TH2	0.3000	0.5000	0.2000
TC1	0.3000	0.5000	0.2000
TC2	0.4000	0	0.6000

} ?

LtL =

```
0.3400  0.3000  0.3600
0.3000  0.5000  0.2000
0.3600  0.2000  0.4400
```

eigLtL =

```
-0.0000
 0.2800
 1.0000
```

RGACN =

```
0 -1.5663e+008i
```

ans =

SVD Anaylysis of 4th K Matrix of Superstrucure-0.1 bypass design

U =

TH2	0.7071	-0.6572	0.2610
TC1	0.7071	0.6572	-0.2610
TC2	0.0000	0.3690	0.9294

S =

```
56.5685  0  0
 0  47.7575  0
 0  0  14.8062
```


V =

```
x\  0  0.9802  0.1979
x\ -1.0000 -0.0000  0.0000
x\ -0.0000  0.1979 -0.9802
```

```
>> SVDCN=56.5685/14.8062
```

SVDCN =

3.8206

```
>>
```

**Appendix 2: Sample Aspen HX-Net Simulation Report of the Proposed Framework
Design**

1	<p>LEGENDS Calgary, Alberta CANADA</p>	Case Name: e:\thesis 2013\studies\2-studying controllability between superstructure a
2		Unit Set: NewUser
3		Date/Time: Sat Mar 22 10:30:46 2014
4		
5		

HI Design Datasheet

HIP1

Case 1

Design1

Performance

Summary

NETWORK COST INDEXES

	Cost Index	% of Target
20 Heating (Cost/year)	0.0000 *	0.0000 *
21 Cooling (Cost/year)	0.0000 *	0.0000 *
22 Operating Cost (Cost/year)	0.0000 *	0.0000 *
23 Capital Cost (Cost)	97344 *	100.1 *
24 Total Cost (Cost/year)	3.138e+004 *	100.1 *

NETWORK PERFORMANCE

	HEN	% of Target
28 Heating (kJ/h)	0.0000 *	0.0000 *
29 Cooling (kJ/h)	5.394e+005 *	99.88 *
30 Number of Units	4.000 *	100.0 *
31 Number of Shells	6.000 *	100.0 *
32 Total Area (m2)	133.6 *	91.68 *

Heat Exchangers

Heat Exchanger	Cost Index (Cost)	Area (m2)	Shells	Load (kJ/h)
37 HE2	30557 *	48.65 *	2 *	1.026e+007
38 HE3	20388 *	24.65 *	1 *	6.481e+006
39 COOLER	17023 *	15.11	1 *	5.394e+005
40 HE1	29376 *	45.18 *	2 *	8.460e+006
41 Total	97344 *	133.6 *	6 *	2.574e+007 *

Utilities

Utility	Type	Cost Index (Cost/year)	Load (kJ/h)	% of Target
46 Air	COLD	0.0000 *	5.394e+005 *	99.88 *
47 Total		0.0000 *	---	---

WorkSheet

Heat Exchanger	Cold Stream	Cold T in (C)	Tied	Cold T out (C)	Tied	Hot Stream	Hot T in (C)	Tied	Hot T out (C)	Tied	Load (kJ/h)	Area (m2)	Status	dT Min Hot	dT Min Cold
53 HE2	C1	144.3	T	302.7		H2	446.9	T	256.8	T	1.026e+007	48.6 *	Small Status OK	144.2	112.5
54 HE3	C2	6.850	T	73.52		H2	256.8	T	136.8	T	6.481e+006	24.6 *	Small Status OK	183.3	130.0
55 COOLER	Air	30.00		35.00		H2	136.8	T	126.9	T	5.394e+005	15.1	Small Status OK	101.8	96.85
56 HE1	C1	26.85	T	144.3		H1	346.9	T	85.74		8.460e+006	45.2 *	Small Status OK	202.5	58.89

1	LEGENDS Calgary, Alberta CANADA	Case Name: e:\thesis 2013\studies\2-studying controllability between superstructure a
2		Unit Set: NewUser
3		Date/Time: Sat Mar 22 10:30:46 2014
4		

HI Design Datasheet

HIP1

Case 1

Design1

Heat Exchangers

Summary

ALL HEAT EXCHANGERS

Heat Exchanger	Load (kJ/h)	Cost	Area (m2)	Shells	LMTD (C)	HTC (kJ/h-m2-C)	F Factor	Fouling
HE2	1.026e+007	30557 *	48.65 *	2 *	127.7	1800	0.9176	0.0000 *
HE3	6.481e+006	20388 *	24.65 *	1 *	155.1	1800	0.9415	0.0000 *
COOLER	5.394e+005	17023 *	15.11	1 *	99.32	359.7	0.9992	0.0000 *
HE1	8.460e+006	29376 *	45.18 *	2 *	116.3	1800	0.8946	0.0000 *

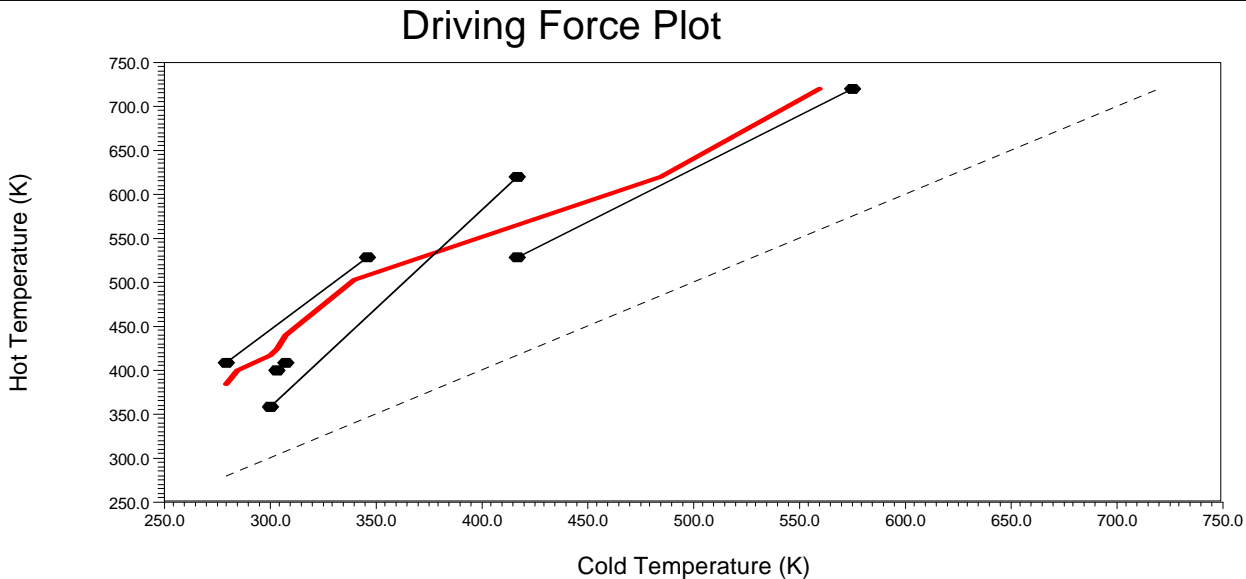
All Heat Exchangers (Continued)

Heat Exchanger	Hot Stream	Hot T in (C)	Hot T out (C)	Cold Stream	Cold T in (C)	Cold T out (C)	dT Min Hot (C)	dT Min Cold (C)
HE2	H2	446.9	256.8	C1	144.3	302.7	144.2	112.5
HE3	H2	256.8	136.8	C2	6.850	73.52	183.3	130.0
COOLER	H2	136.8	126.9	Air	30.00	35.00	101.8	96.85
HE1	H1	346.9	85.74	C1	26.85	144.3	202.5	58.89

HEAT EXCHANGERS FOR STREAM: C2

Heat Exchanger	Load (kJ/h)	Cost Index (Cost)	Area (m2)	Shells	LMTD (C)	HTC (kJ/h-m2-C)	T in (C)	T out (C)	Matched With
HE3	6.481e+006 *	20388 *	24.65 *	1 *	155.1 *	1800 *	6.850 *	73.52 *	H2

DRIVING FORCE PLOT



1	LEGENDS Calgary, Alberta CANADA	Case Name:	e:\thesis 2013\studies\2-studying controllability between superstructure a	
2		Unit Set:	NewUser	
3		Date/Time:	Sat Mar 22 10:30:46 2014	
4				
5				

HI Design Datasheet

HIP1

Case 1

Design1

Targets

15	Heating	0.0000 kJ/h *	Operating Cost Index	---
16	Cooling	5.400e+005 kJ/h *	Capital Cost Index	97239 Cost *
17	Number of Units	4 *	Total Cost Index	3.134e+004 Cost/year *
18	Total Area	145.7 m2 *		

Topology Data

Sub-Networks

24	Number of Sub-Networks	1	*	
25	Network Number	Streams in Network		
26				H1
27				C1
28				H2
29				C2

Loops

32	Independant Loops:	0	*	Dependant Loops:	0	*
33	Loop Number	Exchangers in Loop				
34						

Paths

37	Path Number	Hot Utility	Heat Exchangers in Path	Cold Utility
38				

Utilities

41	Utilities in Design	Utility Included in Searches for Sub-Nets, Loops and Paths
42	Air	Not Included

Notes

Design Notes

Modification Log

Added splitter-mixer TEE-100-MIX-100 manually;Heat exchanger E-100 is added manually;Added splitter-mixer TEE-101-MIX-101 manually;Heat exchanger E-101 is added manually;Added splitter-mixer TEE-102-MIX-102 manually;

Grid Design

Infeasible HX: 0, HX Not Calculated: 0Unsatisfied Streams: 0

Cross Pinch

60	Pinch				
61	Network Cross Pinch Load	(kJ/h)			
62					

1	LEGENDS Calgary, Alberta CANADA	Case Name: e:\thesis 2013\studies\2-studying controllability between superstructure a
2		Unit Set: NewUser
3		Date/Time: Sat Mar 22 10:30:46 2014
4		
5		

HI Design Datasheet

HIP1

Case 1

Design1

Grid Design

Heat Exchanger Status

Degrees of Freedom: 0

Heat Exchangers

Status

Stream Load Status

Streams

Type

Unsatisfied

% of Total

Total

Network Heating

Utility

Type

Cost Index

Load

% of Target

Total

0.0000 *

0.0000 *

0.0000 *

Network Cooling

Utility

Type

Cost Index

Load

% of Target

(Cost/year)

(kJ/h)

Air

COLD

0.0000 *

5.394e+005 *

99.88 *

Total


0.0000 *

5.394e+005 *

99.88 *

Appendix 3: Sample Aspen HYSY Simulation Report of the Proposed Framework

Design


1	 LEGENDS Calgary, Alberta CANADA	Case Name:	E:\THESIS 2013\STUDIES\8- STUDYING DYNAMICS USING HYSYS\1
2		Unit Set:	NewUser
3		Date/Time:	Sat May 03 08:55:09 2014
4			
5			

Workbook: Case (Main)

Material Streams						Fluid Pkg:	All
11	Name	H1 Bypass 1	H1 HE1 in	H1 Bypass 2	H1 HE1 2	C1 HE1 out	
12	Vapour Fraction	0.0000	0.0000	0.0000	0.0000	0.0000	
13	Temperature (K)	619.9	619.9	619.8	350.8	417.4	
14	Pressure (bar)	16.51	16.51	16.00	16.00	7.995	
15	Molar Flow (kgmole/h)	6.756	58.73	6.756	58.73	168.7	
16	Mass Flow (kg/s)	0.319652	2.77870	0.319652	2.77870	7.98153	
17	Liquid Volume Flow (m3/h)	1.532	13.32	1.532	13.32	38.25	
18	Heat Flow (kJ/h)	-1.326e+006	-1.152e+007	-1.326e+006	-1.935e+007	-5.095e+007	
19	Name	H1 out	C1 HE2 in	C1 HE2 Bypass	H2 HE2 out	C1 HE2 out	
20	Vapour Fraction	0.0000	0.0000	0.0000	0.0000	0.0000	
21	Temperature (K)	385.0	417.4	417.4	529.2	575.1	
22	Pressure (bar)	16.00 *	7.995	7.995	49.99	7.500	
23	Molar Flow (kgmole/h)	65.48	150.4	18.28	106.1	150.4	
24	Mass Flow (kg/s)	3.09835	7.11652	0.865009	5.02242	7.11652	
25	Liquid Volume Flow (m3/h)	14.85	34.11	4.146	24.07	34.11	
26	Heat Flow (kJ/h)	-2.067e+007	-4.543e+007	-5.522e+006	-2.633e+007	-3.352e+007	
27	Name	C1 out	C2 HE3 in	C2 HE3 Bypass	C2 HE3 out	H2 HE3 out	
28	Vapour Fraction	0.0000	0.0000	0.0000	0.0000	0.0000	
29	Temperature (K)	560.0	280.0	280.0	345.6	408.4	
30	Pressure (bar)	7.500 *	5.512	5.512	5.000	49.49	
31	Molar Flow (kgmole/h)	168.7	256.3	25.67	256.3	106.1	
32	Mass Flow (kg/s)	7.98153	12.1262	1.21477	12.1262	5.02242	
33	Liquid Volume Flow (m3/h)	38.25	58.12	5.822	58.12	24.07	
34	Heat Flow (kJ/h)	-3.904e+007	-9.107e+007	-9.123e+006	-8.501e+007	-3.240e+007	
35	Name	C2 out	H2 out	C1 HE2 Bypass-2	C2 HE3 Bypass-2	H1	
36	Vapour Fraction	0.0000	0.0000	0.0000	0.0000	0.0000	
37	Temperature (K)	340.0	398.3	417.4	280.1	620.0 *	
38	Pressure (bar)	5.000 *	49.00 *	7.500	5.000	17.00 *	
39	Molar Flow (kgmole/h)	282.0	106.1	18.28	25.67	65.48	
40	Mass Flow (kg/s)	13.3410	5.02242	0.865009	1.21477	3.09835	
41	Liquid Volume Flow (m3/h)	63.94	24.07	4.146	5.822	14.85	
42	Heat Flow (kJ/h)	-9.413e+007	-3.286e+007	-5.522e+006	-9.123e+006	-1.285e+007	
43	Name	H2	C1	C2	H1--1	H2-1	
44	Vapour Fraction	0.0000	0.0000	0.0000	0.0000	0.0000	
45	Temperature (K)	720.0 *	300.0 *	280.0 *	619.9	719.9	
46	Pressure (bar)	51.00 *	9.000 *	6.000 *	16.51	50.50	
47	Molar Flow (kgmole/h)	106.1	168.7	282.0	65.48	106.1	
48	Mass Flow (kg/s)	5.02242	7.98153	13.3410	3.09835	5.02242	
49	Liquid Volume Flow (m3/h)	24.07	38.25	63.94	14.85	24.07	
50	Heat Flow (kJ/h)	-1.442e+007	-5.877e+007	-1.002e+008	-1.285e+007	-1.442e+007	
51	Name	C1-2	C2-1				
52	Vapour Fraction	0.0000	0.0000				
53	Temperature (K)	300.0	280.0				
54	Pressure (bar)	8.497	5.512				
55	Molar Flow (kgmole/h)	168.7	282.0				
56	Mass Flow (kg/s)	7.98153	13.3410				
57	Liquid Volume Flow (m3/h)	38.25	63.94				
58	Heat Flow (kJ/h)	-5.877e+007	-1.002e+008				

Compositions

Compositions						Fluid Pkg:	All
61	Name	H1 Bypass 1	H1 HE1 in	H1 Bypass 2	H1 HE1 2	C1 HE1 out	
62	Comp Mole Frac (n-C12)	1.0000	1.0000	1.0000	1.0000	1.0000	

1	 LEGENDS Calgary, Alberta CANADA	Case Name: E:\THESIS 2013\STUDIES\8- STUDYING DYNAMICS USING HYSYS\1
2		Unit Set: NewUser
3		Date/Time: Sat May 03 08:55:09 2014
4		
5		

Workbook: Case (Main) (continued)

Compositions (continued)

Fluid Pkg: All

Name	H1 out	C1 HE2 in	C1 HE2 Bypass	H2 HE2 out	C1 HE2 out
Comp Mole Frac (n-C12)	1.0000	1.0000	1.0000	1.0000	1.0000
Name	C1 out	C2 HE3 in	C2 HE3 Bypass	C2 HE3 out	H2 HE3 out
Comp Mole Frac (n-C12)	1.0000	1.0000	1.0000	1.0000	1.0000
Name	C2 out	H2 out	C1 HE2 Bypass-2	C2 HE3 Bypass-2	H1
Comp Mole Frac (n-C12)	1.0000	1.0000	1.0000	1.0000	1.0000 *
Name	H2	C1	C2	H1--1	H2-1
Comp Mole Frac (n-C12)	1.0000 *	1.0000 *	1.0000 *	1.0000	1.0000
Name	C1-2	C2-1			
Comp Mole Frac (n-C12)	1.0000	1.0000			


Energy Streams

Fluid Pkg: All

Name	QCooler			
Heat Flow (kJ/h)	4.605e+005 *			

Unit Ops

Operation Name	Operation Type	Feeds	Products	Ignored	Calc Level
TEE-100	Tee	H1--1	H1 Bypass 1	No	500.0 *
			H1 HE1 in		
TEE-101	Tee	C1 HE1 out	C1 HE2 in	No	500.0 *
			C1 HE2 Bypass		
TEE-102	Tee	C2-1	C2 HE3 in	No	500.0 *
			C2 HE3 Bypass		
VLV-100	Valve	H1 Bypass 1	H1 Bypass 2	No	500.0 *
VLV-101	Valve	C1 HE2 Bypass	C1 HE2 Bypass-2	No	500.0 *
VLV-102	Valve	C2 HE3 Bypass	C2 HE3 Bypass-2	No	500.0 *
VLV-103	Valve	H1	H1--1	No	500.0 *
VLV-104	Valve	H2	H2-1	No	500.0 *
VLV-105	Valve	C1	C1-2	No	500.0 *
VLV-106	Valve	C2	C2-1	No	500.0 *
HE1	Heat Exchanger	H1 HE1 in	H1 HE1 2	No	500.0 *
		C1-2	C1 HE1 out		
HE2	Heat Exchanger	H2-1	H2 HE2 out	No	500.0 *
		C1 HE2 in	C1 HE2 out		
E-100	Heat Exchanger	H2 HE2 out	H2 HE3 out	No	500.0 *
		C2 HE3 in	C2 HE3 out		
MIX-100	Mixer	H1 Bypass 2	H1 out	No	500.0 *
			H1 HE1 2		
MIX-101	Mixer	C1 HE2 out	C1 out	No	500.0 *
			C1 HE2 Bypass-2		
MIX-102	Mixer	C2 HE3 out	C2 out	No	500.0 *
			C2 HE3 Bypass-2		
Cooler	Cooler	H2 HE3 out	H2 out	No	500.0 *
			QCooler		
TIC-100	PID Controller			No	500.0 *
TIC-101	PID Controller			No	500.0 *
TIC-102	PID Controller			No	500.0 *
FIC-100	PID Controller			No	500.0 *
FIC-101	PID Controller			No	500.0 *
FIC-102	PID Controller			No	500.0 *
FIC-103	PID Controller			No	500.0 *

1	 LEGENDS Calgary, Alberta CANADA	Case Name:	E:\THESIS 2013\STUDIES\8- STUDYING DYNAMICS USING HYSYS\1
2		Unit Set:	NewUser
3		Date/Time:	Sat May 03 08:55:09 2014
4			
5			


Tee: TEE-100

CONDITIONS

11	Name	H1--1	H1 Bypass 1	H1 HE1 in
12	Vapour	0.0000	0.0000	0.0000
13	Temperature (K)	619.9065	619.9065	619.9065
14	Pressure (bar)	16.5090	16.5090	16.5090
15	Molar Flow (kgmole/h)	65.4815	6.7556	58.7259
16	Mass Flow (kg/s)	3.0983	0.3197	2.7787
17	Std Ideal Liq Vol Flow (m3/h)	14.8494	1.5320	13.3174
18	Molar Enthalpy (kJ/kgmole)	-1.962e+005	-1.962e+005	-1.962e+005
19	Molar Entropy (kJ/kgmole-C)	604.2	604.2	604.2
20	Heat Flow (kJ/h)	-1.2849e+07	-1.3256e+06	-1.1523e+07

PROPERTIES

23	Name	H1--1	H1 Bypass 1	H1 HE1 in
24	Molecular Weight	170.3	170.3	170.3
25	Molar Density (kgmole/m3)	2.599	2.599	2.599
26	Mass Density (kg/m3)	442.7	442.7	442.7
27	Act. Volume Flow (m3/h)	25.20	2.599	22.60
28	Mass Enthalpy (kJ/kg)	-1152	-1152	-1152
29	Mass Entropy (kJ/kg-K)	3.547	3.547	3.547
30	Heat Capacity (kJ/kgmole-C)	644.9	644.9	644.9
31	Mass Heat Capacity (kJ/kg-K)	3.786	3.786	3.786
32	Lower Heating Value (kJ/kgmole)	7.579e+006	7.579e+006	7.579e+006
33	Mass Lower Heating Value (kJ/kg)	4.449e+004	4.449e+004	4.449e+004
34	Phase Fraction [Vol. Basis]	---	---	---
35	Phase Fraction [Mass Basis]	2.122e-314	2.122e-314	2.122e-314
36	Partial Pressure of CO2 (bar)	0.0000	0.0000	0.0000
37	Cost Based on Flow (Cost/s)	0.0000	0.0000	0.0000
38	Act. Gas Flow (ACT_m3/h)	---	---	---
39	Avg. Liq. Density (kgmole/m3)	4.410	4.410	4.410
40	Specific Heat (kJ/kgmole-C)	644.9	644.9	644.9
41	Std. Gas Flow (STD_m3/h)	1548	159.7	1389
42	Std. Ideal Liq. Mass Density (kg/m3)	751.1	751.1	751.1
43	Act. Liq. Flow (m3/s)	6.999e-003	7.221e-004	6.277e-003
44	Z Factor	---	---	---
45	Watson K	12.74	12.74	12.74
46	User Property	---	---	---
47	Partial Pressure of H2S (bar)	0.0000	0.0000	0.0000
48	Cp/(Cp - R)	1.013	1.013	1.013
49	Cp/Cv	1.188	1.188	1.188
50	Heat of Vap. (kJ/kgmole)	1.128e+004	1.128e+004	1.128e+004
51	Kinematic Viscosity (cSt)	0.1808	0.1808	0.1808
52	Liq. Mass Density (Std. Cond) (kg/m3)	753.0	753.0	753.0
53	Liq. Vol. Flow (Std. Cond) (m3/h)	14.81	1.528	13.28
54	Liquid Fraction	1.000	1.000	1.000
55	Molar Volume (m3/kgmole)	0.3848	0.3848	0.3848
56	Mass Heat of Vap. (kJ/kg)	66.21	66.21	66.21
57	Phase Fraction [Molar Basis]	0.0000	0.0000	0.0000
58	Surface Tension (dyne/cm)	1.582	1.582	1.582
59	Thermal Conductivity (W/m-K)	5.257e-002	5.257e-002	5.257e-002
60	Viscosity (cP)	8.002e-002	8.002e-002	8.002e-002
61	Cv (Semi-Ideal) (kJ/kgmole-C)	636.6	636.6	636.6
62	Mass Cv (Semi-Ideal) (kJ/kg-K)	3.737	3.737	3.737

1	 LEGENDS Calgary, Alberta CANADA	Case Name:	E:\THESIS 2013\STUDIES\8- STUDYING DYNAMICS USING HYSYS\C1
2		Unit Set:	NewUser
3		Date/Time:	Sat May 03 08:55:09 2014
4			
5			

Tee: TEE-100 (continued)

PROPERTIES

11	Name	H1--1	H1 Bypass 1	H1 HE1 in	
12	Cv (kJ/kgmole-C)	542.9	542.9	542.9	
13	Mass Cv (kJ/kg-K)	3.187	3.187	3.187	
14	Cv (Ent. Method) (kJ/kgmole-C)	---	---	---	
15	Mass Cv (Ent. Method) (kJ/kg-K)	---	---	---	
16	Cp/Cv (Ent. Method)	---	---	---	
17	Reid VP at 37.8 C (bar)	---	---	---	
18	True VP at 37.8 C (bar)	6.294e-004	6.294e-004	6.294e-004	
19	Liq. Vol. Flow - Sum(Std. Cond) (m3/h)	14.81	1.528	13.28	


Tee: TEE-101

CONDITIONS

25	Name	C1 HE1 out	C1 HE2 in	C1 HE2 Bypass	
26	Vapour	0.0000	0.0000	0.0000	
27	Temperature (K)	417.3812	417.3812	417.3812	
28	Pressure (bar)	7.9946	7.9946	7.9946	
29	Molar Flow (kgmole/h)	168.6843	150.4029	18.2814	
30	Mass Flow (kg/s)	7.9815	7.1165	0.8650	
31	Std Ideal Liq Vol Flow (m3/h)	38.2529	34.1072	4.1457	
32	Molar Enthalpy (kJ/kgmole)	-3.020e+005	-3.020e+005	-3.020e+005	
33	Molar Entropy (kJ/kgmole-C)	400.4	400.4	400.4	
34	Heat Flow (kJ/h)	-5.0949e+07	-4.5427e+07	-5.5217e+06	

PROPERTIES

37	Name	C1 HE1 out	C1 HE2 in	C1 HE2 Bypass	
38	Molecular Weight	170.3	170.3	170.3	
39	Molar Density (kgmole/m3)	3.848	3.848	3.848	
40	Mass Density (kg/m3)	655.5	655.5	655.5	
41	Act. Volume Flow (m3/h)	43.84	39.09	4.751	
42	Mass Enthalpy (kJ/kg)	-1773	-1773	-1773	
43	Mass Entropy (kJ/kg-K)	2.351	2.351	2.351	
44	Heat Capacity (kJ/kgmole-C)	439.3	439.3	439.3	
45	Mass Heat Capacity (kJ/kg-K)	2.579	2.579	2.579	
46	Lower Heating Value (kJ/kgmole)	7.579e+006	7.579e+006	7.579e+006	
47	Mass Lower Heating Value (kJ/kg)	4.449e+004	4.449e+004	4.449e+004	
48	Phase Fraction [Vol. Basis]	---	---	---	
49	Phase Fraction [Mass Basis]	2.122e-314	2.122e-314	2.122e-314	
50	Partial Pressure of CO2 (bar)	0.0000	0.0000	0.0000	
51	Cost Based on Flow (Cost/s)	0.0000	0.0000	0.0000	
52	Act. Gas Flow (ACT_m3/h)	---	---	---	
53	Avg. Liq. Density (kgmole/m3)	4.410	4.410	4.410	
54	Specific Heat (kJ/kgmole-C)	439.3	439.3	439.3	
55	Std. Gas Flow (STD_m3/h)	3988	3556	432.3	
56	Std. Ideal Liq. Mass Density (kg/m3)	751.1	751.1	751.1	
57	Act. Liq. Flow (m3/s)	1.218e-002	1.086e-002	1.320e-003	
58	Z Factor	---	---	---	
59	Watson K	12.74	12.74	12.74	
60	User Property	---	---	---	
61	Partial Pressure of H2S (bar)	0.0000	0.0000	0.0000	
62	Cp/(Cp - R)	1.019	1.019	1.019	

1	 LEGENDS Calgary, Alberta CANADA	Case Name:	E:\THESIS 2013\STUDIES\8- STUDYING DYNAMICS USING HYSYS\C1
2		Unit Set:	NewUser
3		Date/Time:	Sat May 03 08:55:09 2014
4			
5			

Tee: TEE-101 (continued)

PROPERTIES

11	Name	C1 HE1 out	C1 HE2 in	C1 HE2 Bypass	
12	Cp/Cv	1.134	1.134	1.134	
13	Heat of Vap. (kJ/kgmole)	2.902e+004	2.902e+004	2.902e+004	
14	Kinematic Viscosity (cSt)	0.5204	0.5204	0.5204	
15	Liq. Mass Density (Std. Cond) (kg/m3)	753.0	753.0	753.0	
16	Liq. Vol. Flow (Std. Cond) (m3/h)	38.16	34.02	4.135	
17	Liquid Fraction	1.000	1.000	1.000	
18	Molar Volume (m3/kgmole)	0.2599	0.2599	0.2599	
19	Mass Heat of Vap. (kJ/kg)	170.4	170.4	170.4	
20	Phase Fraction [Molar Basis]	0.0000	0.0000	0.0000	
21	Surface Tension (dyne/cm)	14.93	14.93	14.93	
22	Thermal Conductivity (W/m-K)	0.1097	0.1097	0.1097	
23	Viscosity (cP)	0.3411	0.3411	0.3411	
24	Cv (Semi-Ideal) (kJ/kgmole-C)	431.0	431.0	431.0	
25	Mass Cv (Semi-Ideal) (kJ/kg-K)	2.530	2.530	2.530	
26	Cv (kJ/kgmole-C)	387.3	387.3	387.3	
27	Mass Cv (kJ/kg-K)	2.274	2.274	2.274	
28	Cv (Ent. Method) (kJ/kgmole-C)	---	---	---	
29	Mass Cv (Ent. Method) (kJ/kg-K)	---	---	---	
30	Cp/Cv (Ent. Method)	---	---	---	
31	Reid VP at 37.8 C (bar)	---	---	---	
32	True VP at 37.8 C (bar)	6.294e-004	6.294e-004	6.294e-004	
33	Liq. Vol. Flow - Sum(Std. Cond) (m3/h)	38.16	34.02	4.135	


Tee: TEE-102

CONDITIONS

39	Name	C2-1	C2 HE3 in	C2 HE3 Bypass	
40	Vapour	0.0000	0.0000	0.0000	
41	Temperature (K)	280.0315	280.0315	280.0315	
42	Pressure (bar)	5.5120	5.5120	5.5120	
43	Molar Flow (kgmole/h)	281.9530	256.2797	25.6733	
44	Mass Flow (kg/s)	13.3410	12.1262	1.2148	
45	Std Ideal Liq Vol Flow (m3/h)	63.9392	58.1172	5.8220	
46	Molar Enthalpy (kJ/kgmole)	-3.554e+005	-3.554e+005	-3.554e+005	
47	Molar Entropy (kJ/kgmole-C)	247.0	247.0	247.0	
48	Heat Flow (kJ/h)	-1.0019e+08	-9.1071e+07	-9.1232e+06	

PROPERTIES

51	Name	C2-1	C2 HE3 in	C2 HE3 Bypass	
52	Molecular Weight	170.3	170.3	170.3	
53	Molar Density (kgmole/m3)	4.458	4.458	4.458	
54	Mass Density (kg/m3)	759.4	759.4	759.4	
55	Act. Volume Flow (m3/h)	63.24	57.48	5.759	
56	Mass Enthalpy (kJ/kg)	-2086	-2086	-2086	
57	Mass Entropy (kJ/kg-K)	1.450	1.450	1.450	
58	Heat Capacity (kJ/kgmole-C)	335.7	335.7	335.7	
59	Mass Heat Capacity (kJ/kg-K)	1.971	1.971	1.971	
60	Lower Heating Value (kJ/kgmole)	7.579e+006	7.579e+006	7.579e+006	
61	Mass Lower Heating Value (kJ/kg)	4.449e+004	4.449e+004	4.449e+004	
62	Phase Fraction [Vol. Basis]	---	---	---	

1	 LEGENDS Calgary, Alberta CANADA	Case Name: E:\THESIS 2013\STUDIES\8- STUDYING DYNAMICS USING HYSYS\C1
2		Unit Set: NewUser
3		Date/Time: Sat May 03 08:55:09 2014
4		
5		

Tee: TEE-102 (continued)


PROPERTIES

11	Name	C2-1	C2 HE3 in	C2 HE3 Bypass	
12	Phase Fraction [Mass Basis]	2.122e-314	2.122e-314	2.122e-314	
13	Partial Pressure of CO2 (bar)	0.0000	0.0000	0.0000	
14	Cost Based on Flow (Cost/s)	0.0000	0.0000	0.0000	
15	Act. Gas Flow (ACT_m3/h)	---	---	---	
16	Avg. Liq. Density (kgmole/m3)	4.410	4.410	4.410	
17	Specific Heat (kJ/kgmole-C)	335.7	335.7	335.7	
18	Std. Gas Flow (STD_m3/h)	6667	6060	607.0	
19	Std. Ideal Liq. Mass Density (kg/m3)	751.1	751.1	751.1	
20	Act. Liq. Flow (m3/s)	1.757e-002	1.597e-002	1.600e-003	
21	Z Factor	---	---	---	
22	Watson K	12.74	12.74	12.74	
23	User Property	---	---	---	
24	Partial Pressure of H2S (bar)	0.0000	0.0000	0.0000	
25	Cp/(Cp - R)	1.025	1.025	1.025	
26	Cp/Cv	1.134	1.134	1.134	
27	Heat of Vap. (kJ/kgmole)	3.342e+004	3.342e+004	3.342e+004	
28	Kinematic Viscosity (cSt)	2.370	2.370	2.370	
29	Liq. Mass Density (Std. Cond) (kg/m3)	753.0	753.0	753.0	
30	Liq. Vol. Flow (Std. Cond) (m3/h)	63.78	57.97	5.807	
31	Liquid Fraction	1.000	1.000	1.000	
32	Molar Volume (m3/kgmole)	0.2243	0.2243	0.2243	
33	Mass Heat of Vap. (kJ/kg)	196.2	196.2	196.2	
34	Phase Fraction [Molar Basis]	0.0000	0.0000	0.0000	
35	Surface Tension (dyne/cm)	25.92	25.92	25.92	
36	Thermal Conductivity (W/m-K)	0.1395	0.1395	0.1395	
37	Viscosity (cP)	1.800	1.800	1.800	
38	Cv (Semi-Ideal) (kJ/kgmole-C)	327.4	327.4	327.4	
39	Mass Cv (Semi-Ideal) (kJ/kg-K)	1.922	1.922	1.922	
40	Cv (kJ/kgmole-C)	296.1	296.1	296.1	
41	Mass Cv (kJ/kg-K)	1.738	1.738	1.738	
42	Cv (Ent. Method) (kJ/kgmole-C)	---	---	---	
43	Mass Cv (Ent. Method) (kJ/kg-K)	---	---	---	
44	Cp/Cv (Ent. Method)	---	---	---	
45	Reid VP at 37.8 C (bar)	---	---	---	
46	True VP at 37.8 C (bar)	6.294e-004	6.294e-004	6.294e-004	
47	Liq. Vol. Flow - Sum(Std. Cond) (m3/h)	63.78	57.97	5.807	

Valve: VLV-100

CONDITIONS


53	Name	H1 Bypass 1	H1 Bypass 2	
54	Vapour	0.0000	0.0000	
55	Temperature (K)	619.9065	619.8070	
56	Pressure (bar)	16.5090	16.0000	
57	Molar Flow (kgmole/h)	6.7556	6.7556	
58	Mass Flow (kg/s)	0.3197	0.3197	
59	Std Ideal Liq Vol Flow (m3/h)	1.5320	1.5320	
60	Molar Enthalpy (kJ/kgmole)	-1.962e+005	-1.962e+005	
61	Molar Entropy (kJ/kgmole-C)	604.2	604.2	
62	Heat Flow (kJ/h)	-1.3256e+06	-1.3256e+06	

1	 LEGENDS Calgary, Alberta CANADA	Case Name: E:\THESIS 2013\STUDIES\8- STUDYING DYNAMICS USING HYSYS\C1
2		Unit Set: NewUser
3		Date/Time: Sat May 03 08:55:09 2014
4		
5		

Valve: VLV-100 (continued)

PROPERTIES

11	Name	H1 Bypass 1	H1 Bypass 2		
12	Molecular Weight	170.3	170.3		
13	Molar Density (kgmole/m3)	2.599	2.594		
14	Mass Density (kg/m3)	442.7	441.9		
15	Act. Volume Flow (m3/h)	2.599	2.604		
16	Mass Enthalpy (kJ/kg)	-1152	-1152		
17	Mass Entropy (kJ/kg-K)	3.547	3.547		
18	Heat Capacity (kJ/kgmole-C)	644.9	647.2		
19	Mass Heat Capacity (kJ/kg-K)	3.786	3.799		
20	Lower Heating Value (kJ/kgmole)	7.579e+006	7.579e+006		
21	Mass Lower Heating Value (kJ/kg)	4.449e+004	4.449e+004		
22	Phase Fraction [Vol. Basis]	---	---		
23	Phase Fraction [Mass Basis]	2.122e-314	2.122e-314		
24	Partial Pressure of CO2 (bar)	0.0000	0.0000		
25	Cost Based on Flow (Cost/s)	0.0000	0.0000		
26	Act. Gas Flow (ACT_m3/h)	---	---		
27	Avg. Liq. Density (kgmole/m3)	4.410	4.410		
28	Specific Heat (kJ/kgmole-C)	644.9	647.2		
29	Std. Gas Flow (STD_m3/h)	159.7	159.7		
30	Std. Ideal Liq. Mass Density (kg/m3)	751.1	751.1		
31	Act. Liq. Flow (m3/s)	7.221e-004	7.234e-004		
32	Z Factor	---	---		
33	Watson K	12.74	12.74		
34	User Property	---	---		
35	Partial Pressure of H2S (bar)	0.0000	0.0000		
36	Cp/(Cp - R)	1.013	1.013		
37	Cp/Cv	1.188	1.189		
38	Heat of Vap. (kJ/kgmole)	1.128e+004	1.282e+004		
39	Kinematic Viscosity (cSt)	0.1808	0.1810		
40	Liq. Mass Density (Std. Cond) (kg/m3)	753.0	753.0		
41	Liq. Vol. Flow (Std. Cond) (m3/h)	1.528	1.528		
42	Liquid Fraction	1.000	1.000		
43	Molar Volume (m3/kgmole)	0.3848	0.3855		
44	Mass Heat of Vap. (kJ/kg)	66.21	75.27		
45	Phase Fraction [Molar Basis]	0.0000	0.0000		
46	Surface Tension (dyne/cm)	1.582	1.587		
47	Thermal Conductivity (W/m-K)	5.257e-002	5.262e-002		
48	Viscosity (cP)	8.002e-002	7.996e-002		
49	Cv (Semi-Ideal) (kJ/kgmole-C)	636.6	638.9		
50	Mass Cv (Semi-Ideal) (kJ/kg-K)	3.737	3.751		
51	Cv (kJ/kgmole-C)	542.9	544.3		
52	Mass Cv (kJ/kg-K)	3.187	3.195		
53	Cv (Ent. Method) (kJ/kgmole-C)	---	---		
54	Mass Cv (Ent. Method) (kJ/kg-K)	---	---		
55	Cp/Cv (Ent. Method)	---	---		
56	Reid VP at 37.8 C (bar)	---	---		
57	True VP at 37.8 C (bar)	6.294e-004	6.294e-004		
58	Liq. Vol. Flow - Sum(Std. Cond) (m3/h)	1.528	1.528		

1	 LEGENDS Calgary, Alberta CANADA	Case Name: E:\THESIS 2013\STUDIES\8- STUDYING DYNAMICS USING HYSYS\C1
2		Unit Set: NewUser
3		Date/Time: Sat May 03 08:55:09 2014
4		
5		


Valve: VLV-101

CONDITIONS

11	Name	C1 HE2 Bypass	C1 HE2 Bypass-2		
12	Vapour	0.0000	0.0000		
13	Temperature (K)	417.3812	417.3997		
14	Pressure (bar)	7.9946	7.5000		
15	Molar Flow (kgmole/h)	18.2814	18.2814		
16	Mass Flow (kg/s)	0.8650	0.8650		
17	Std Ideal Liq Vol Flow (m3/h)	4.1457	4.1457		
18	Molar Enthalpy (kJ/kgmole)	-3.020e+005	-3.020e+005		
19	Molar Entropy (kJ/kgmole-C)	400.4	400.4		
20	Heat Flow (kJ/h)	-5.5217e+06	-5.5217e+06		

PROPERTIES

23	Name	C1 HE2 Bypass	C1 HE2 Bypass-2		
24	Molecular Weight	170.3	170.3		
25	Molar Density (kgmole/m3)	3.848	3.847		
26	Mass Density (kg/m3)	655.5	655.4		
27	Act. Volume Flow (m3/h)	4.751	4.752		
28	Mass Enthalpy (kJ/kg)	-1773	-1773		
29	Mass Entropy (kJ/kg-K)	2.351	2.351		
30	Heat Capacity (kJ/kgmole-C)	439.3	439.3		
31	Mass Heat Capacity (kJ/kg-K)	2.579	2.579		
32	Lower Heating Value (kJ/kgmole)	7.579e+006	7.579e+006		
33	Mass Lower Heating Value (kJ/kg)	4.449e+004	4.449e+004		
34	Phase Fraction [Vol. Basis]	---	---		
35	Phase Fraction [Mass Basis]	2.122e-314	2.122e-314		
36	Partial Pressure of CO2 (bar)	0.0000	0.0000		
37	Cost Based on Flow (Cost/s)	0.0000	0.0000		
38	Act. Gas Flow (ACT_m3/h)	---	---		
39	Avg. Liq. Density (kgmole/m3)	4.410	4.410		
40	Specific Heat (kJ/kgmole-C)	439.3	439.3		
41	Std. Gas Flow (STD_m3/h)	432.3	432.3		
42	Std. Ideal Liq. Mass Density (kg/m3)	751.1	751.1		
43	Act. Liq. Flow (m3/s)	1.320e-003	1.320e-003		
44	Z Factor	---	---		
45	Watson K	12.74	12.74		
46	User Property	---	---		
47	Partial Pressure of H2S (bar)	0.0000	0.0000		
48	Cp/(Cp - R)	1.019	1.019		
49	Cp/Cv	1.134	1.134		
50	Heat of Vap. (kJ/kgmole)	2.902e+004	2.988e+004		
51	Kinematic Viscosity (cSt)	0.5204	0.5204		
52	Liq. Mass Density (Std. Cond) (kg/m3)	753.0	753.0		
53	Liq. Vol. Flow (Std. Cond) (m3/h)	4.135	4.135		
54	Liquid Fraction	1.000	1.000		
55	Molar Volume (m3/kgmole)	0.2599	0.2599		
56	Mass Heat of Vap. (kJ/kg)	170.4	175.4		
57	Phase Fraction [Molar Basis]	0.0000	0.0000		
58	Surface Tension (dyne/cm)	14.93	14.93		
59	Thermal Conductivity (W/m-K)	0.1097	0.1097		
60	Viscosity (cP)	0.3411	0.3410		
61	Cv (Semi-Ideal) (kJ/kgmole-C)	431.0	431.0		
62	Mass Cv (Semi-Ideal) (kJ/kg-K)	2.530	2.530		

1	 LEGENDS Calgary, Alberta CANADA	Case Name: E:\THESIS 2013\STUDIES\8- STUDYING DYNAMICS USING HYSYS\C1
2		Unit Set: NewUser
3		Date/Time: Sat May 03 08:55:09 2014
4		
5		

Valve: VLV-101 (continued)

PROPERTIES

11	Name	C1 HE2 Bypass	C1 HE2 Bypass-2		
12	Cv (kJ/kgmole-C)	387.3	387.3		
13	Mass Cv (kJ/kg-K)	2.274	2.274		
14	Cv (Ent. Method) (kJ/kgmole-C)	---	---		
15	Mass Cv (Ent. Method) (kJ/kg-K)	---	---		
16	Cp/Cv (Ent. Method)	---	---		
17	Reid VP at 37.8 C (bar)	---	---		
18	True VP at 37.8 C (bar)	6.294e-004	6.294e-004		
19	Liq. Vol. Flow - Sum(Std. Cond) (m3/h)	4.135	4.135		


Valve: VLV-102

CONDITIONS

25	Name	C2 HE3 Bypass	C2 HE3 Bypass-2		
26	Vapour	0.0000	0.0000		
27	Temperature (K)	280.0315	280.0645		
28	Pressure (bar)	5.5120	5.0000		
29	Molar Flow (kgmole/h)	25.6733	25.6733		
30	Mass Flow (kg/s)	1.2148	1.2148		
31	Std Ideal Liq Vol Flow (m3/h)	5.8220	5.8220		
32	Molar Enthalpy (kJ/kgmole)	-3.554e+005	-3.554e+005		
33	Molar Entropy (kJ/kgmole-C)	247.0	247.1		
34	Heat Flow (kJ/h)	-9.1232e+06	-9.1232e+06		

PROPERTIES

37	Name	C2 HE3 Bypass	C2 HE3 Bypass-2		
38	Molecular Weight	170.3	170.3		
39	Molar Density (kgmole/m3)	4.458	4.458		
40	Mass Density (kg/m3)	759.4	759.3		
41	Act. Volume Flow (m3/h)	5.759	5.759		
42	Mass Enthalpy (kJ/kg)	-2086	-2086		
43	Mass Entropy (kJ/kg-K)	1.450	1.450		
44	Heat Capacity (kJ/kgmole-C)	335.7	335.7		
45	Mass Heat Capacity (kJ/kg-K)	1.971	1.971		
46	Lower Heating Value (kJ/kgmole)	7.579e+006	7.579e+006		
47	Mass Lower Heating Value (kJ/kg)	4.449e+004	4.449e+004		
48	Phase Fraction [Vol. Basis]	---	---		
49	Phase Fraction [Mass Basis]	2.122e-314	2.122e-314		
50	Partial Pressure of CO2 (bar)	0.0000	0.0000		
51	Cost Based on Flow (Cost/s)	0.0000	0.0000		
52	Act. Gas Flow (ACT_m3/h)	---	---		
53	Avg. Liq. Density (kgmole/m3)	4.410	4.410		
54	Specific Heat (kJ/kgmole-C)	335.7	335.7		
55	Std. Gas Flow (STD_m3/h)	607.0	607.0		
56	Std. Ideal Liq. Mass Density (kg/m3)	751.1	751.1		
57	Act. Liq. Flow (m3/s)	1.600e-003	1.600e-003		
58	Z Factor	---	---		
59	Watson K	12.74	12.74		
60	User Property	---	---		
61	Partial Pressure of H2S (bar)	0.0000	0.0000		
62	Cp/(Cp - R)	1.025	1.025		

1	 LEGENDS Calgary, Alberta CANADA	Case Name: E:\THESIS 2013\STUDIES\8- STUDYING DYNAMICS USING HYSYS\1
2		Unit Set: NewUser
3		Date/Time: Sat May 03 08:55:09 2014
4		
5		

Valve: VLV-102 (continued)

PROPERTIES

11	Name	C2 HE3 Bypass	C2 HE3 Bypass-2		
12	Cp/Cv	1.134	1.134		
13	Heat of Vap. (kJ/kgmole)	3.342e+004	3.437e+004		
14	Kinematic Viscosity (cSt)	2.370	2.368		
15	Liq. Mass Density (Std. Cond) (kg/m3)	753.0	753.0		
16	Liq. Vol. Flow (Std. Cond) (m3/h)	5.807	5.807		
17	Liquid Fraction	1.000	1.000		
18	Molar Volume (m3/kgmole)	0.2243	0.2243		
19	Mass Heat of Vap. (kJ/kg)	196.2	201.7		
20	Phase Fraction [Molar Basis]	0.0000	0.0000		
21	Surface Tension (dyne/cm)	25.92	25.92		
22	Thermal Conductivity (W/m-K)	0.1395	0.1395		
23	Viscosity (cP)	1.800	1.798		
24	Cv (Semi-Ideal) (kJ/kgmole-C)	327.4	327.4		
25	Mass Cv (Semi-Ideal) (kJ/kg-K)	1.922	1.922		
26	Cv (kJ/kgmole-C)	296.1	296.1		
27	Mass Cv (kJ/kg-K)	1.738	1.738		
28	Cv (Ent. Method) (kJ/kgmole-C)	---	---		
29	Mass Cv (Ent. Method) (kJ/kg-K)	---	---		
30	Cp/Cv (Ent. Method)	---	---		
31	Reid VP at 37.8 C (bar)	---	---		
32	True VP at 37.8 C (bar)	6.294e-004	6.294e-004		
33	Liq. Vol. Flow - Sum(Std. Cond) (m3/h)	5.807	5.807		


Valve: VLV-103

CONDITIONS

39	Name	H1	H1--1		
40	Vapour	0.0000	0.0000		
41	Temperature (K)	620.0000 *	619.9065		
42	Pressure (bar)	17.0000 *	16.5090		
43	Molar Flow (kgmole/h)	65.4815	65.4815		
44	Mass Flow (kg/s)	3.0983	3.0983		
45	Std Ideal Liq Vol Flow (m3/h)	14.8494	14.8494		
46	Molar Enthalpy (kJ/kgmole)	-1.962e+005	-1.962e+005		
47	Molar Entropy (kJ/kgmole-C)	604.2	604.2		
48	Heat Flow (kJ/h)	-1.2849e+07	-1.2849e+07		

PROPERTIES

51	Name	H1	H1--1		
52	Molecular Weight	170.3	170.3		
53	Molar Density (kgmole/m3)	2.604	2.599		
54	Mass Density (kg/m3)	443.5	442.7		
55	Act. Volume Flow (m3/h)	25.15	25.20		
56	Mass Enthalpy (kJ/kg)	-1152	-1152		
57	Mass Entropy (kJ/kg-K)	3.547	3.547		
58	Heat Capacity (kJ/kgmole-C)	642.8	644.9		
59	Mass Heat Capacity (kJ/kg-K)	3.773	3.786		
60	Lower Heating Value (kJ/kgmole)	7.579e+006	7.579e+006		
61	Mass Lower Heating Value (kJ/kg)	4.449e+004	4.449e+004		
62	Phase Fraction [Vol. Basis]	---	---		

1	 LEGENDS Calgary, Alberta CANADA	Case Name:	E:\THESIS 2013\STUDIES\8- STUDYING DYNAMICS USING HYSYS\1
2		Unit Set:	NewUser
3		Date/Time:	Sat May 03 08:55:09 2014
4			
5			

Valve: VLV-103 (continued)

PROPERTIES

11	Name	H1	H1--1		
12	Phase Fraction [Mass Basis]	2.122e-314	2.122e-314		
13	Partial Pressure of CO2 (bar)	0.0000	0.0000		
14	Cost Based on Flow (Cost/s)	0.0000	0.0000		
15	Act. Gas Flow (ACT_m3/h)	---	---		
16	Avg. Liq. Density (kgmole/m3)	4.410	4.410		
17	Specific Heat (kJ/kgmole-C)	642.8	644.9		
18	Std. Gas Flow (STD_m3/h)	1548	1548		
19	Std. Ideal Liq. Mass Density (kg/m3)	751.1	751.1		
20	Act. Liq. Flow (m3/s)	6.986e-003	6.999e-003		
21	Z Factor	---	---		
22	Watson K	12.74	12.74		
23	User Property	---	---		
24	Partial Pressure of H2S (bar)	0.0000	0.0000		
25	Cp/(Cp - R)	1.013	1.013		
26	Cp/Cv	1.187	1.188		
27	Heat of Vap. (kJ/kgmole)	9579	1.128e+004		
28	Kinematic Viscosity (cSt)	0.1806	0.1808		
29	Liq. Mass Density (Std. Cond) (kg/m3)	753.0	753.0		
30	Liq. Vol. Flow (Std. Cond) (m3/h)	14.81	14.81		
31	Liquid Fraction	1.000	1.000		
32	Molar Volume (m3/kgmole)	0.3841	0.3848		
33	Mass Heat of Vap. (kJ/kg)	56.24	66.21		
34	Phase Fraction [Molar Basis]	0.0000	0.0000		
35	Surface Tension (dyne/cm)	1.578	1.582		
36	Thermal Conductivity (W/m-K)	5.252e-002	5.257e-002		
37	Viscosity (cP)	8.008e-002	8.002e-002		
38	Cv (Semi-Ideal) (kJ/kgmole-C)	634.4	636.6		
39	Mass Cv (Semi-Ideal) (kJ/kg-K)	3.725	3.737		
40	Cv (kJ/kgmole-C)	541.6	542.9		
41	Mass Cv (kJ/kg-K)	3.180	3.187		
42	Cv (Ent. Method) (kJ/kgmole-C)	---	---		
43	Mass Cv (Ent. Method) (kJ/kg-K)	---	---		
44	Cp/Cv (Ent. Method)	---	---		
45	Reid VP at 37.8 C (bar)	---	---		
46	True VP at 37.8 C (bar)	6.294e-004	6.294e-004		
47	Liq. Vol. Flow - Sum(Std. Cond) (m3/h)	14.81	14.81		

Valve: VLV-104

CONDITIONS

53	Name	H2	H2-1		
54	Vapour	0.0000	0.0000		
55	Temperature (K)	720.0000 *	719.8633		
56	Pressure (bar)	51.0000 *	50.5007		
57	Molar Flow (kgmole/h)	106.1455	106.1455		
58	Mass Flow (kg/s)	5.0224	5.0224		
59	Std Ideal Liq Vol Flow (m3/h)	24.0709	24.0709		
60	Molar Enthalpy (kJ/kgmole)	-1.359e+005	-1.359e+005		
61	Molar Entropy (kJ/kgmole-C)	691.8	691.9		
62	Heat Flow (kJ/h)	-1.4420e+07	-1.4420e+07		




LEGENDS
Calgary, Alberta
CANADA

Case Name: E:\THESIS 2013\STUDIES\8- STUDYING DYNAMICS USING HYSYS\C1
Unit Set: NewUser
Date/Time: Sat May 03 08:55:09 2014

Valve: VLV-104 (continued)

PROPERTIES

Name	H2	H2-1			
Molecular Weight	170.3	170.3			
Molar Density (kgmole/m3)	---	1.717			
Mass Density (kg/m3)	---	292.5			
Act. Volume Flow (m3/h)	---	61.82			
Mass Enthalpy (kJ/kg)	-797.5	-797.5			
Mass Entropy (kJ/kg-K)	4.062	4.062			
Heat Capacity (kJ/kgmole-C)	657.2	658.2			
Mass Heat Capacity (kJ/kg-K)	3.858	3.864			
Lower Heating Value (kJ/kgmole)	7.579e+006	7.579e+006			
Mass Lower Heating Value (kJ/kg)	4.449e+004	4.449e+004			
Phase Fraction [Vol. Basis]	---	---			
Phase Fraction [Mass Basis]	2.122e-314	2.122e-314			
Partial Pressure of CO2 (bar)	0.0000	0.0000			
Cost Based on Flow (Cost/s)	0.0000	0.0000			
Act. Gas Flow (ACT_m3/h)	---	---			
Avg. Liq. Density (kgmole/m3)	4.410	4.410			
Specific Heat (kJ/kgmole-C)	657.2	658.2			
Std. Gas Flow (STD_m3/h)	2510	2510			
Std. Ideal Liq. Mass Density (kg/m3)	751.1	751.1			
Act. Liq. Flow (m3/s)	1.708e-002	1.717e-002			
Z Factor	---	---			
Watson K	12.74	12.74			
User Property	---	---			
Partial Pressure of H2S (bar)	0.0000	0.0000			
Cp/(Cp - R)	1.013	1.013			
Cp/Cv	1.197	1.199			
Heat of Vap. (kJ/kgmole)	---	---			
Kinematic Viscosity (cSt)	0.1082	0.1084			
Liq. Mass Density (Std. Cond) (kg/m3)	753.0	753.0			
Liq. Vol. Flow (Std. Cond) (m3/h)	24.01	24.01			
Liquid Fraction	1.000	1.000			
Molar Volume (m3/kgmole)	0.5792	0.5824			
Mass Heat of Vap. (kJ/kg)	---	---			
Phase Fraction [Molar Basis]	0.0000	0.0000			
Surface Tension (dyne/cm)	0.0000	0.0000			
Thermal Conductivity (W/m-K)	1.929e-003	1.929e-003			
Viscosity (cP)	3.182e-002	3.170e-002			
Cv (Semi-Ideal) (kJ/kgmole-C)	648.9	649.9			
Mass Cv (Semi-Ideal) (kJ/kg-K)	3.810	3.815			
Cv (kJ/kgmole-C)	549.3	549.1			
Mass Cv (kJ/kg-K)	3.224	3.224			
Cv (Ent. Method) (kJ/kgmole-C)	628.7	629.2			
Mass Cv (Ent. Method) (kJ/kg-K)	3.691	3.694			
Cp/Cv (Ent. Method)	1.045	1.046			
Reid VP at 37.8 C (bar)	---	---			
True VP at 37.8 C (bar)	6.294e-004	6.294e-004			
Liq. Vol. Flow - Sum(Std. Cond) (m3/h)	24.01	24.01			

1	 LEGENDS Calgary, Alberta CANADA	Case Name:	E:\THESIS 2013\STUDIES\8- STUDYING DYNAMICS USING HYSYS\C1
2		Unit Set:	NewUser
3		Date/Time:	Sat May 03 08:55:09 2014
4			
5			


Valve: VLV-105

CONDITIONS

11	Name	C1	C1-2
12	Vapour	0.0000	0.0000
13	Temperature (K)	300.0000 *	300.0305
14	Pressure (bar)	9.0000 *	8.4973
15	Molar Flow (kgmole/h)	168.6843	168.6843
16	Mass Flow (kg/s)	7.9815	7.9815
17	Std Ideal Liq Vol Flow (m3/h)	38.2529	38.2529
18	Molar Enthalpy (kJ/kgmole)	-3.484e+005	-3.484e+005
19	Molar Entropy (kJ/kgmole-C)	270.6	270.7
20	Heat Flow (kJ/h)	-5.8774e+07	-5.8774e+07

PROPERTIES

23	Name	C1	C1-2
24	Molecular Weight	170.3	170.3
25	Molar Density (kgmole/m3)	4.376	4.375
26	Mass Density (kg/m3)	745.3	745.2
27	Act. Volume Flow (m3/h)	38.55	38.56
28	Mass Enthalpy (kJ/kg)	-2045	-2045
29	Mass Entropy (kJ/kg-K)	1.589	1.589
30	Heat Capacity (kJ/kgmole-C)	351.0	351.0
31	Mass Heat Capacity (kJ/kg-K)	2.061	2.061
32	Lower Heating Value (kJ/kgmole)	7.579e+006	7.579e+006
33	Mass Lower Heating Value (kJ/kg)	4.449e+004	4.449e+004
34	Phase Fraction [Vol. Basis]	---	---
35	Phase Fraction [Mass Basis]	2.122e-314	2.122e-314
36	Partial Pressure of CO2 (bar)	0.0000	0.0000
37	Cost Based on Flow (Cost/s)	0.0000	0.0000
38	Act. Gas Flow (ACT_m3/h)	---	---
39	Avg. Liq. Density (kgmole/m3)	4.410	4.410
40	Specific Heat (kJ/kgmole-C)	351.0	351.0
41	Std. Gas Flow (STD_m3/h)	3988	3988
42	Std. Ideal Liq. Mass Density (kg/m3)	751.1	751.1
43	Act. Liq. Flow (m3/s)	1.071e-002	1.071e-002
44	Z Factor	---	---
45	Watson K	12.74	12.74
46	User Property	---	---
47	Partial Pressure of H2S (bar)	0.0000	0.0000
48	Cp/(Cp - R)	1.024	1.024
49	Cp/Cv	1.141	1.141
50	Heat of Vap. (kJ/kgmole)	2.727e+004	2.814e+004
51	Kinematic Viscosity (cSt)	1.719	1.718
52	Liq. Mass Density (Std. Cond) (kg/m3)	753.0	753.0
53	Liq. Vol. Flow (Std. Cond) (m3/h)	38.16	38.16
54	Liquid Fraction	1.000	1.000
55	Molar Volume (m3/kgmole)	0.2285	0.2286
56	Mass Heat of Vap. (kJ/kg)	160.1	165.2
57	Phase Fraction [Molar Basis]	0.0000	0.0000
58	Surface Tension (dyne/cm)	24.26	24.25
59	Thermal Conductivity (W/m-K)	0.1354	0.1354
60	Viscosity (cP)	1.281	1.281
61	Cv (Semi-Ideal) (kJ/kgmole-C)	342.7	342.7
62	Mass Cv (Semi-Ideal) (kJ/kg-K)	2.012	2.012

1	 LEGENDS Calgary, Alberta CANADA	Case Name: E:\THESIS 2013\STUDIES\8- STUDYING DYNAMICS USING HYSYS\C1
2		Unit Set: NewUser
3		Date/Time: Sat May 03 08:55:09 2014
4		
5		

Valve: VLV-105 (continued)

PROPERTIES

11	Name	C1	C1-2		
12	Cv (kJ/kgmole-C)	307.7	307.7		
13	Mass Cv (kJ/kg-K)	1.806	1.807		
14	Cv (Ent. Method) (kJ/kgmole-C)	---	---		
15	Mass Cv (Ent. Method) (kJ/kg-K)	---	---		
16	Cp/Cv (Ent. Method)	---	---		
17	Reid VP at 37.8 C (bar)	---	---		
18	True VP at 37.8 C (bar)	6.294e-004	6.294e-004		
19	Liq. Vol. Flow - Sum(Std. Cond) (m3/h)	38.16	38.16		


Valve: VLV-106

CONDITIONS

25	Name	C2	C2-1		
26	Vapour	0.0000	0.0000		
27	Temperature (K)	280.0000 *	280.0315		
28	Pressure (bar)	6.0000 *	5.5120		
29	Molar Flow (kgmole/h)	281.9530	281.9530		
30	Mass Flow (kg/s)	13.3410	13.3410		
31	Std Ideal Liq Vol Flow (m3/h)	63.9392	63.9392		
32	Molar Enthalpy (kJ/kgmole)	-3.554e+005	-3.554e+005		
33	Molar Entropy (kJ/kgmole-C)	247.0	247.0		
34	Heat Flow (kJ/h)	-1.0019e+08	-1.0019e+08		

PROPERTIES

37	Name	C2	C2-1		
38	Molecular Weight	170.3	170.3		
39	Molar Density (kgmole/m3)	4.459	4.458		
40	Mass Density (kg/m3)	759.5	759.4		
41	Act. Volume Flow (m3/h)	63.24	63.24		
42	Mass Enthalpy (kJ/kg)	-2086	-2086		
43	Mass Entropy (kJ/kg-K)	1.450	1.450		
44	Heat Capacity (kJ/kgmole-C)	335.6	335.7		
45	Mass Heat Capacity (kJ/kg-K)	1.970	1.971		
46	Lower Heating Value (kJ/kgmole)	7.579e+006	7.579e+006		
47	Mass Lower Heating Value (kJ/kg)	4.449e+004	4.449e+004		
48	Phase Fraction [Vol. Basis]	---	---		
49	Phase Fraction [Mass Basis]	2.122e-314	2.122e-314		
50	Partial Pressure of CO2 (bar)	0.0000	0.0000		
51	Cost Based on Flow (Cost/s)	0.0000	0.0000		
52	Act. Gas Flow (ACT_m3/h)	---	---		
53	Avg. Liq. Density (kgmole/m3)	4.410	4.410		
54	Specific Heat (kJ/kgmole-C)	335.6	335.7		
55	Std. Gas Flow (STD_m3/h)	6667	6667		
56	Std. Ideal Liq. Mass Density (kg/m3)	751.1	751.1		
57	Act. Liq. Flow (m3/s)	1.757e-002	1.757e-002		
58	Z Factor	---	---		
59	Watson K	12.74	12.74		
60	User Property	---	---		
61	Partial Pressure of H2S (bar)	0.0000	0.0000		
62	Cp/(Cp - R)	1.025	1.025		

1	 LEGENDS Calgary, Alberta CANADA	Case Name:	E:\THESIS 2013\STUDIES\8- STUDYING DYNAMICS USING HYSYS\C1
2		Unit Set:	NewUser
3		Date/Time:	Sat May 03 08:55:09 2014
4			
5			

Valve: VLV-106 (continued)

PROPERTIES

11	Name	C2	C2-1		
12	Cp/Cv	1.134	1.134		
13	Heat of Vap. (kJ/kgmole)	3.253e+004	3.342e+004		
14	Kinematic Viscosity (cSt)	2.371	2.370		
15	Liq. Mass Density (Std. Cond) (kg/m3)	753.0	753.0		
16	Liq. Vol. Flow (Std. Cond) (m3/h)	63.78	63.78		
17	Liquid Fraction	1.000	1.000		
18	Molar Volume (m3/kgmole)	0.2243	0.2243		
19	Mass Heat of Vap. (kJ/kg)	191.0	196.2		
20	Phase Fraction [Molar Basis]	0.0000	0.0000		
21	Surface Tension (dyne/cm)	25.92	25.92		
22	Thermal Conductivity (W/m-K)	0.1395	0.1395		
23	Viscosity (cP)	1.801	1.800		
24	Cv (Semi-Ideal) (kJ/kgmole-C)	327.3	327.4		
25	Mass Cv (Semi-Ideal) (kJ/kg-K)	1.922	1.922		
26	Cv (kJ/kgmole-C)	296.0	296.1		
27	Mass Cv (kJ/kg-K)	1.738	1.738		
28	Cv (Ent. Method) (kJ/kgmole-C)	---	---		
29	Mass Cv (Ent. Method) (kJ/kg-K)	---	---		
30	Cp/Cv (Ent. Method)	---	---		
31	Reid VP at 37.8 C (bar)	---	---		
32	True VP at 37.8 C (bar)	6.294e-004	6.294e-004		
33	Liq. Vol. Flow - Sum(Std. Cond) (m3/h)	63.78	63.78		


Heat Exchanger: HE1

CONDITIONS

39	Name	H1 HE1 in	C1-2	H1 HE1 2	C1 HE1 out
40	Vapour	0.0000	0.0000	0.0000	0.0000
41	Temperature (K)	619.9065	300.0305	350.8094	417.3812
42	Pressure (bar)	16.5090	8.4973	16.0000	7.9946
43	Molar Flow (kgmole/h)	58.7259	168.6843	58.7259	168.6843
44	Mass Flow (kg/s)	2.7787	7.9815	2.7787	7.9815
45	Std Ideal Liq Vol Flow (m3/h)	13.3174	38.2529	13.3174	38.2529
46	Molar Enthalpy (kJ/kgmole)	-1.962e+005	-3.484e+005	-3.295e+005	-3.020e+005
47	Molar Entropy (kJ/kgmole-C)	604.2	270.7	328.4	400.4
48	Heat Flow (kJ/h)	-1.1523e+07	-5.8774e+07	-1.9349e+07	-5.0949e+07

PROPERTIES

51	Name	H1 HE1 in	C1-2	H1 HE1 2	C1 HE1 out
52	Molecular Weight	170.3	170.3	170.3	170.3
53	Molar Density (kgmole/m3)	2.599	4.375	4.160	3.848
54	Mass Density (kg/m3)	442.7	745.2	708.6	655.5
55	Act. Volume Flow (m3/h)	22.60	38.56	14.12	43.84
56	Mass Enthalpy (kJ/kg)	-1152	-2045	-1934	-1773
57	Mass Entropy (kJ/kg-K)	3.547	1.589	1.928	2.351
58	Heat Capacity (kJ/kgmole-C)	644.9	351.0	389.3	439.3
59	Mass Heat Capacity (kJ/kg-K)	3.786	2.061	2.286	2.579
60	Lower Heating Value (kJ/kgmole)	7.579e+006	7.579e+006	7.579e+006	7.579e+006
61	Mass Lower Heating Value (kJ/kg)	4.449e+004	4.449e+004	4.449e+004	4.449e+004
62	Phase Fraction [Vol. Basis]	---	---	---	---

1	 LEGENDS Calgary, Alberta CANADA	Case Name: E:\THESIS 2013\STUDIES\8- STUDYING DYNAMICS USING HYSYS\C1
2		Unit Set: NewUser
3		Date/Time: Sat May 03 08:55:09 2014
4		
5		

Heat Exchanger: HE1 (continued)

PROPERTIES

11	Name	H1 HE1 in	C1-2	H1 HE1 2	C1 HE1 out
12	Phase Fraction [Mass Basis]	2.122e-314	2.122e-314	2.122e-314	2.122e-314
13	Partial Pressure of CO2 (bar)	0.0000	0.0000	0.0000	0.0000
14	Cost Based on Flow (Cost/s)	0.0000	0.0000	0.0000	0.0000
15	Act. Gas Flow (ACT_m3/h)	---	---	---	---
16	Avg. Liq. Density (kgmole/m3)	4.410	4.410	4.410	4.410
17	Specific Heat (kJ/kgmole-C)	644.9	351.0	389.3	439.3
18	Std. Gas Flow (STD_m3/h)	1389	3988	1389	3988
19	Std. Ideal Liq. Mass Density (kg/m3)	751.1	751.1	751.1	751.1
20	Act. Liq. Flow (m3/s)	6.277e-003	1.071e-002	3.921e-003	1.218e-002
21	Z Factor	---	---	---	---
22	Watson K	12.74	12.74	12.74	12.74
23	User Property	---	---	---	---
24	Partial Pressure of H2S (bar)	0.0000	0.0000	0.0000	0.0000
25	Cp/(Cp - R)	1.013	1.024	1.022	1.019
26	Cp/Cv	1.188	1.141	1.141	1.134
27	Heat of Vap. (kJ/kgmole)	1.128e+004	2.814e+004	1.282e+004	2.902e+004
28	Kinematic Viscosity (cSt)	0.1808	1.718	0.9208	0.5204
29	Liq. Mass Density (Std. Cond) (kg/m3)	753.0	753.0	753.0	753.0
30	Liq. Vol. Flow (Std. Cond) (m3/h)	13.28	38.16	13.28	38.16
31	Liquid Fraction	1.000	1.000	1.000	1.000
32	Molar Volume (m3/kgmole)	0.3848	0.2286	0.2404	0.2599
33	Mass Heat of Vap. (kJ/kg)	66.21	165.2	75.27	170.4
34	Phase Fraction [Molar Basis]	0.0000	0.0000	0.0000	0.0000
35	Surface Tension (dyne/cm)	1.582	24.25	20.12	14.93
36	Thermal Conductivity (W/m-K)	5.257e-002	0.1354	0.1247	0.1097
37	Viscosity (cP)	8.002e-002	1.281	0.6525	0.3411
38	Cv (Semi-Ideal) (kJ/kgmole-C)	636.6	342.7	381.0	431.0
39	Mass Cv (Semi-Ideal) (kJ/kg-K)	3.737	2.012	2.237	2.530
40	Cv (kJ/kgmole-C)	542.9	307.7	341.1	387.3
41	Mass Cv (kJ/kg-K)	3.187	1.807	2.002	2.274
42	Cv (Ent. Method) (kJ/kgmole-C)	---	---	---	---
43	Mass Cv (Ent. Method) (kJ/kg-K)	---	---	---	---
44	Cp/Cv (Ent. Method)	---	---	---	---
45	Reid VP at 37.8 C (bar)	---	---	---	---
46	True VP at 37.8 C (bar)	6.294e-004	6.294e-004	6.294e-004	6.294e-004
47	Liq. Vol. Flow - Sum(Std. Cond) (m3/h)	13.28	38.16	13.28	38.16

Heat Exchanger: HE2


CONDITIONS

53	Name	H2-1	C1 HE2 in	H2 HE2 out	C1 HE2 out
54	Vapour	0.0000	0.0000	0.0000	0.0000
55	Temperature (K)	719.8633	417.3812	529.2090	575.1032
56	Pressure (bar)	50.5007	7.9946	49.9911	7.5000
57	Molar Flow (kgmole/h)	106.1455	150.4029	106.1455	150.4029
58	Mass Flow (kg/s)	5.0224	7.1165	5.0224	7.1165
59	Std Ideal Liq Vol Flow (m3/h)	24.0709	34.1072	24.0709	34.1072
60	Molar Enthalpy (kJ/kgmole)	-1.359e+005	-3.020e+005	-2.481e+005	-2.228e+005
61	Molar Entropy (kJ/kgmole-C)	691.9	400.4	512.0	560.3
62	Heat Flow (kJ/h)	-1.4420e+07	-4.5427e+07	-2.6332e+07	-3.3516e+07

Heat Exchanger: HE2 (continued)

PROPERTIES

Name	H2-1	C1 HE2 in	H2 HE2 out	C1 HE2 out
12 Molecular Weight	170.3	170.3	170.3	170.3
13 Molar Density (kgmole/m3)	1.717	3.848	3.366	2.939
14 Mass Density (kg/m3)	292.5	655.5	573.4	500.7
15 Act. Volume Flow (m3/h)	61.82	39.09	31.53	51.17
16 Mass Enthalpy (kJ/kg)	-797.5	-1773	-1456	-1308
17 Mass Entropy (kJ/kg-K)	4.062	2.351	3.006	3.289
18 Heat Capacity (kJ/kgmole-C)	658.2	439.3	515.7	578.4
19 Mass Heat Capacity (kJ/kg-K)	3.864	2.579	3.028	3.396
20 Lower Heating Value (kJ/kgmole)	7.579e+006	7.579e+006	7.579e+006	7.579e+006
21 Mass Lower Heating Value (kJ/kg)	4.449e+004	4.449e+004	4.449e+004	4.449e+004
22 Phase Fraction [Vol. Basis]	---	---	---	---
23 Phase Fraction [Mass Basis]	2.122e-314	2.122e-314	2.122e-314	2.122e-314
24 Partial Pressure of CO2 (bar)	0.0000	0.0000	0.0000	0.0000
25 Cost Based on Flow (Cost/s)	0.0000	0.0000	0.0000	0.0000
26 Act. Gas Flow (ACT_m3/h)	---	---	---	---
27 Avg. Liq. Density (kgmole/m3)	4.410	4.410	4.410	4.410
28 Specific Heat (kJ/kgmole-C)	658.2	439.3	515.7	578.4
29 Std. Gas Flow (STD_m3/h)	2510	3556	2510	3556
30 Std. Ideal Liq. Mass Density (kg/m3)	751.1	751.1	751.1	751.1
31 Act. Liq. Flow (m3/s)	1.717e-002	1.086e-002	8.758e-003	1.421e-002
32 Z Factor	---	---	---	---
33 Watson K	12.74	12.74	12.74	12.74
34 User Property	---	---	---	---
35 Partial Pressure of H2S (bar)	0.0000	0.0000	0.0000	0.0000
36 Cp/(Cp - R)	1.013	1.019	1.016	1.015
37 Cp/Cv	1.199	1.134	1.111	1.141
38 Heat of Vap. (kJ/kgmole)	---	2.902e+004	---	2.988e+004
39 Kinematic Viscosity (cSt)	0.1084	0.5204	0.2672	0.2191
40 Liq. Mass Density (Std. Cond) (kg/m3)	753.0	753.0	753.0	753.0
41 Liq. Vol. Flow (Std. Cond) (m3/h)	24.01	34.02	24.01	34.02
42 Liquid Fraction	1.000	1.000	1.000	1.000
43 Molar Volume (m3/kgmole)	0.5824	0.2599	0.2970	0.3402
44 Mass Heat of Vap. (kJ/kg)	---	170.4	---	175.4
45 Phase Fraction [Molar Basis]	0.0000	0.0000	0.0000	0.0000
46 Surface Tension (dyne/cm)	0.0000	14.93	6.965	4.072
47 Thermal Conductivity (W/m-K)	1.929e-003	0.1097	8.557e-002	7.141e-002
48 Viscosity (cP)	3.170e-002	0.3411	0.1532	0.1097
49 Cv (Semi-Ideal) (kJ/kgmole-C)	649.9	431.0	507.4	570.1
50 Mass Cv (Semi-Ideal) (kJ/kg-K)	3.815	2.530	2.979	3.347
51 Cv (kJ/kgmole-C)	549.1	387.3	464.4	507.0
52 Mass Cv (kJ/kg-K)	3.224	2.274	2.726	2.976
53 Cv (Ent. Method) (kJ/kgmole-C)	629.2	---	---	---
54 Mass Cv (Ent. Method) (kJ/kg-K)	3.694	---	---	---
55 Cp/Cv (Ent. Method)	1.046	---	---	---
56 Reid VP at 37.8 C (bar)	---	---	---	---
57 True VP at 37.8 C (bar)	6.294e-004	6.294e-004	6.294e-004	6.294e-004
58 Liq. Vol. Flow - Sum(Std. Cond) (m3/h)	24.01	34.02	24.01	34.02

1	 LEGENDS Calgary, Alberta CANADA	Case Name: E:\THESIS 2013\STUDIES\8- STUDYING DYNAMICS USING HYSYS\C1
2		Unit Set: NewUser
3		Date/Time: Sat May 03 08:55:09 2014
4		
5		


Heat Exchanger: E-100

CONDITIONS

11	Name	H2 HE2 out	C2 HE3 in	H2 HE3 out	C2 HE3 out
12	Vapour	0.0000	0.0000	0.0000	0.0000
13	Temperature (K)	529.2090	280.0315	408.4491	345.6375
14	Pressure (bar)	49.9911	5.5120	49.4875	5.0000
15	Molar Flow (kgmole/h)	106.1455	256.2797	106.1455	256.2797
16	Mass Flow (kg/s)	5.0224	12.1262	5.0224	12.1262
17	Std Ideal Liq Vol Flow (m3/h)	24.0709	58.1172	24.0709	58.1172
18	Molar Enthalpy (kJ/kgmole)	-2.481e+005	-3.554e+005	-3.052e+005	-3.317e+005
19	Molar Entropy (kJ/kgmole-C)	512.0	247.0	390.0	322.8
20	Heat Flow (kJ/h)	-2.6332e+07	-9.1071e+07	-3.2396e+07	-8.5007e+07

PROPERTIES

23	Name	H2 HE2 out	C2 HE3 in	H2 HE3 out	C2 HE3 out
24	Molecular Weight	170.3	170.3	170.3	170.3
25	Molar Density (kgmole/m3)	3.366	4.458	3.936	4.174
26	Mass Density (kg/m3)	573.4	759.4	670.5	711.0
27	Act. Volume Flow (m3/h)	31.53	57.48	26.96	61.40
28	Mass Enthalpy (kJ/kg)	-1456	-2086	-1792	-1947
29	Mass Entropy (kJ/kg-K)	3.006	1.450	2.289	1.895
30	Heat Capacity (kJ/kgmole-C)	515.7	335.7	430.2	385.8
31	Mass Heat Capacity (kJ/kg-K)	3.028	1.971	2.526	2.265
32	Lower Heating Value (kJ/kgmole)	7.579e+006	7.579e+006	7.579e+006	7.579e+006
33	Mass Lower Heating Value (kJ/kg)	4.449e+004	4.449e+004	4.449e+004	4.449e+004
34	Phase Fraction [Vol. Basis]	---	---	---	---
35	Phase Fraction [Mass Basis]	2.122e-314	2.122e-314	2.122e-314	2.122e-314
36	Partial Pressure of CO2 (bar)	0.0000	0.0000	0.0000	0.0000
37	Cost Based on Flow (Cost/s)	0.0000	0.0000	0.0000	0.0000
38	Act. Gas Flow (ACT_m3/h)	---	---	---	---
39	Avg. Liq. Density (kgmole/m3)	4.410	4.410	4.410	4.410
40	Specific Heat (kJ/kgmole-C)	515.7	335.7	430.2	385.8
41	Std. Gas Flow (STD_m3/h)	2510	6060	2510	6060
42	Std. Ideal Liq. Mass Density (kg/m3)	751.1	751.1	751.1	751.1
43	Act. Liq. Flow (m3/s)	8.758e-003	1.597e-002	7.490e-003	1.705e-002
44	Z Factor	---	---	---	---
45	Watson K	12.74	12.74	12.74	12.74
46	User Property	---	---	---	---
47	Partial Pressure of H2S (bar)	0.0000	0.0000	0.0000	0.0000
48	Cp/(Cp - R)	1.016	1.025	1.020	1.022
49	Cp/Cv	1.111	1.134	1.128	1.143
50	Heat of Vap. (kJ/kgmole)	---	3.342e+004	---	3.437e+004
51	Kinematic Viscosity (cSt)	0.2672	2.370	0.5536	0.9726
52	Liq. Mass Density (Std. Cond) (kg/m3)	753.0	753.0	753.0	753.0
53	Liq. Vol. Flow (Std. Cond) (m3/h)	24.01	57.97	24.01	57.97
54	Liquid Fraction	1.000	1.000	1.000	1.000
55	Molar Volume (m3/kgmole)	0.2970	0.2243	0.2540	0.2396
56	Mass Heat of Vap. (kJ/kg)	---	196.2	---	201.7
57	Phase Fraction [Molar Basis]	0.0000	0.0000	0.0000	0.0000
58	Surface Tension (dyne/cm)	6.965	25.92	15.61	20.54
59	Thermal Conductivity (W/m-K)	8.557e-002	0.1395	0.1118	0.1258
60	Viscosity (cP)	0.1532	1.800	0.3712	0.6915
61	Cv (Semi-Ideal) (kJ/kgmole-C)	507.4	327.4	421.9	377.5
62	Mass Cv (Semi-Ideal) (kJ/kg-K)	2.979	1.922	2.477	2.216

1	 LEGENDS Calgary, Alberta CANADA	Case Name: E:\THESIS 2013\STUDIES\8- STUDYING DYNAMICS USING HYSYS\1
2		Unit Set: NewUser
3		Date/Time: Sat May 03 08:55:09 2014
4		
5		

Heat Exchanger: E-100 (continued)

PROPERTIES

11	Name	H2 HE2 out	C2 HE3 in	H2 HE3 out	C2 HE3 out
12	Cv (kJ/kgmole-C)	464.4	296.1	381.3	337.5
13	Mass Cv (kJ/kg-K)	2.726	1.738	2.239	1.981
14	Cv (Ent. Method) (kJ/kgmole-C)	---	---	---	---
15	Mass Cv (Ent. Method) (kJ/kg-K)	---	---	---	---
16	Cp/Cv (Ent. Method)	---	---	---	---
17	Reid VP at 37.8 C (bar)	---	---	---	---
18	True VP at 37.8 C (bar)	6.294e-004	6.294e-004	6.294e-004	6.294e-004
19	Liq. Vol. Flow - Sum(Std. Cond) (m3/h)	24.01	57.97	24.01	57.97


Mixer: MIX-100

CONDITIONS

25	Name	H1 Bypass 2	H1 HE1 2	H1 out
26	Vapour	0.0000	0.0000	0.0000
27	Temperature (K)	619.8070	350.8094	385.0000
28	Pressure (bar)	16.0000	16.0000	16.0000 *
29	Molar Flow (kgmole/h)	6.7556	58.7259	65.4815
30	Mass Flow (kg/s)	0.3197	2.7787	3.0983
31	Std Ideal Liq Vol Flow (m3/h)	1.5320	13.3174	14.8494
32	Molar Enthalpy (kJ/kgmole)	-1.962e+005	-3.295e+005	-3.157e+005
33	Molar Entropy (kJ/kgmole-C)	604.2	328.4	365.7
34	Heat Flow (kJ/h)	-1.3256e+06	-1.9349e+07	-2.0674e+07

PROPERTIES

37	Name	H1 Bypass 2	H1 HE1 2	H1 out
38	Molecular Weight	170.3	170.3	170.3
39	Molar Density (kgmole/m3)	2.594	4.160	4.007
40	Mass Density (kg/m3)	441.9	708.6	682.6
41	Act. Volume Flow (m3/h)	2.604	14.12	16.34
42	Mass Enthalpy (kJ/kg)	-1152	-1934	-1854
43	Mass Entropy (kJ/kg-K)	3.547	1.928	2.147
44	Heat Capacity (kJ/kgmole-C)	647.2	389.3	414.8
45	Mass Heat Capacity (kJ/kg-K)	3.799	2.286	2.435
46	Lower Heating Value (kJ/kgmole)	7.579e+006	7.579e+006	7.579e+006
47	Mass Lower Heating Value (kJ/kg)	4.449e+004	4.449e+004	4.449e+004
48	Phase Fraction [Vol. Basis]	---	---	---
49	Phase Fraction [Mass Basis]	2.122e-314	2.122e-314	2.122e-314
50	Partial Pressure of CO2 (bar)	0.0000	0.0000	0.0000
51	Cost Based on Flow (Cost/s)	0.0000	0.0000	0.0000
52	Act. Gas Flow (ACT_m3/h)	---	---	---
53	Avg. Liq. Density (kgmole/m3)	4.410	4.410	4.410
54	Specific Heat (kJ/kgmole-C)	647.2	389.3	414.8
55	Std. Gas Flow (STD_m3/h)	159.7	1389	1548
56	Std. Ideal Liq. Mass Density (kg/m3)	751.1	751.1	751.1
57	Act. Liq. Flow (m3/s)	7.234e-004	3.921e-003	4.539e-003
58	Z Factor	---	---	---
59	Watson K	12.74	12.74	12.74
60	User Property	---	---	---
61	Partial Pressure of H2S (bar)	0.0000	0.0000	0.0000
62	Cp/(Cp - R)	1.013	1.022	1.020

1	 LEGENDS Calgary, Alberta CANADA	Case Name:	E:\THESIS 2013\STUDIES\8- STUDYING DYNAMICS USING HYSYS\C1
2		Unit Set:	NewUser
3		Date/Time:	Sat May 03 08:55:09 2014
4			
5			

Mixer: MIX-100 (continued)

PROPERTIES

11	Name	H1 Bypass 2	H1 HE1 2	H1 out	
12	Cp/Cv	1.189	1.141	1.137	
13	Heat of Vap. (kJ/kgmole)	1.282e+004	1.282e+004	1.282e+004	
14	Kinematic Viscosity (cSt)	0.1810	0.9208	0.6696	
15	Liq. Mass Density (Std. Cond) (kg/m3)	753.0	753.0	753.0	
16	Liq. Vol. Flow (Std. Cond) (m3/h)	1.528	13.28	14.81	
17	Liquid Fraction	1.000	1.000	1.000	
18	Molar Volume (m3/kgmole)	0.3855	0.2404	0.2495	
19	Mass Heat of Vap. (kJ/kg)	75.27	75.27	75.27	
20	Phase Fraction [Molar Basis]	0.0000	0.0000	0.0000	
21	Surface Tension (dyne/cm)	1.587	20.12	17.42	
22	Thermal Conductivity (W/m-K)	5.262e-002	0.1247	0.1172	
23	Viscosity (cP)	7.996e-002	0.6525	0.4571	
24	Cv (Semi-Ideal) (kJ/kgmole-C)	638.9	381.0	406.5	
25	Mass Cv (Semi-Ideal) (kJ/kg-K)	3.751	2.237	2.386	
26	Cv (kJ/kgmole-C)	544.3	341.1	364.9	
27	Mass Cv (kJ/kg-K)	3.195	2.002	2.142	
28	Cv (Ent. Method) (kJ/kgmole-C)	---	---	---	
29	Mass Cv (Ent. Method) (kJ/kg-K)	---	---	---	
30	Cp/Cv (Ent. Method)	---	---	---	
31	Reid VP at 37.8 C (bar)	---	---	---	
32	True VP at 37.8 C (bar)	6.294e-004	6.294e-004	6.294e-004	
33	Liq. Vol. Flow - Sum(Std. Cond) (m3/h)	1.528	13.28	14.81	


Mixer: MIX-101

CONDITIONS

39	Name	C1 HE2 out	C1 HE2 Bypass-2	C1 out	
40	Vapour	0.0000	0.0000	0.0000	
41	Temperature (K)	575.1032	417.3997	560.0000	
42	Pressure (bar)	7.5000	7.5000	7.5000 *	
43	Molar Flow (kgmole/h)	150.4029	18.2814	168.6843	
44	Mass Flow (kg/s)	7.1165	0.8650	7.9815	
45	Std Ideal Liq Vol Flow (m3/h)	34.1072	4.1457	38.2529	
46	Molar Enthalpy (kJ/kgmole)	-2.228e+005	-3.020e+005	-2.314e+005	
47	Molar Entropy (kJ/kgmole-C)	560.3	400.4	545.1	
48	Heat Flow (kJ/h)	-3.3516e+07	-5.5217e+06	-3.9037e+07	

PROPERTIES

51	Name	C1 HE2 out	C1 HE2 Bypass-2	C1 out	
52	Molecular Weight	170.3	170.3	170.3	
53	Molar Density (kgmole/m3)	2.939	3.847	3.052	
54	Mass Density (kg/m3)	500.7	655.4	519.8	
55	Act. Volume Flow (m3/h)	51.17	4.752	55.27	
56	Mass Enthalpy (kJ/kg)	-1308	-1773	-1359	
57	Mass Entropy (kJ/kg-K)	3.289	2.351	3.200	
58	Heat Capacity (kJ/kgmole-C)	578.4	439.3	558.9	
59	Mass Heat Capacity (kJ/kg-K)	3.396	2.579	3.281	
60	Lower Heating Value (kJ/kgmole)	7.579e+006	7.579e+006	7.579e+006	
61	Mass Lower Heating Value (kJ/kg)	4.449e+004	4.449e+004	4.449e+004	
62	Phase Fraction [Vol. Basis]	---	---	---	

1	 LEGENDS Calgary, Alberta CANADA	Case Name: E:\THESIS 2013\STUDIES\8- STUDYING DYNAMICS USING HYSYS\C1
2		Unit Set: NewUser
3		Date/Time: Sat May 03 08:55:09 2014
4		
5		

Mixer: MIX-101 (continued)

PROPERTIES

11	Name	C1 HE2 out	C1 HE2 Bypass-2	C1 out	
12	Phase Fraction [Mass Basis]	2.122e-314	2.122e-314	2.122e-314	
13	Partial Pressure of CO2 (bar)	0.0000	0.0000	0.0000	
14	Cost Based on Flow (Cost/s)	0.0000	0.0000	0.0000	
15	Act. Gas Flow (ACT_m3/h)	---	---	---	
16	Avg. Liq. Density (kgmole/m3)	4.410	4.410	4.410	
17	Specific Heat (kJ/kgmole-C)	578.4	439.3	558.9	
18	Std. Gas Flow (STD_m3/h)	3556	432.3	3988	
19	Std. Ideal Liq. Mass Density (kg/m3)	751.1	751.1	751.1	
20	Act. Liq. Flow (m3/s)	1.421e-002	1.320e-003	1.535e-002	
21	Z Factor	---	---	---	
22	Watson K	12.74	12.74	12.74	
23	User Property	---	---	---	
24	Partial Pressure of H2S (bar)	0.0000	0.0000	0.0000	
25	Cp/(Cp - R)	1.015	1.019	1.015	
26	Cp/Cv	1.141	1.134	1.135	
27	Heat of Vap. (kJ/kgmole)	2.988e+004	2.988e+004	2.988e+004	
28	Kinematic Viscosity (cSt)	0.2191	0.5204	0.2341	
29	Liq. Mass Density (Std. Cond) (kg/m3)	753.0	753.0	753.0	
30	Liq. Vol. Flow (Std. Cond) (m3/h)	34.02	4.135	38.16	
31	Liquid Fraction	1.000	1.000	1.000	
32	Molar Volume (m3/kgmole)	0.3402	0.2599	0.3277	
33	Mass Heat of Vap. (kJ/kg)	175.4	175.4	175.4	
34	Phase Fraction [Molar Basis]	0.0000	0.0000	0.0000	
35	Surface Tension (dyne/cm)	4.072	14.93	4.992	
36	Thermal Conductivity (W/m-K)	7.141e-002	0.1097	7.642e-002	
37	Viscosity (cP)	0.1097	0.3410	0.1217	
38	Cv (Semi-Ideal) (kJ/kgmole-C)	570.1	431.0	550.6	
39	Mass Cv (Semi-Ideal) (kJ/kg-K)	3.347	2.530	3.232	
40	Cv (kJ/kgmole-C)	507.0	387.3	492.2	
41	Mass Cv (kJ/kg-K)	2.976	2.274	2.890	
42	Cv (Ent. Method) (kJ/kgmole-C)	---	---	---	
43	Mass Cv (Ent. Method) (kJ/kg-K)	---	---	---	
44	Cp/Cv (Ent. Method)	---	---	---	
45	Reid VP at 37.8 C (bar)	---	---	---	
46	True VP at 37.8 C (bar)	6.294e-004	6.294e-004	6.294e-004	
47	Liq. Vol. Flow - Sum(Std. Cond) (m3/h)	34.02	4.135	38.16	

Mixer: MIX-102


CONDITIONS

53	Name	C2 HE3 out	C2 HE3 Bypass-2	C2 out	
54	Vapour	0.0000	0.0000	0.0000	
55	Temperature (K)	345.6375	280.0645	340.0219	
56	Pressure (bar)	5.0000	5.0000	5.0000 *	
57	Molar Flow (kgmole/h)	256.2797	25.6733	281.9530	
58	Mass Flow (kg/s)	12.1262	1.2148	13.3410	
59	Std Ideal Liq Vol Flow (m3/h)	58.1172	5.8220	63.9392	
60	Molar Enthalpy (kJ/kgmole)	-3.317e+005	-3.554e+005	-3.339e+005	
61	Molar Entropy (kJ/kgmole-C)	322.8	247.1	316.5	
62	Heat Flow (kJ/h)	-8.5007e+07	-9.1232e+06	-9.4130e+07	

Mixer: MIX-102 (continued)

PROPERTIES

11	Name	C2 HE3 out	C2 HE3 Bypass-2	C2 out	
12	Molecular Weight	170.3	170.3	170.3	
13	Molar Density (kgmole/m3)	4.174	4.458	4.199	
14	Mass Density (kg/m3)	711.0	759.3	715.2	
15	Act. Volume Flow (m3/h)	61.40	5.759	67.15	
16	Mass Enthalpy (kJ/kg)	-1947	-2086	-1960	
17	Mass Entropy (kJ/kg-K)	1.895	1.450	1.858	
18	Heat Capacity (kJ/kgmole-C)	385.8	335.7	381.6	
19	Mass Heat Capacity (kJ/kg-K)	2.265	1.971	2.240	
20	Lower Heating Value (kJ/kgmole)	7.579e+006	7.579e+006	7.579e+006	
21	Mass Lower Heating Value (kJ/kg)	4.449e+004	4.449e+004	4.449e+004	
22	Phase Fraction [Vol. Basis]	---	---	---	
23	Phase Fraction [Mass Basis]	2.122e-314	2.122e-314	2.122e-314	
24	Partial Pressure of CO2 (bar)	0.0000	0.0000	0.0000	
25	Cost Based on Flow (Cost/s)	0.0000	0.0000	0.0000	
26	Act. Gas Flow (ACT_m3/h)	---	---	---	
27	Avg. Liq. Density (kgmole/m3)	4.410	4.410	4.410	
28	Specific Heat (kJ/kgmole-C)	385.8	335.7	381.6	
29	Std. Gas Flow (STD_m3/h)	6060	607.0	6667	
30	Std. Ideal Liq. Mass Density (kg/m3)	751.1	751.1	751.1	
31	Act. Liq. Flow (m3/s)	1.705e-002	1.600e-003	1.865e-002	
32	Z Factor	---	---	---	
33	Watson K	12.74	12.74	12.74	
34	User Property	---	---	---	
35	Partial Pressure of H2S (bar)	0.0000	0.0000	0.0000	
36	Cp/(Cp - R)	1.022	1.025	1.022	
37	Cp/Cv	1.143	1.134	1.143	
38	Heat of Vap. (kJ/kgmole)	3.437e+004	3.437e+004	3.437e+004	
39	Kinematic Viscosity (cSt)	0.9726	2.368	1.033	
40	Liq. Mass Density (Std. Cond) (kg/m3)	753.0	753.0	753.0	
41	Liq. Vol. Flow (Std. Cond) (m3/h)	57.97	5.807	63.78	
42	Liquid Fraction	1.000	1.000	1.000	
43	Molar Volume (m3/kgmole)	0.2396	0.2243	0.2382	
44	Mass Heat of Vap. (kJ/kg)	201.7	201.7	201.7	
45	Phase Fraction [Molar Basis]	0.0000	0.0000	0.0000	
46	Surface Tension (dyne/cm)	20.54	25.92	20.99	
47	Thermal Conductivity (W/m-K)	0.1258	0.1395	0.1270	
48	Viscosity (cP)	0.6915	1.798	0.7392	
49	Cv (Semi-Ideal) (kJ/kgmole-C)	377.5	327.4	373.2	
50	Mass Cv (Semi-Ideal) (kJ/kg-K)	2.216	1.922	2.191	
51	Cv (kJ/kgmole-C)	337.5	296.1	333.7	
52	Mass Cv (kJ/kg-K)	1.981	1.738	1.959	
53	Cv (Ent. Method) (kJ/kgmole-C)	---	---	---	
54	Mass Cv (Ent. Method) (kJ/kg-K)	---	---	---	
55	Cp/Cv (Ent. Method)	---	---	---	
56	Reid VP at 37.8 C (bar)	---	---	---	
57	True VP at 37.8 C (bar)	6.294e-004	6.294e-004	6.294e-004	
58	Liq. Vol. Flow - Sum(Std. Cond) (m3/h)	57.97	5.807	63.78	

1	 LEGENDS Calgary, Alberta CANADA	Case Name:	E:\THESIS 2013\STUDIES\8- STUDYING DYNAMICS USING HYSYS\C1
2		Unit Set:	NewUser
3		Date/Time:	Sat May 03 08:55:09 2014
4			
5			


Cooler: Cooler

CONDITIONS

11	Name	H2 HE3 out	H2 out	QCooler
12	Vapour	0.0000	0.0000	---
13	Temperature (K)	408.4491	398.3000	---
14	Pressure (bar)	49.4875	49.0000 *	---
15	Molar Flow (kgmole/h)	106.1455	106.1455	---
16	Mass Flow (kg/s)	5.0224	5.0224	---
17	Std Ideal Liq Vol Flow (m3/h)	24.0709	24.0709	---
18	Molar Enthalpy (kJ/kgmole)	-3.052e+005	-3.095e+005	---
19	Molar Entropy (kJ/kgmole-C)	390.0	379.2	---
20	Heat Flow (kJ/h)	-3.2396e+07	-3.2856e+07	4.6050e+05 *

PROPERTIES

23	Name	H2 HE3 out	H2 out		
24	Molecular Weight	170.3	170.3		
25	Molar Density (kgmole/m3)	3.936	3.981		
26	Mass Density (kg/m3)	670.5	678.1		
27	Act. Volume Flow (m3/h)	26.96	26.66		
28	Mass Enthalpy (kJ/kg)	-1792	-1817		
29	Mass Entropy (kJ/kg-K)	2.289	2.226		
30	Heat Capacity (kJ/kgmole-C)	430.2	422.9		
31	Mass Heat Capacity (kJ/kg-K)	2.526	2.483		
32	Lower Heating Value (kJ/kgmole)	7.579e+006	7.579e+006		
33	Mass Lower Heating Value (kJ/kg)	4.449e+004	4.449e+004		
34	Phase Fraction [Vol. Basis]	---	---		
35	Phase Fraction [Mass Basis]	2.122e-314	2.122e-314		
36	Partial Pressure of CO2 (bar)	0.0000	0.0000		
37	Cost Based on Flow (Cost/s)	0.0000	0.0000		
38	Act. Gas Flow (ACT_m3/h)	---	---		
39	Avg. Liq. Density (kgmole/m3)	4.410	4.410		
40	Specific Heat (kJ/kgmole-C)	430.2	422.9		
41	Std. Gas Flow (STD_m3/h)	2510	2510		
42	Std. Ideal Liq. Mass Density (kg/m3)	751.1	751.1		
43	Act. Liq. Flow (m3/s)	7.490e-003	7.407e-003		
44	Z Factor	---	---		
45	Watson K	12.74	12.74		
46	User Property	---	---		
47	Partial Pressure of H2S (bar)	0.0000	0.0000		
48	Cp/(Cp - R)	1.020	1.020		
49	Cp/Cv	1.128	1.130		
50	Heat of Vap. (kJ/kgmole)	---	---		
51	Kinematic Viscosity (cSt)	0.5536	0.5989		
52	Liq. Mass Density (Std. Cond) (kg/m3)	753.0	753.0		
53	Liq. Vol. Flow (Std. Cond) (m3/h)	24.01	24.01		
54	Liquid Fraction	1.000	1.000		
55	Molar Volume (m3/kgmole)	0.2540	0.2512		
56	Mass Heat of Vap. (kJ/kg)	---	---		
57	Phase Fraction [Molar Basis]	0.0000	0.0000		
58	Surface Tension (dyne/cm)	15.61	16.39		
59	Thermal Conductivity (W/m-K)	0.1118	0.1142		
60	Viscosity (cP)	0.3712	0.4061		
61	Cv (Semi-Ideal) (kJ/kgmole-C)	421.9	414.6		
62	Mass Cv (Semi-Ideal) (kJ/kg-K)	2.477	2.434		

1	 LEGENDS Calgary, Alberta CANADA	Case Name: E:\THESIS 2013\STUDIES\8- STUDYING DYNAMICS USING HYSYS\C1
2		Unit Set: NewUser
3		Date/Time: Sat May 03 08:55:09 2014
4		
5		

Cooler: Cooler (continued)

PROPERTIES

11	Name	H2 HE3 out	H2 out			
12	Cv (kJ/kgmole-C)	381.3	374.3			
13	Mass Cv (kJ/kg-K)	2.239	2.198			
14	Cv (Ent. Method) (kJ/kgmole-C)	---	---			
15	Mass Cv (Ent. Method) (kJ/kg-K)	---	---			
16	Cp/Cv (Ent. Method)	---	---			
17	Reid VP at 37.8 C (bar)	---	---			
18	True VP at 37.8 C (bar)	6.294e-004	6.294e-004			
19	Liq. Vol. Flow - Sum(Std. Cond) (m3/h)	24.01	24.01			

PID Controller: TIC-100

PID Controller: TIC-101

PID Controller: TIC-102

PID Controller: FIC-100

PID Controller: FIC-101

PID Controller: FIC-102

PID Controller: FIC-103

Vita

Ibrahim Tamer Masoud was born on January 19, 1987, in Port Said, Egypt. He was educated in private schools in UAE. He graduated from Fujairah Private Academy in 2005 and enrolled in the American University of Sharjah to graduate with a bachelor degree of chemical engineering in spring 2009. He joined the MSc program of chemical engineering at the American University of Sharjah in fall 2009.

Mr. Masoud started his professional career as a process engineer in Petrofac International Limited, Sharjah, where he worked there from 2009 to 2012. In 2012 he then moved to work for Tenaris Global Services S.A. as an inside sales analyst. In 2013 Mr. Masoud took the role of commercial manager within Tenaris Global Services S.A. for the markets of Qatar, Pakistan and Lebanon.